“CFD Analysis of rectangular micro-channel heat sink”
Major project-II

Submitted to Delhi Technological University in partial fulfillment of the requirement for the award of Degree of

Master of Technology

In

Thermal Engineering

UNDER THE SUPERVISION OF

Mr. MD. ZUNAID

Asst. Professor

Department Of Mechanical Engineering

Delhi Technological University

Delhi-110042

SUBMITTED BY-

AVINASH GUPCHUP

2k13/THE/09

Department of Mechanical Engineering
Delhi Technological University
(Formerly DELHI COLLEGE OF ENGINEERING)
Bawana road, Delhi -110042

CERTIFICATE

DELHI TECHNOLOGICAL UNIVERSITY
(Formerly DELHI COLLEGE OF ENGINEERING)

Date:-_____

This is to certify that report entitled **"CFD Analysis of rectangular micro-channel heat sink"** by **AVINASH GUPCHUP** in the requirement of the partial fulfilment for the award of Degree of **Master of Technology (M.Tech)** in **Thermal Engineering** at **Delhi Technological University**. This work was completed under my supervision and guidance. He has completed his work with utmost sincerity and diligence. The work embodied in this project has not been submitted for the award of any other degree to the best of my knowledge.

Supervisor-
Mr. MD. ZUNAID
(Asst. professor)
Delhi technological university
Delhi

DECLARATION

I declare that the work presented in this thesis titled “CFD analysis of rectangular micro-channel heat sink”,submitted to Department of Mechanical Engineering, is an authentic record of my own work carried out under the supervision of asst. prof. Mr. MD. ZUNAID, Department of Mechanical Engineering, Delhi technological university, Delhi.

This report does not, to the best of my knowledge, contain part of my work which has been submitted for the award of any other degree either of this university or any other university without proper citation.

Date:

Place : DTU ,Delhi Signature of candidate

ACKNOWLEDGEMENT

First of all, I would like to express my gratitude to God for giving me ideas and strengths to make my dreams true and accomplish this thesis.

To achieve success in any work, guidance plays an important role. It makes us put right amount of energy in the right direction and at right time to obtain the desired result. Express my sincere gratitude to my guide, **MR. MD. ZUNAID**, Asst. Professor, Mechanical Engineering Department for giving valuable guidance during the course of this work, for his ever encouraging and timely moral support.

I am greatly thankful to **DR. R. S. MISHRA**, Professor and Head, Mechanical Engineering Department, Delhi Technological University, for his encouragement and inspiration for execution of the this work. I express my feelings of thanks to the entire faculty and staff, Department of Mechanical Engineering, Delhi Technological University, and Delhi for their help, inspiration and moral support, which went a long way in the successful completion of my report work.

AVINASH GUCHUP

(Roll No-2K13/THE/09)

ABSTRACT

In the present study fluid flow, pressure drop and heat transfer characteristics in two types of micro-channel heat sinks have been analyzed using computational fluid dynamics. One of them is a straight rectangular micro-channel heat sink on which validation is done by comparing experimental results with numerical results while the other is a wavy edge type rectangular micro-channel heat sink for which simulation results are obtained. Water is used as a coolant for the simulation. The material for heat sink is copper. Both the micro-channels have a width of 0.23mm and height of 0.71mm. The aspect ratio (ɣ) and the length of both the channels is kept same as 0.32 and 44.7mm respectively. The analysis for both the micro-channels is done for five sets of Reynolds number which are 400, 600, 800, 1000 and 1200 respectively. The two values of heat flux used are 100W/ cm^2 and 200W/ cm^2 .After constructing the geometry in solid works the simulation is done on ANSYS CFX. For both the straight micro-channel and the wavy micro-channel investigated, it is found that the thermal performance of wavy edge micro-channels is better in comparison to that of straight micro-channels. The temperature rise of water is more in wavy edge type micro-channels in comparison to that of straight micro-channels of the same hydraulic diameter for different sets of Reynolds number for different values of heat flux. Further the pressure drop is more in wavy type of channels which can be compensated due to the high heat transfer characteristics of wavy micro-channels.

CONTENTS

LIST OF FIGURES

LIST OF TABLES

NOMENCLATURE

A_c	Cross-sectional area of channel
C_p	Specific heat at constant pressure
D_h	Hydraulic diameter of channel. perimeter
H	Height of micro-channel heat sink
H_{ch}	Height of micro-channel
H_{w1}	Substrate thickness on insulated side of micro-channel heat sink
H_{w2}	Substrate thickness on heated side of micro-channel heat sink
K	Thermal conductivity
L	Length of micro-channel heat sink
P	Pressure
q	Heat flux
Re	Reynolds number based on channel hydraulic diameter
R_{th}	Thermal resistance
T	Temperature
T_{in}	Fluid inlet temperature
T_{bm}	Fluid bulk temperature
W	Width of micro-channel heat sink unit cell
W_{ch}	Width of micro-channel
W_{w1}, W_{w2}	Half-thickness of wall separating micro-channels
ɣ	aspect ratio

Greek symbols

μ	dynamic viscosity
ρ	density

CHAPTER 1

INTRODUCTION

1.1 Micro-channel heat sink-

Since the most recent decade, smaller scale machining technology is utilized at an expanded rate for the improvement of exceptionally productive cooling gadgets known as micro-channel heat sinks due to its greater advantages, for example, less coolant requirement and small measurements. Thus, the investigation of heat transfer and fluid flow in smaller scale channels which are two important parts of such gadgets, have pulled in additional considerations with expansive applications in both designing and performance issues. Heat sinks can be classified into two phase or single phase depending on if bubbling of fluid happens inside the smaller scale channels. Essential parameters that defines the single phase and two-phase working administrations are heat flux through the channel wall and volume flow rate of the coolant .

The construction of the heat sink is done from a material with high thermal conductivity, for example, copper or silicon with the smaller scale channels created into its surface by either exactness machining or miniaturized scale fabrication technology. These small scale channels have trademark measurements going from 10 to 500 μm, and serve as flow entries for the cooling fluid. These micro-channels possess advantage of very small volume to surface area ,small mass, large convective heat transfer coefficient. Miniaturization of electronic gadgets has become necessity of today. The reduced size of the microchips has led to an increase in the heat flux density , which causes overheating of gadgets and makes the general prosperity and working of these gadgets a major test for scientists. So there is a need to grow profoundly proficient cooling innovation and heat dissemination strategies to meet the safety standards.

across the channel walls, though transport of mass happens through the cross-sectional area of the heat sink. The cross –sectional area of the heat sink serves as a course to transport liquid to and far from the wall of the channel.

Due to high value of flux density, dissipating from the rapid and high speed devices the study on micro-channels is gaining importance. The advancements in the micro-electromechanical gadgets actually need a heat evacuation system which are capable of convecting high heat and are also equally small at the same time.

1.2 Requirement of micro-channels-

The flow section measurements in convective exchange of heat applications have been moving towards littler measurements for the accompanying three main reasons:

1. Heat transfer enhancement.
2. Increased heat flux dissemination in microelectronic gadgets.
3. Rise of micro-scale gadgets that support cooling utilizing littler direct measurements brings about higher heat exchange execution.

Micro-channel coolers comprise of a very powerful way for dissipating very large amounts of heat from small surfaces. The heat sinks possess several features that make them very prime devices which can be used for the next generation of cooling technology in various high performance supercomputer chips and diodes of laser. The construction of a typical micro-cooler comprise of very large number coolant channels. Heat sinks can be classified as single-phase or two-phase depending as to whether the fluid or liquid boils inside the micro–channels or not.

The study on single phase micro-channel heat sink has a very extensive coverage since the last two decades. Since the last two decades,micro-channel coolers having different dimensions and and different material of substrate have been fabricated and tested with numerous cooling liquids. Test results have demonstrated several technical merits of single-phase micro-channel heat sinks, namely, the ability to produce very large heat transfer coefficients, small size and volume per heat load, and small coolant inventory requirements. The main objective of these studies is to develop heat transfer modelling tools that are essential to the design and optimization of heat sink geometry.

1.3 Coolants used and heat sink material-

Various types of coolants can be employed in a micro-channel cooler for heat removal. A commonly used coolant in a heat sink is water. However, for better cooling performance of the micro-channel cooler nano-fluids can be used. The material of the heat sink is usually a material with high thermal conductivity such as silicon, copper and aluminium.

1.4 Solid works-

Solid works is a computer aided design (CAD) and solid modelling software program which runs on windows. The Solid Works is product of the Daussalt systems .Solid Works is a solid modeler, and in turn uses a parametric element based way to deal with assemblies , parts and models. Parameters allude to imperatives whose qualities focus the shape or geometry of the parts or assemblies. Parameters can be either numeric parameters, for example, line lengths or circle measurements, or geometric parameters, for example, parallel, tangent vertical etc.

1.5 ANSYS CFX package-

ANSYS CFX software is a high performance and elite, fluid dynamics software package. The package has been in use for solving fluid flow and heat transfer problems since the last 20 years. Application of ANSYS CFX includes-

1. Fluid flow problems.

2. Conjugate heat transfer problems, involving heat transfer between a solid and a fluid.

The ANSYS CFX solver uses a finite elements (cell vertex numerics), similar to those used in mechanical analysis, to discretize the domain. ANSYS CFX software package involves only one approach for solving the necessary governing equations . Major advantage of using ANSYS CFX is seen in problems on conjugate heat transfer where selection of interface is the main criteria. ANSYS CFX sets a default interface and hence is more user friendly in comparison to other software packages for problems on heat transfer and fluid flow.

1.6 CFD

Computational Fluid Dynamics (CFD) is a PC based numerical simulation tool used to examine the heat exchange and fluid flow characteristic furthermore its related phenomena, for example, substance response. An arrangement of numerical model and mathematical statements are initially created after conservation laws. These mathematical statements are then solved utilizing a PC program to get the stream variables all through the computational space. Approval of CFD models is regularly needed to survey the exactness of the computational model. Approval or validation is accomplished by comparing CFD results with

the experimental data. Approved models get to be set up as reliable, while those which come up short the approval test should be altered and revalidated.

1.7 Conjugate heat transfer-

The term conjugate heat transfer is used to describe processes which involve variations of temperature within solids and fluids, due to thermal interaction between the solids and fluids. Most common example of a conjugate heat transfer problem is a micro-channel heat sink.

Conjugate heat transfer in fluids and solids is the key to designing effective coolers, heaters, or heat exchangers. The fluid usually plays the role of energy carrier on large distances. Forced convection is the most common way to achieve high heat transfer rate. In some applications, the performances are further improved by combining convection with phase change.

1.8 Applications-

1. Laser diodes

2. Micro-chips.

3. Soldering circuit boards.

CHAPTER 2

LITERATURE REVIEW

Experimental studies-

Peng and Peterson (1996) investigated experimentally the single-phase forced convective heat transfer micro-channel structures with small rectangular channels having hydraulic diameters of 0.133–0.367 mm for different types of geometric configurations. The results shows heat transfer and flow characteristics. The laminar heat transfer found to be dependent upon the aspect ratio i.e. the ratio of hydraulic diameter to the centre to centre distance of micro-channels.

Fedorov and Viskanta (2000) developed a three dimensional model to investigate the conjugate heat transfer in a micro channel heat sink with the same channel geometry used in the experimental work done. This investigation indicated that the average channel wall temperature along the flow direction was nearly uniform except in the region close to the channel inlet, where very large temperature gradients were observed. This allowed them to conclude that the thermo–properties are temperature dependent.

Jiang et al. (2001) performed an experimental comparison of microchannel heat exchanger with microchannel and porous media. The effect of the dimensions on heat transfer was analyzed numerically. It was emphasized that the heat transfer performance of the microchannel heat exchanger using porous media is better than using of microchannels, but the pressure drop of the former is much larger.

Qu and Mudawar (2002) have performed experimental and numerical investigations of pressure drop and heat transfer characteristics of single-phase laminar flow in 0.231 mm by 0.713 mm channels. Deionized water was employed as the cooling liquid and two heat flux levels, 100 W/cm^2 and 200 W/cm^2. Good agreement was found between the measurements and numerical predictions, validating the use of conventional Navier–Stokes equations for micro channels. For the channel bottom wall, much higher heat flux and Nusselt number values are encountered near the channel inlet.

Lee and Mudawar (2007) have done experimental work to explore the micro-channel cooling benefits of water-based nano-fluids containing small concentrations of Al2O3. It was

observed that the presence of nano-particles enhances the single-phase heat transfer coefficient, especially for laminar flow. For two-phase cooling, nanoparticles caused catastrophic failure by depositing into large clusters near the channel exit due to localized evaporation once boiling commenced.

Chein and Chuang (2007) have addressed micro-channel heat sink (MCHS) performance using nanofluids as coolants. They have carried out a simple theoretical analysis that indicated more energy and lower micro-channel wall temperature could be obtained under the assumption that heat transfer could be enhanced by the presence of nano-particles. It was observed that nano fluid cooled MCHS could absorb more energy than water-cooled MCHS.

Numerical studies-

Liu and Garimella (2004) have studied numerically on fluid flow and heat transfer in micro channels and confirmed that the behaviour of micro channels is quite similar to that of conventional channels. And their analysis showed that conventional correlations offer reliable predictions for the laminar flow characteristics in rectangular micro channels over a hydraulic diameter in the range of 244–974 μm.

Roy et al. (2004) has studied a steady, laminar flow and heat transfer of a nanofluid flowing inside a radial channel between two coaxial and parallel discs. The non-dimensional governing equations of mass, momentum and energy were solved by computational fluid dynamics method. Results have shown that the inclusion of nanoparticles in a traditional coolant can provide considerable improvement in heat transfer rates, even at small particle volume fractions. Increases in the resulting wall shear stresses were also noticed.

Hetsroni et al. (2005) has further verified the capacity of conventional theory to predict the hydrodynamic and thermal features of laminar Newtonian incompressible flows in micro channels in the range of hydraulic diameter from D_h =15 □m to D_h = 401 μm . They have compared their results with the data available in open literature. The theoretical models were subdivided in two groups depending on the degree of correctness of the assumptions. The first group includes the simplest one-dimensional models assuming uniform heat flux, constant heat ransfer coefficient, etc. The comparison of these models with experiment shows significant discrepancy between the measurements and the theoretical predictions.

Khanafer et al. (2003) has investigated heat transfer enhancement in a two-dimensional rectangular enclosure using nanofluids. The material used is water/copper. The transport equations were solved numerically using the finite-volume approach along with the alternating direct implicit procedure. The effect of suspended ultrafine metallic nanoparticles on the fluid flow and heat transfer processes within the enclosure was analyzed. The heat transfer correlation of the average Nusselt number for various Grashof numbers and volume fractions was also presented.

Jou and Tzeng (2006) have used the Khanafer's model to analyze heat transfer performance of nanofluids inside an enclosure taking into account the solid particle dispersion. Transport equations were modeled by a stream function-vorticity formulation and solved numerically by finite difference approach. Based upon the numerical predictions, the effects of Rayleigh number (Ra) and aspect ratio on the flow pattern and energy transport within the thermal boundary layer were presented. It was observed that increasing the buoyancy parameter and volume fraction of nanofluids cause an increase in the average heat transfer coefficient. Finally, the empirical equation was built between average Nusselt number and volume fraction.

Allen (2007) had investigated fluid flow and heat transfer in microchannels experimentally and numerically. Fluid flow and heat transfer experiments were conducted on a copper micro channel heat exchanger with constant surface temperature. The experimentally obtained friction factor were found fairly well agreement with theoretical correlations and moreover the experimental Nusselt number results agreed with theory very well in the transition and turbulent regime, but the results show a higher Nusselt number in the laminar regime than predicted by theoretical correlations. Philips created a CFD model to simulate the fluid in the inlet plenum and the micro-channels. The results from these simulations showed good agreement with the experimental data in the transition/turbulent regime as well as with theoretical correlations for laminar and turbulent flow.

Sabbah et al. (2008) observed that the prediction of heat transfer in micro-channels becomes difficult with increase in complicacy of the geometry of the micro-channels, requiring three dimensional analysis of heat transfer in both solid and liquid phases. Computational Fluid Dynamics (CFD) models were implemented in order to study and optimize the thermal and hydraulic performance of micro channel heat sinks. Despite the small width of the channels, the conventional Navier Stokes and energy conservation equations still apply to the flow due

to the continuum of the working fluid where the channel width is many times larger than the mean free path of liquid molecules (water). The micro-channel is characterized by the laminar flow in it, due to the small hydraulic diameter of the channel which results in low Reynolds numbers.

Mokrani et al. (2009) developed a reliable experimental device and adequate methodology to characterize the flow and convective heat transfer in flat micro channels. The study was concerned with measurement of pressure drop and heat transfer by a Newtonian fluid flow inside a flat micro channel of rectangular cross-section whose aspect ratio is sufficiently high that the flow can be considered two dimensional They considered the hydraulic diameter as twice of the channel height. The mathematical model used to describe the convective heat transfer between the walls and the fluid takes into account the whole field (solid wall and fluid layer) and the coupling between the conduction and the convection modes. Finally they concluded that the conventional laws and correlations describing the flow and convective heat transfer in ducts of large dimension are directly applicable to the micro channels of heights between 500 and 50 microns

Mathew and Hegab (2009) theoretically analyzed the thermal performance of parallel flow micro heat exchanger subjected to constant external heat transfer. The model equations predicts temperature distributions as well as effectiveness of the heat exchanger. Moreover, the model can be used when the individual fluids are subjected to either equal or unequal amounts of external heat transfer.

Rebrov et al. (2011) has reviewed the experimental and numerical results on fluid flow distribution, heat transfer and combination thereof, available in the open literature. They have found that the experiments with single channels are in good agreement with predictions using the published correlations. The review consists of two parts. In the first, the main methods to control flow distribution were reviewed. Several different designs of inlet/outlet chambers were presented together with corresponding models used for optimization of flow distribution.

CHAPTER 3

MATHEMATICAL FORMULATION

3.1 CFD equations –

In the present study the single phase model of computational fluid dynamics is used for the purpose of computing and solving the problem of particular category. This single phase model will solve and calculate one transport equation for continuity and one for momentum for each phase, and after this the energy equations are solved for studying the fluid and thermal performance of the system. The simulation for this single phase model is done using ANSYS CFX.

3.2 Simulation equations-

The equations used in this model include the equation of momentum, equation of continuity and energy equation (ANSYS CFX). The use of energy equation is done for finding out temperature distribution on the wall. The equation for conservation of mass, continuity equation, can be written as follows:

Mass conservation equation-

The equation for conservation of mass, or continuity equation, can be written as follows:

$$\frac{\partial \rho}{\partial t} + \nabla.(\rho \vec{v}) = S_m$$

The equation written above is a general equation for conservation of mass. Here S_m is the mass added from any user defined sources.

Momentum conservation equation-

Momentum conservation in a reference frame which is non accelerating can be written as

$$\frac{\partial}{\partial t}(\rho \vec{v}) + \nabla.(\rho \vec{v}\vec{v}) = -\nabla p + \nabla.(\bar{\bar{\tau}}) + \rho g + \vec{F}$$

Where,

p is the static pressure ,τ is the stress tensor

F and ρg are the external forces on body and gravitational force on body.

Energy equation-

ANSYS CFX solves the energy equation in the following form:

$$\frac{\partial}{\partial t}(\rho E) + \nabla.(\vec{v}\,(\rho E + p)\,) = \nabla.\left(k_{eff}\,\nabla T + \sum_{J} h_j \overrightarrow{J_j} + \overline{\overline{\tau_{eff}}}.\vec{v} \right) + S_h$$

Where,

k_{eff} is the effective conductivity ($k+k_t$), where k_t is the turbulent thermal conductivity, defined on the basis of turbulence model being used, and J_j is the diffusion flux of species J. On the right-hand side of the equation the first three terms represents energy transfer due to species diffusion, conduction, and viscous dissipation, respectively, S_h denotes the chemical reaction heat, and some other sources of heat.

Standard relations and associated equations –

The bulk mean temperature, T_{bm} and the wall temperature, T_{wx} with distance x from the micro-channel entrance can be obtained by doing the thermal energy balance around the micro-channel which is given by the following equations.

$$T_{bm} = T_{in} + \frac{q\pi D\, hx}{mCp}$$

Where,

T_{bm} is the bulk mean temperature.

T_{in} is inlet temperature.

q is the heat flux.

D_h is hydraulic diameter of channel.

m is mass flow rate across channel.

The relation between the hydraulic diameter and Reynolds number in a channel is given by

$$Re=\rho v D_h/ \text{□}$$

Where,

ρ is density

v is average velocity.

□ is dynamic viscocity.

D_h is hydraulic diameter of channel.

CHAPTER 4

METHODOLOGY

Problem 1-

4.1 Simulation of heat transfer and pressure drop in straight rectangular micro-channel heat sink-

In this chapter a three dimensional CFD simulation is done for the heat transfer and pressure drop characteristics of rectangular micro-channel. Material used for heat sink construction is copper. The experimental set up shown in figure was developed by mudawar and Qu (2002).

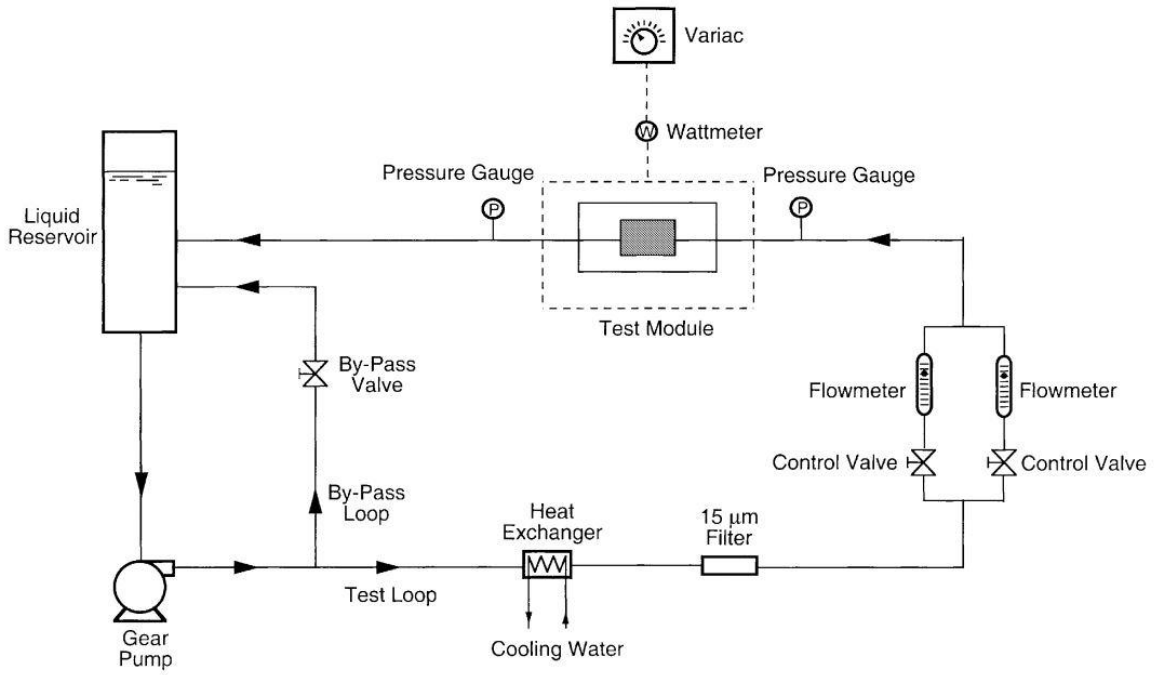

Figure 4.1: Schematic diagrams of flow loop [7]

Description of problem-

The experimental work done by Qu and Mudawar, (2001) on the test apparatus is modelled and simulated in this present study. Water is moving through a straight rectangular smaller scale channel implanted in a test module. 21 rectangular smaller scale openings were machined into micro- channel surface by an accuracy machining procedure. The miniaturized scale openings were equidistantly divided inside of the 1-cm heat sink width and had the

cross-sectional measurements of 231 µ m wide and 712 µm profound. There are 21 parallel rectangular small scale directs in the module.

4.2 Geometry of the heat sink-

In the present analysis, only one micro channel of the remaining 21 micro-channels is considered as a computational domain. Figure shows the micro-channel heat sink with single unit cell used for simulation.

Table 1: Dimensions of the unit cell used for simulation

W_{wall}(µm)	$W_{channel}$(µm)	H_{wall2}(µm)	$H_{channel}$(µm)	H_{wall1}(µm)	L(mm)
118	231	12700	713	5637	44.7

Geometry construction-

For this computational fluid dynamics problem , the geometry of the heat sink was constructed using solid works, and was imported to ANSYS workbench CFX for further meshing and CFD simulations.

For creating geometry, first the heat sink was made in solid works as per the dimensions given in table 1 and was named as solid part while fluid channel was created of the same dimensions as of the rectangular slot along the length of heat sink for proper mating and was given the name of fluid part.

Both parts were created separately using solid works and were later assembled by inserting fluid channel in solid heat sink using the insert components and mate option in solid works.

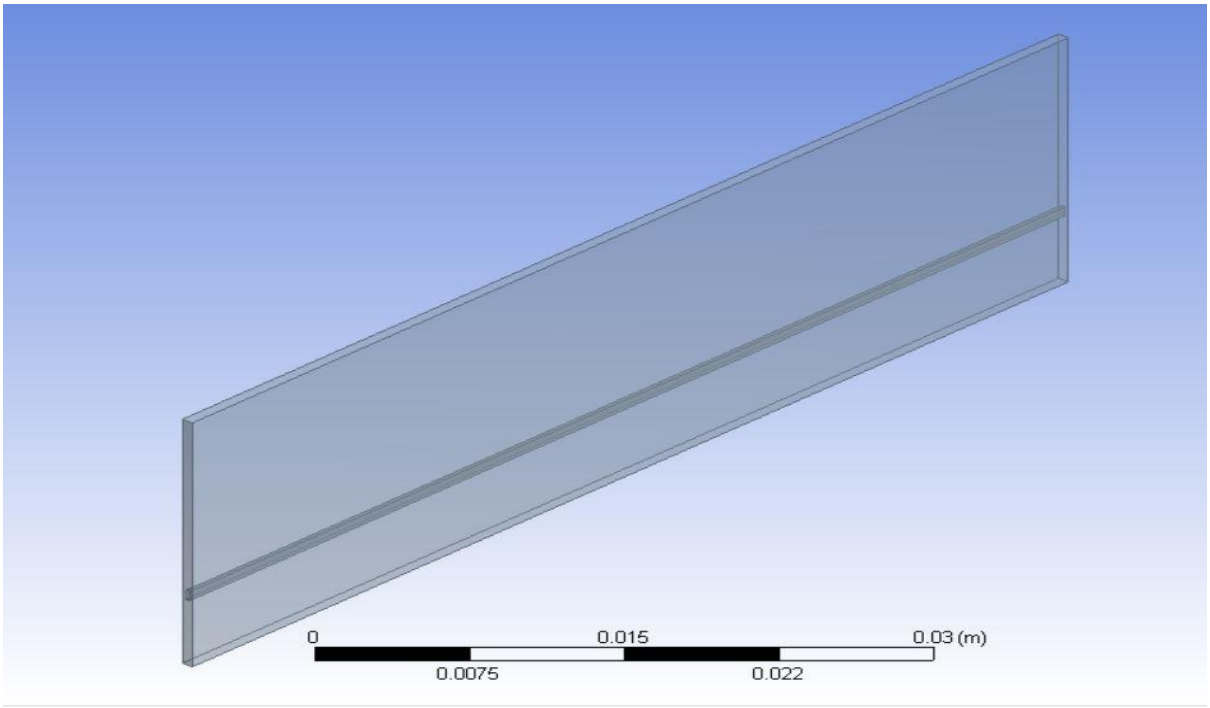

Figure 4.2: Geometry of straight micro-cannel heat sink used in simulation

4.3 Meshing-

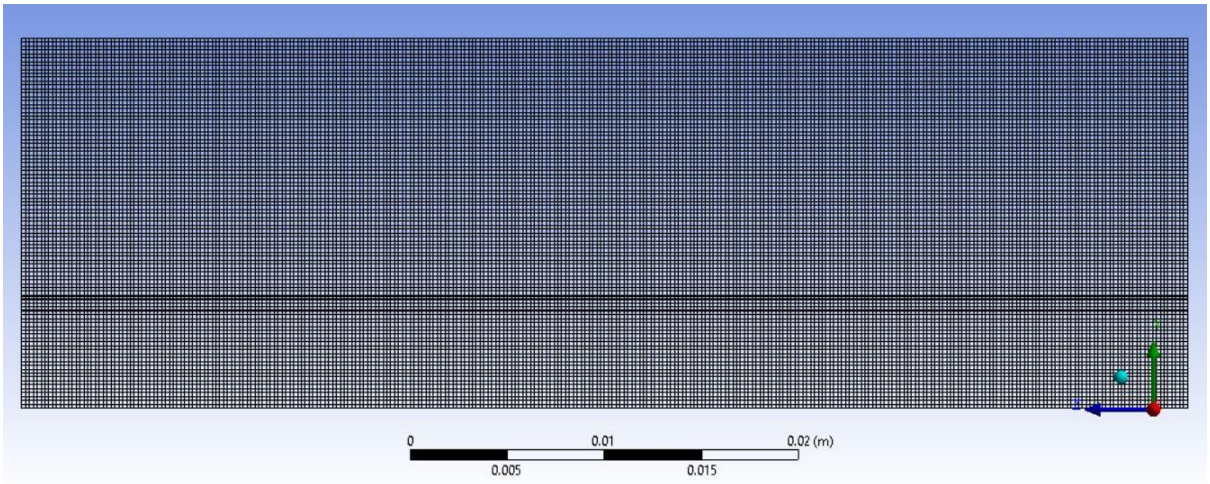

Figure 4.3: Meshing of the geometry in ANSYS CFX

Table 2: Mesh details-

Physics preference	CFD
Solver preference	CFX
Smoothing	Medium
Transition	Slow
Transition ratio	0.272
Minimum size	2e-5
Maximum face size	2.5e-4
Maximum size	2e-4
Nodes	118594
Elements	85500

The mesh was generated using proximity on option. For the straight micro-channel the mesh was created as a structured mesh and for checking the solutions the mesh was made finer and the solutions obtained were mesh independent. After the meshing, the named selection were given, which are to be considered as boundary conditions .

4.4 Set up details-

Before giving the boundary conditions two domains were created in the ANSYS CFX set up. Out of the two domains created one domain was given the name as fluid while the other domain was assigned the name as solid domain. The fluid channel constructed in solid works was given the name fluid domain while the heat sink constructed in solid works was given the name solid domain.

After making the domains in the set up the boundary conditions were created in the solid domain and the fluid domain. Inlet and outlet boundary conditions were given in the fluid domain whereas the bottom wall heat flux and adiabatic conditions for the remaining walls were given in the solid domain.

Boundary conditions-

1. No slip on the surface.

2. Uniform inlet temperature and static pressure were given at the entry of the channel.

3. Outlet of the channel is based on mass flow rate.

4. A uniform heat flux of $10^6 W/m^2$ and $2*10^6$ W/m^2 at the bottom wall of the heat sink.

Table 3 : Zone specification –

Heat sink front wall	Wall
Heat sink top wall	Wall
Heat sink back wall	Wall
Heat sink bottom wall	Heat flux
Heat sink right wall	Wall
Heat sink left wall	Wall
Channel entry	Static pressure
Channel outlet	Mass flow outlet
Default Interface	Wall

Table 4: Solver settings-

Following are the solver settings which are to be used in simulation.

Min. Iterations	1
Max. Iterations	250
Residual type	RMS
Residual target	1E-4
Time scale control	Auto time scale

Problem 2 -

4.5 Simulation of heat transfer and pressure drop in wavy edge type rectangular micro-channel heat sink-

In this chapter a three dimensional CFD simulation is done for the heat transfer and pressure drop characteristics of wavy edge rectangular micro-channel heat sink. Material used for heat sink construction is copper.

Problem description-

Water is moving through a wavy edge rectangular smaller scale channel heat sink assembly In this analysis a design for wavy edge type of micro-channel heat sink is constructed . The dimensions of the micro-channel assembly are same as that of the micro-channels simulated in chapter 4 the only difference being the length is made wavy.

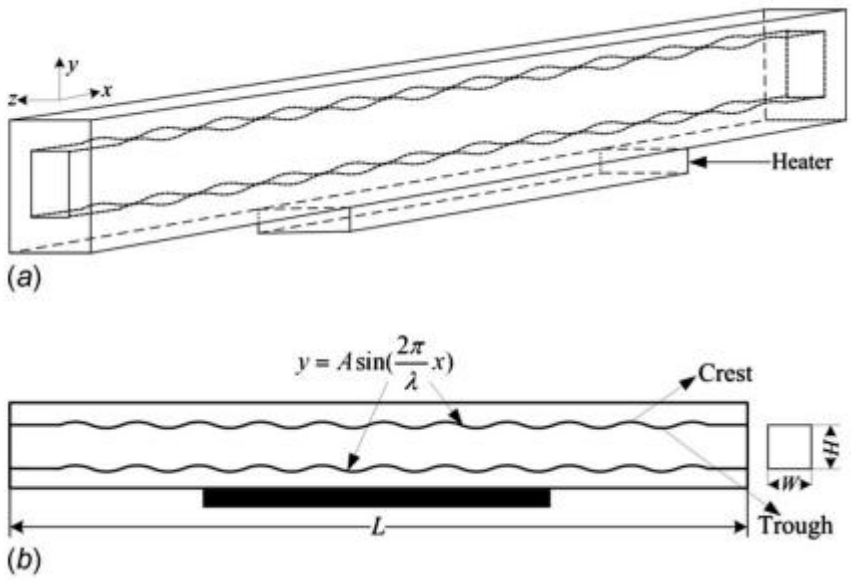

Figure 4.4: Schematic of wavy micro-channel heat sink. [18]

Table- 5: Dimensions of the unit cell used for simulation

W_{wall}(μm)	W(μm)	H_{wall2}(μm)	H(μm)	H_{wall1}(μm)	L(mm)
118	231	12700	713	5637	44.7

In this analysis the only the length of the micro-channel heat sink is made wavy and the pressure drop and heat transfer characteristics are simulated.

Wave equation used- In this analysis ,for the construction of geometry a sine wave is used which has the following equation.

$$y = Asin(2\pi x/\lambda)$$

Here , A is wave amplitude and $\lambda\ is\ wavelength$.

4.6 Geometry construction-

For the analysis of computational fluid dynamics problem , the geometry of the heat sink was constructed using solid works, and was imported to ANSYS workbench CFX for further meshing and CFD simulations.

For creating geometry, first the heat sink was made in solid works as per the dimensions given in table 2. The wave dimensions were given according to the length of the channel which is 44.7 mm.

A sinusoidal wave was assumed and was constructed in the solid heat sink. The amplitude of the wave was taken as 0.15 mm while the wavelength was taken as 2 mm. However, fluid channel was created of the same dimensions as of the wavy rectangular slot along the length of heat sink for proper mating and was given the name of fluid part.

Both parts were created separately using solid works and were later assembled by inserting fluid channel in solid heat sink using the insert components and mate option in solid works.

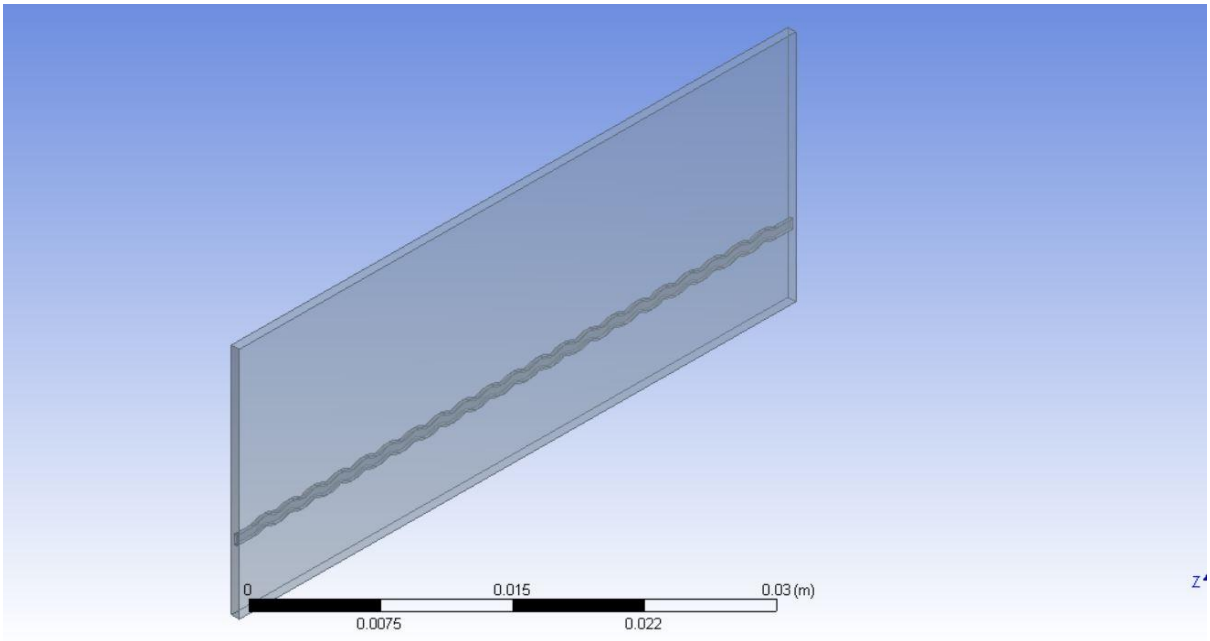

Figure 4.5: Geometry of wavy micro-cannel heat sink used in simulation

4.7 Meshing-

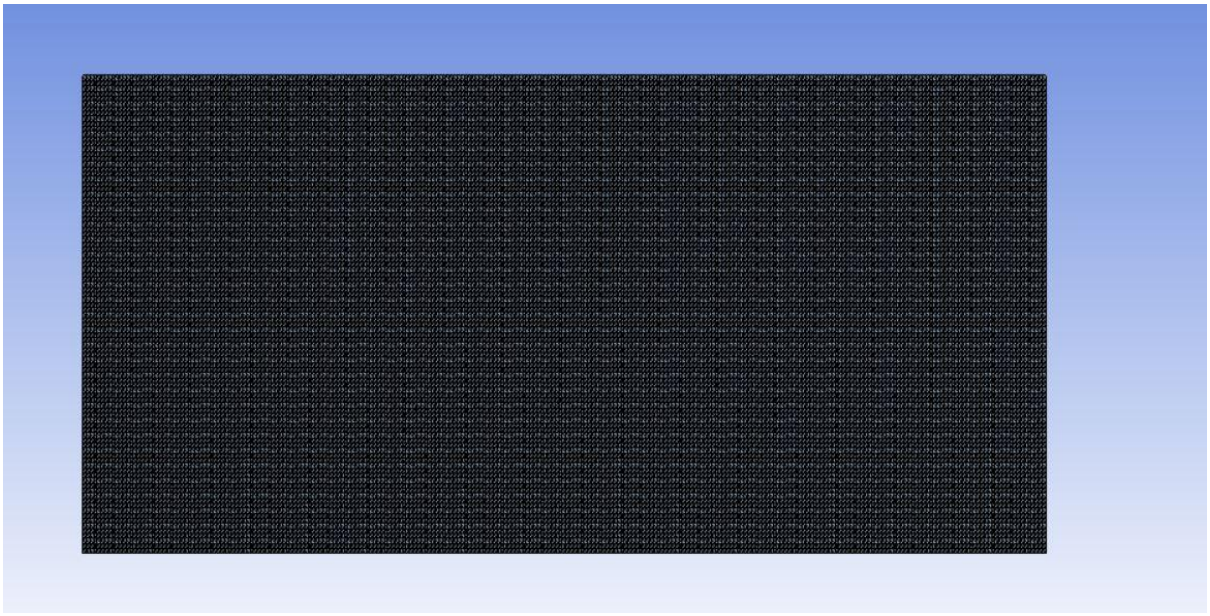

Figure 4.6: Meshing of geometry in ANSYS CFX

Table 6: Mesh details-

Physics preference	CFD
Solver preference	CFX
Smoothing	Medium
Transition	Slow
Transition ratio	0.277
Minimum size	2e-5
Maximum face size	2.5e-4
Maximum size	2e-4
Nodes	118594
Elements	178556

The mesh was generated using proximity and curvature on option. For checking the solutions the mesh was made finer and the solutions obtained were mesh independent. After the meshing, the named selection were given, which are to be considered as boundary conditions.

4.8 Set up details-

Before giving the boundary conditions two domains were created in the ANSYS CFX set up. Out of the two domains created, one domain was given the name as fluid while the other domain was assigned the name as solid domain. The fluid channel constructed in solid works 2013 was given the name fluid domain while the heat sink constructed in solid works 2013 was given the name solid domain.

After making the domains in the set up the boundary conditions were created in the solid domain and the fluid domain. Inlet and outlet boundary conditions were given in the fluid domain whereas the bottom wall heat flux and adiabatic conditions for the remaining walls were given in the solid domain.

Boundary conditions-

1. No slip on the surface.

2. Uniform inlet temperature and static pressure were given at the entry of the channel.

3. Outlet of the channel is based on mass flow rate.

4. A uniform heat flux of 100W/cm^2 and 200 W/cm^2 at the bottom wall of the heat sink for two separate cases was applied.

Table 7: Zone specification –

Front wall of solid heat sink	Wall
Top wall of solid heat sink	Wall
Back wall of solid heat sink	Wall
Bottom wall of solid heat sink	Heat flux
Heat sink right wall	Wall
Heat sink left wall	Wall
Channel entry	Static pressure
Channel exit	Mass flow rate
Default Interface	Wall

Table 8: Solver settings-

Following are the solver settings which are to be used in simulation.

Min. Iterations	1
Max. Iterations	250
Residual type	RMS
Residual target	1E-4
Time scale control	Auto time scale

CHAPTER 5

VALIDATION

5.1 Straight rectangular micro-channel -

In this computational analysis validation is done for straight rectangular micro-channel heat sink and the results are plotted for pressure drop and heat transfer in straight rectangular micro-channel for two different values of heat fluxes applied at the bottom of the heat sink for varying set of values of Reynolds number. The value of heat flux used in the analysis are 100W/$cm^2$and 200W/cm^2. Five values of Reynolds number are taken for the analysis which are 400, 600, 800, 1000, 1200 respectively.

Results for bottom wall heat flux value of 100W/cm^2 and different sets of Reynolds number-

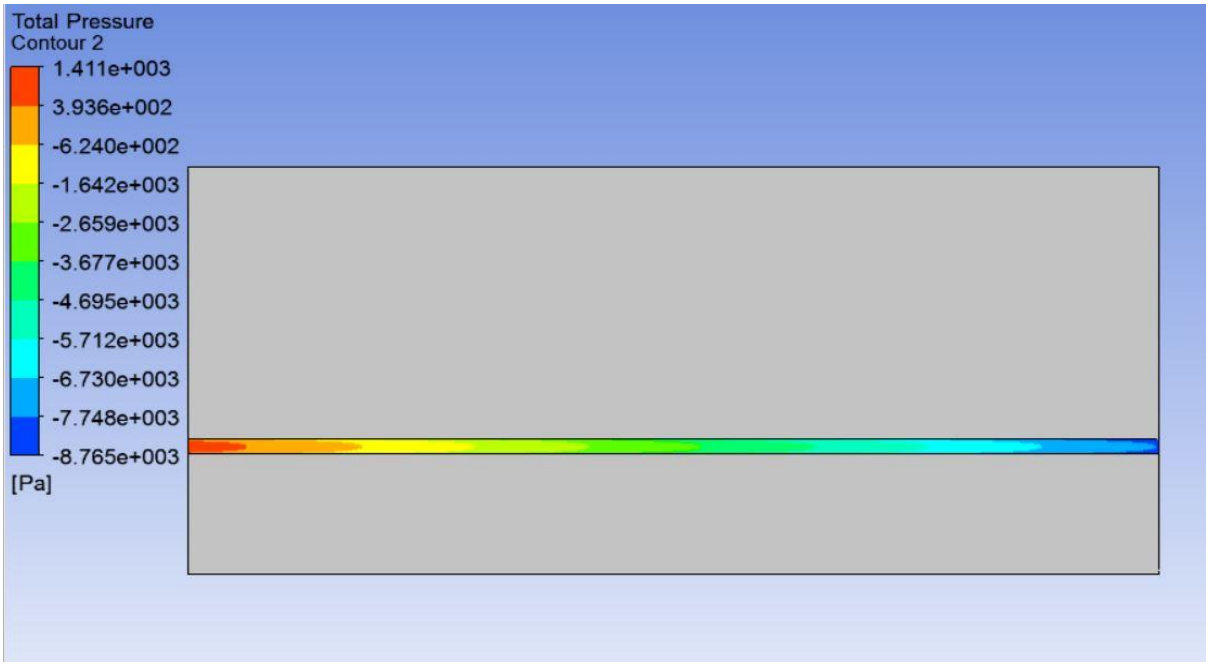

Figure 5.1: Pressure contours of water at Re=400

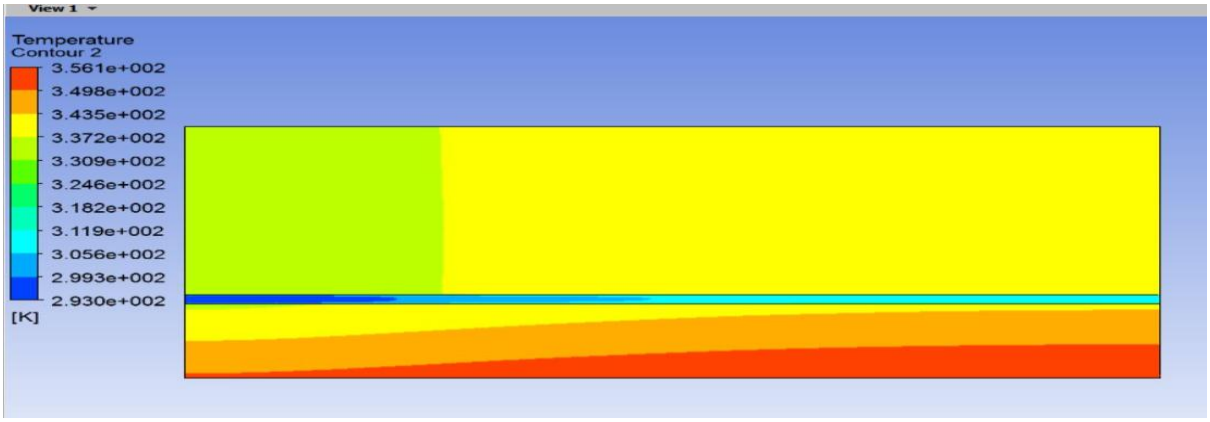

Figure 5.2: Temperature contours of water and heat sink at Re=400

- In the figures 5.1 and 5.2, the contours for pressure and temperature in a straight rectangular channel for Reynolds number value equal to 400 are shown.
- In figure 5.1 pressure drop along the channel is found to be 0.1 bar.
- In figure 5.2 temperature at the outlet of the channel is found to be 313 K
- In figure 5.3 maximum wall temperature is found to be 356 K at the bottom wall of the channel and wall temperature increases in the direction of flow.

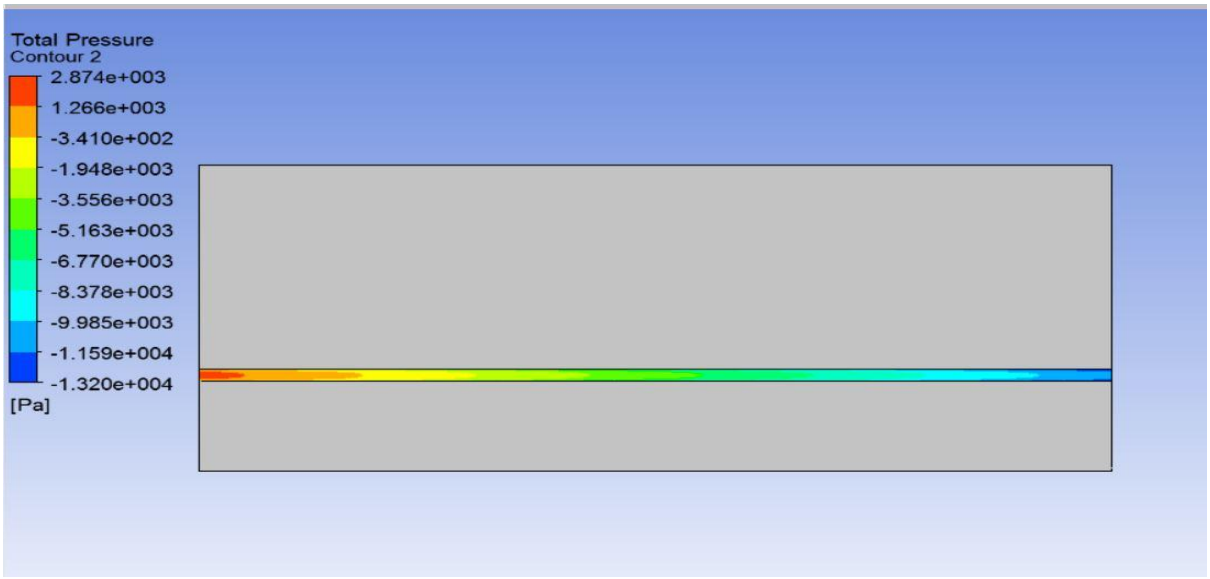

Figure 5.3: pressure contours for water at Re=600

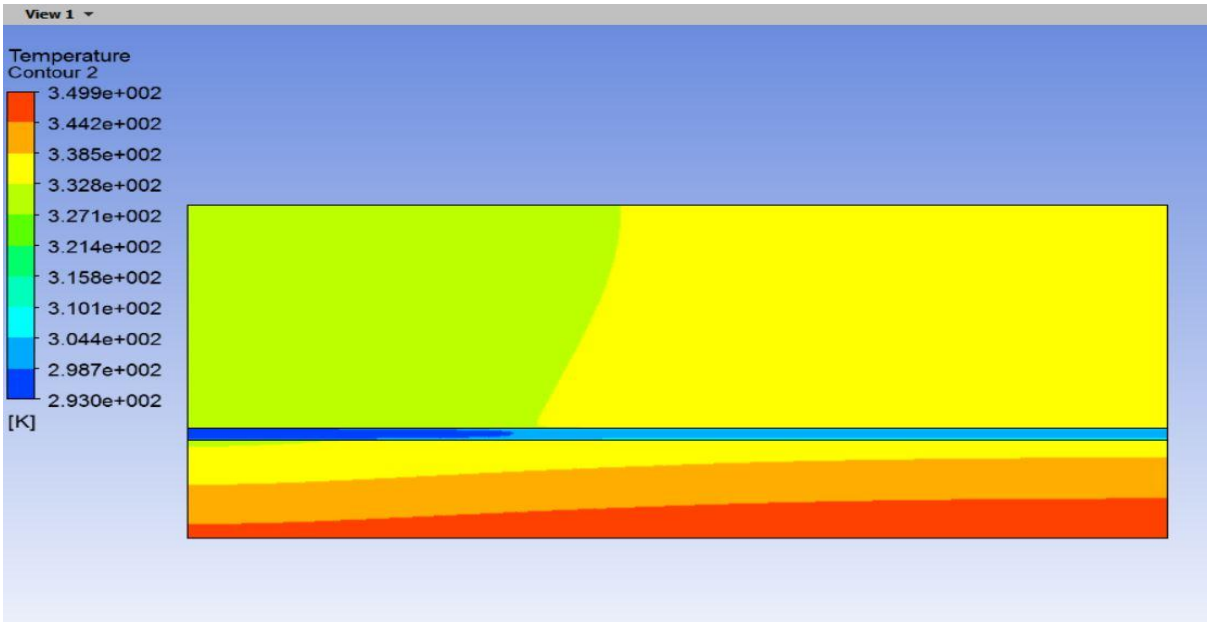

Figure 5.4: Temperature contours for water and heat sink at Re=600

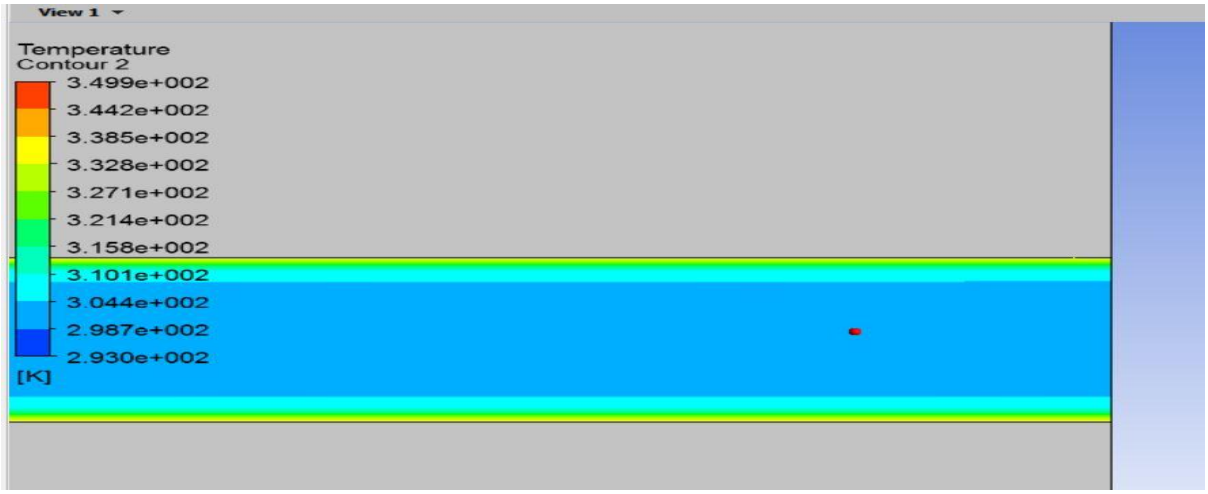

Figure 5.5: Temperature contours at the outlet of the channel at Re=600

- In the figures 5.3 to 5.5, the contours for pressure and temperature in a straight rectangular channel for Reynolds number value equal to 600 are shown.
- In figure 5.3 pressure drop along the channel is found to be 0.16 bar.
- In figure 5.5 temperature at the outlet of the channel is found to be 306.5 K.
- In figure 5.4 maximum wall temperature is found to be 349.8 K at the bottom wall of the channel and wall temperature increases in the direction of flow.

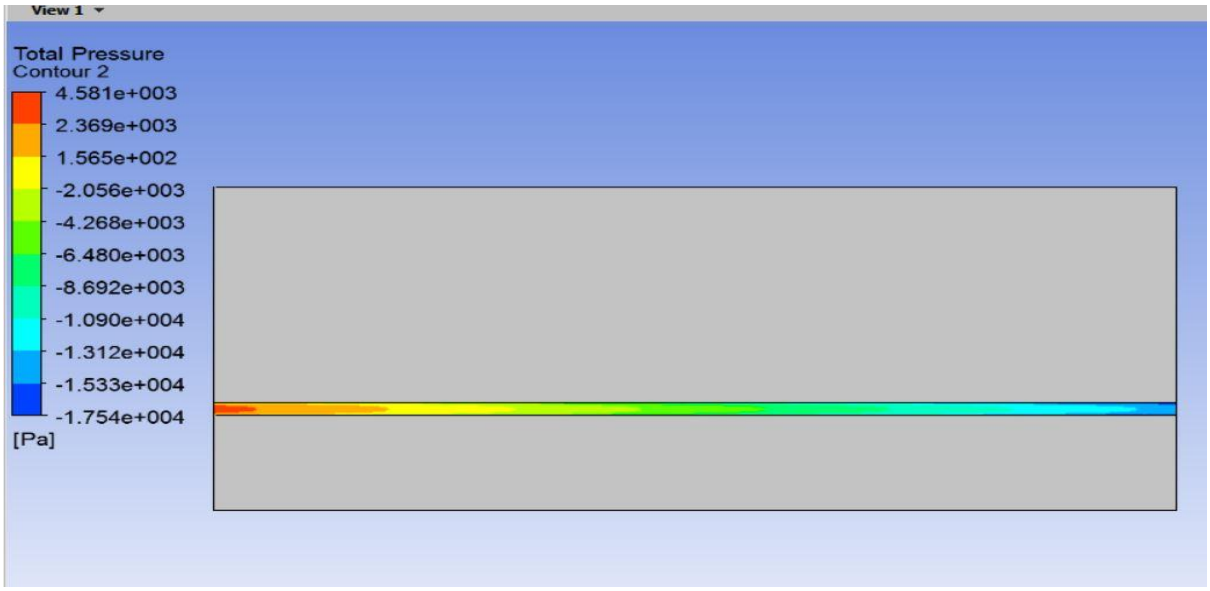

Figure 5.6 : Pressure contours for water at Re=800

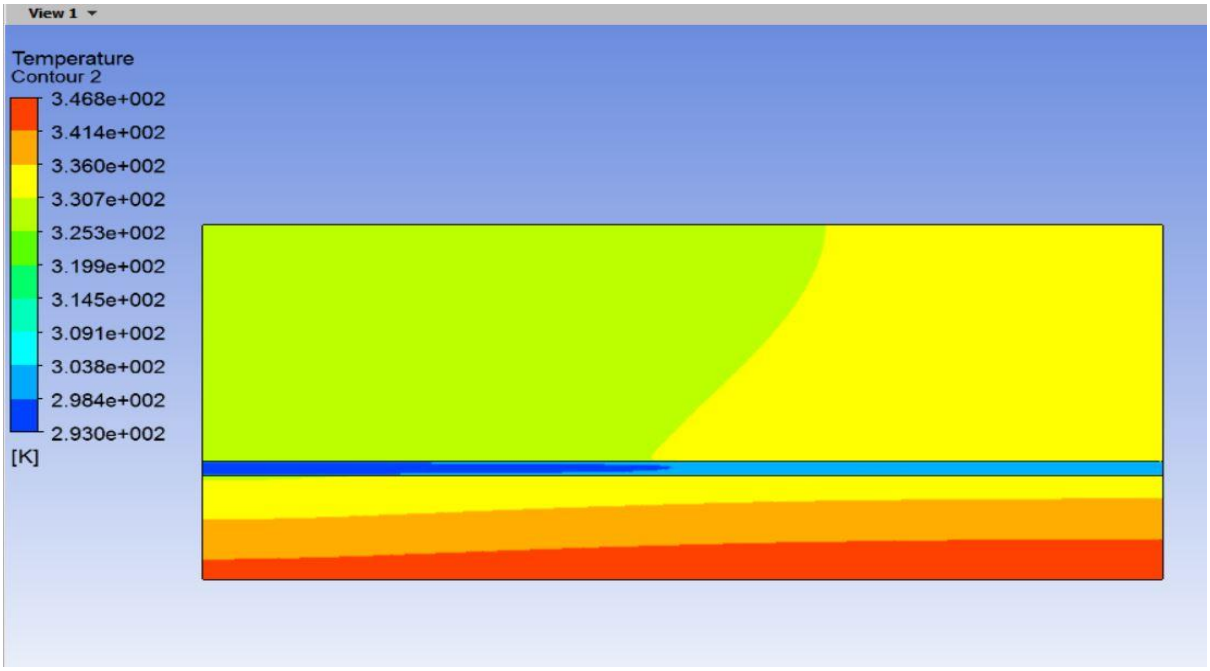

Figure 5.7: Temperature contours for water and heat sink at Re=800

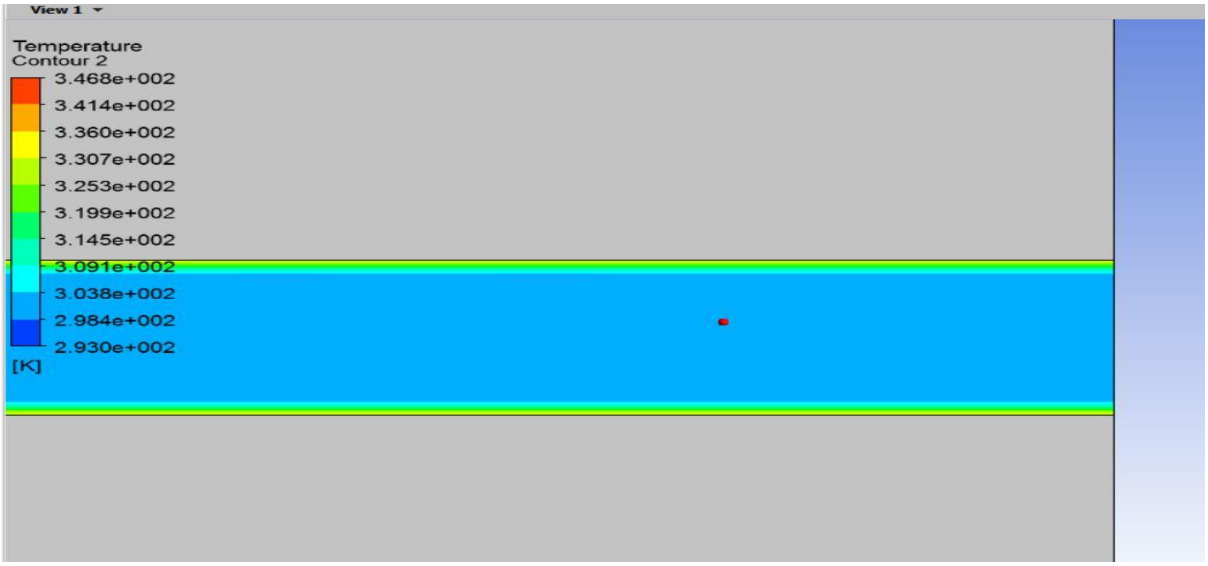

Figure 5.8: Temperature contour for water at channel outlet at Re=800

- In the figures 5.6 to 5.8, the contours for pressure and temperature in a straight rectangular channel for Reynolds number value equal to 800 are shown.
- In figure 5.6 pressure drop along the channel is found to be 0.22 bar.
- In figure 5.8 temperature at the outlet of the channel is found to be 303 K.
- In figure 5.7 maximum wall temperature is found to be 346.8 K at the bottom wall of the channel and wall temperature increases in the direction of flow.

Figure 5.9: Pressure contours for water at Re=1000

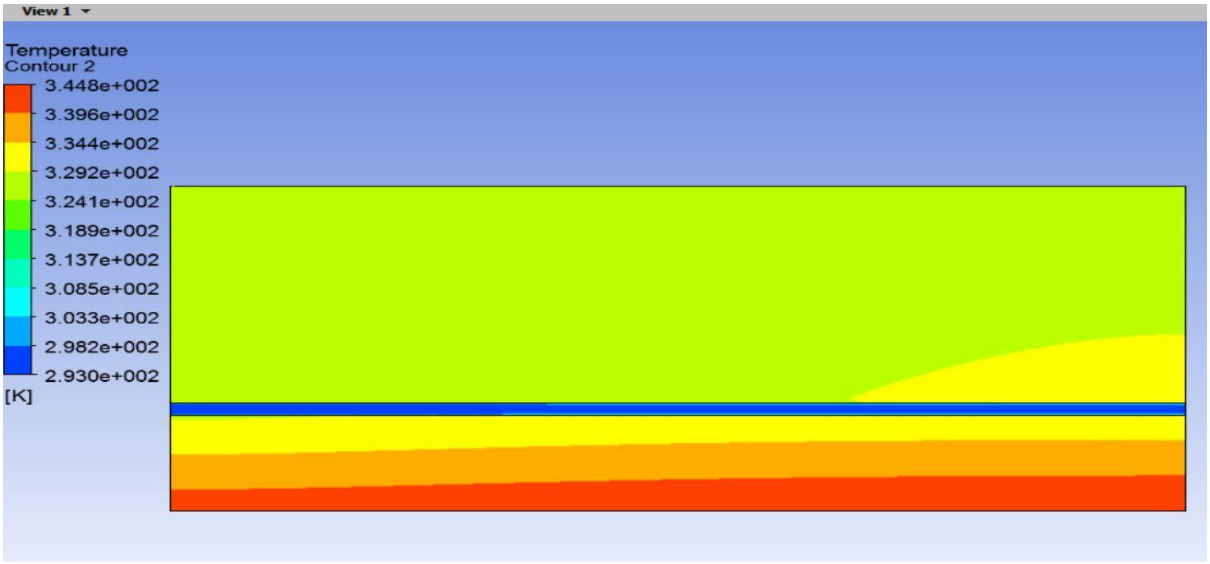

Figure 5.10: Temperature contours for heat sink and water at Re=1000.

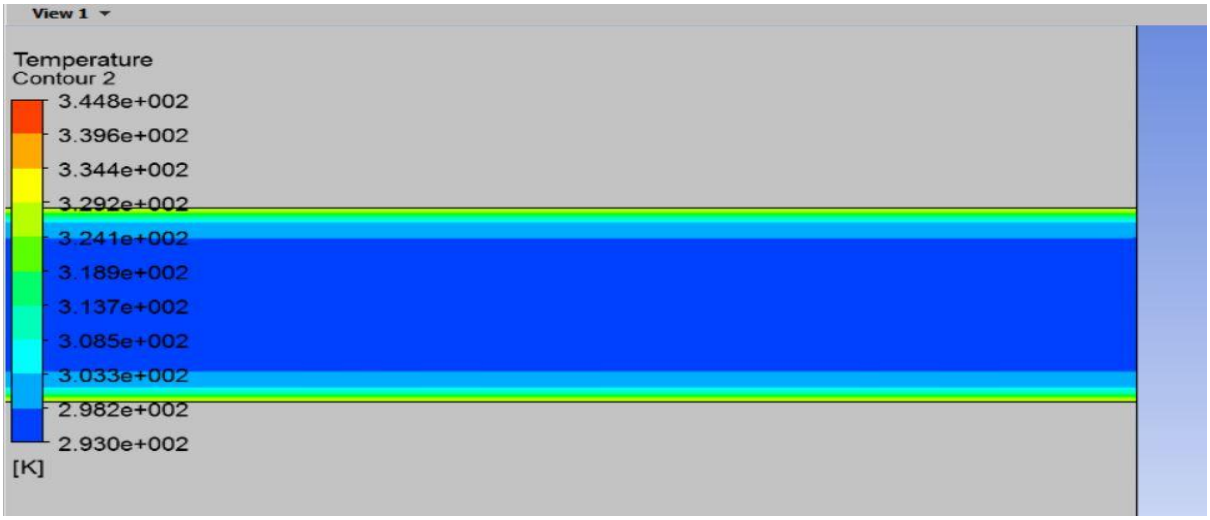

Figure 5.11: Temperature contours for water closer to channel outlet at Re=1000.

- In the figures 5.9 to 5.11, the contours for pressure and temperature in a straight rectangular channel for Reynolds number value equal to 1000 are shown.
- In figure 5.9 pressure drop along the channel is found to be 0.29 bar.
- In figure 5.11 temperature at the outlet of the channel is found to be 298 K.
- In figure 5.10 maximum wall temperature is at the bottom wall of the heat sink and is found to be 344.8 K and the wall temperature increases in the direction of flow.

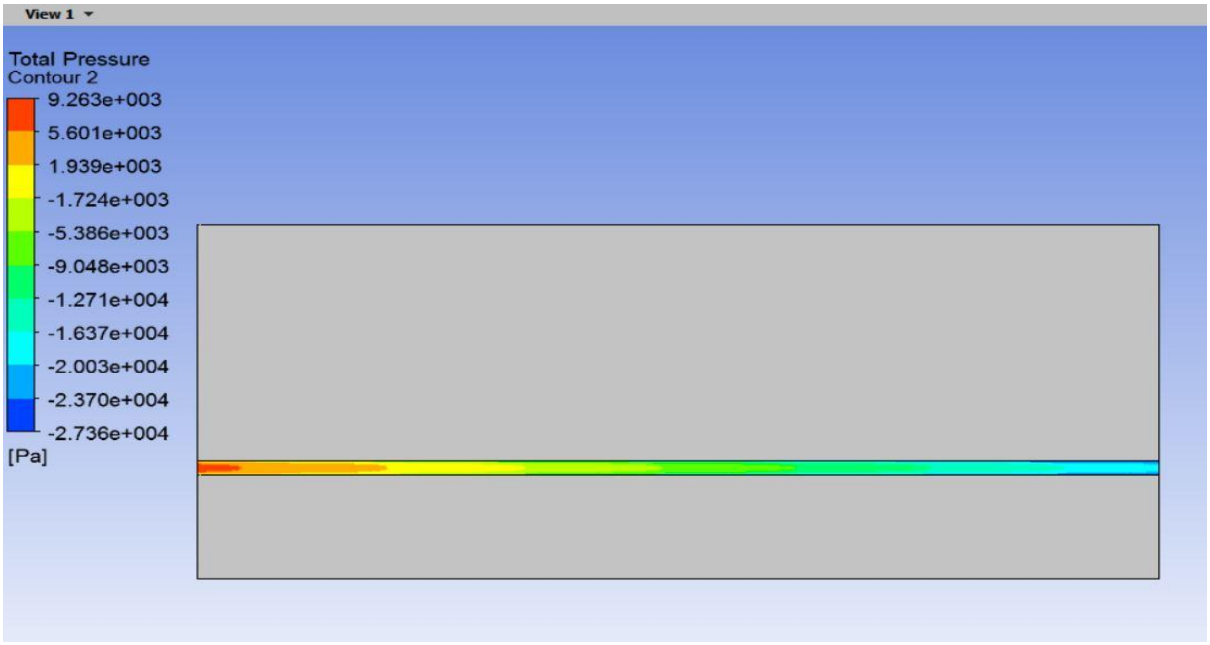

Figure 5.12: Pressure contours for water at Re=1200.

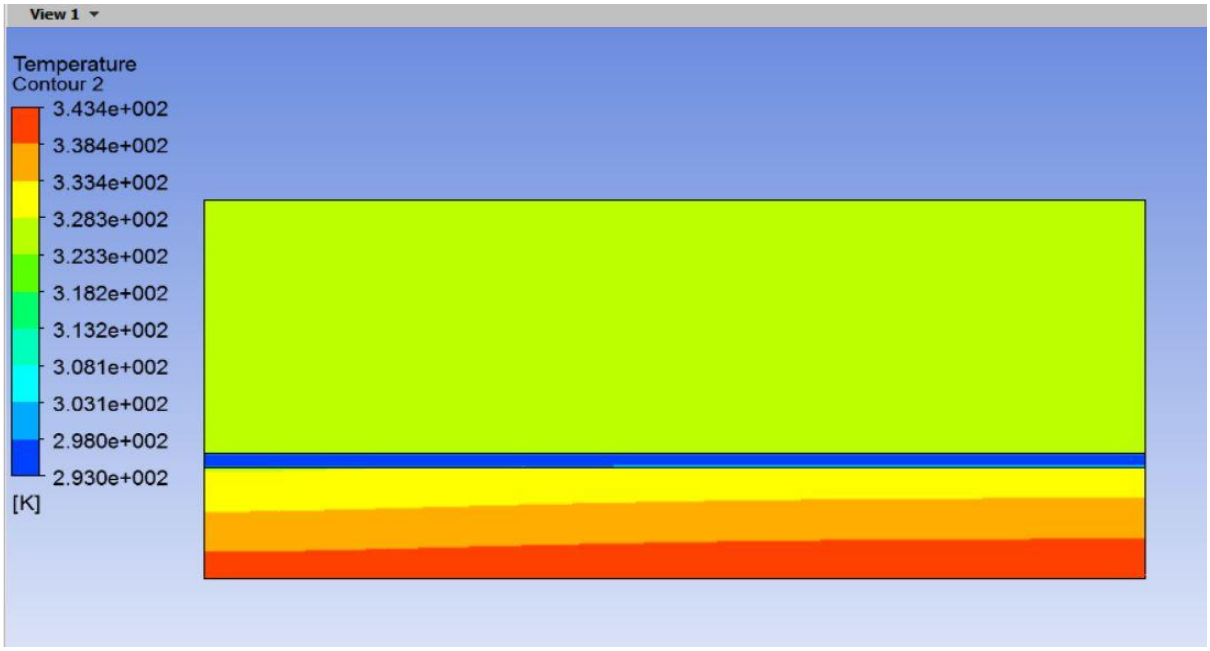

Figure 5.13: Temperature contours for heat sink and channel at Re=1200.

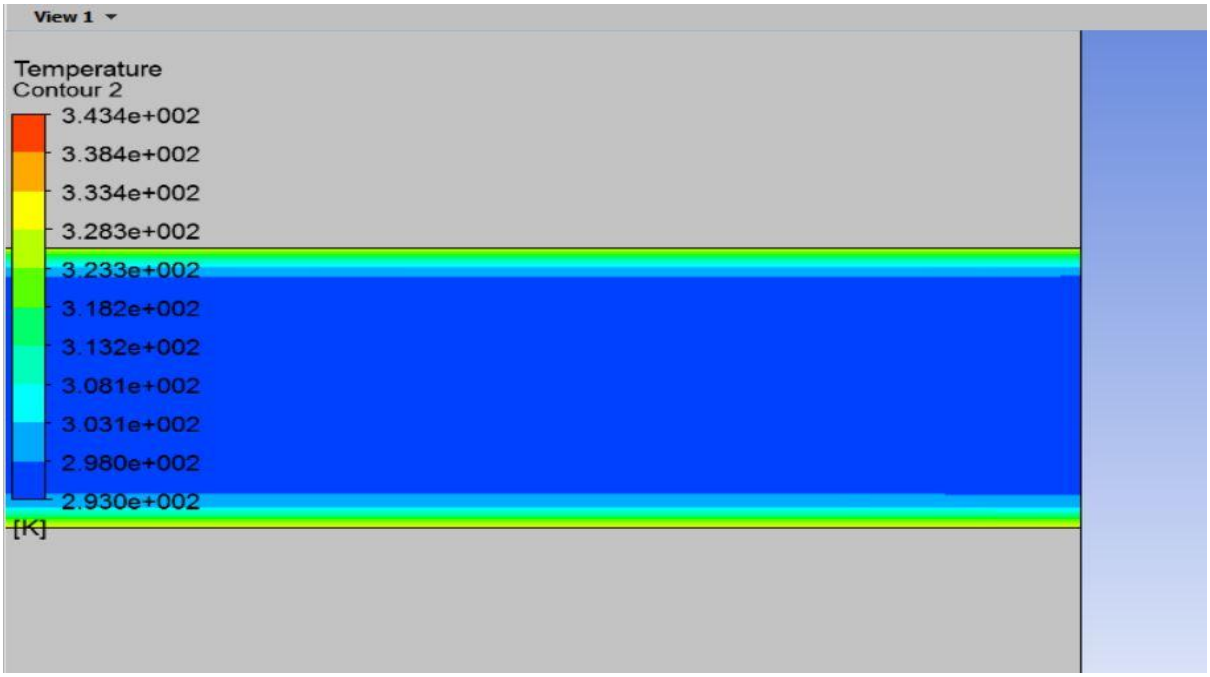

Figure 5.14: Temperature contours of water closer to outlet at Re=1200.

- In the figures 5.12 to 5.14, the contours for pressure and temperature in a straight rectangular channel for Reynolds number value equal to 1000 are shown.
- In figure 5.12 pressure drop along the channel is found to be 0.366 bar.
- In figure 5.14 temperature at the outlet of the channel is found to be 297 K.
- In figure 5.13 maximum wall temperature is at the bottom wall of the heat sink and is found to be 344.8 K and further the wall temperature increases in the direction of flow.

Results for bottom wall heat flux value of 200W/cm^2 and different sets of Reynolds number -

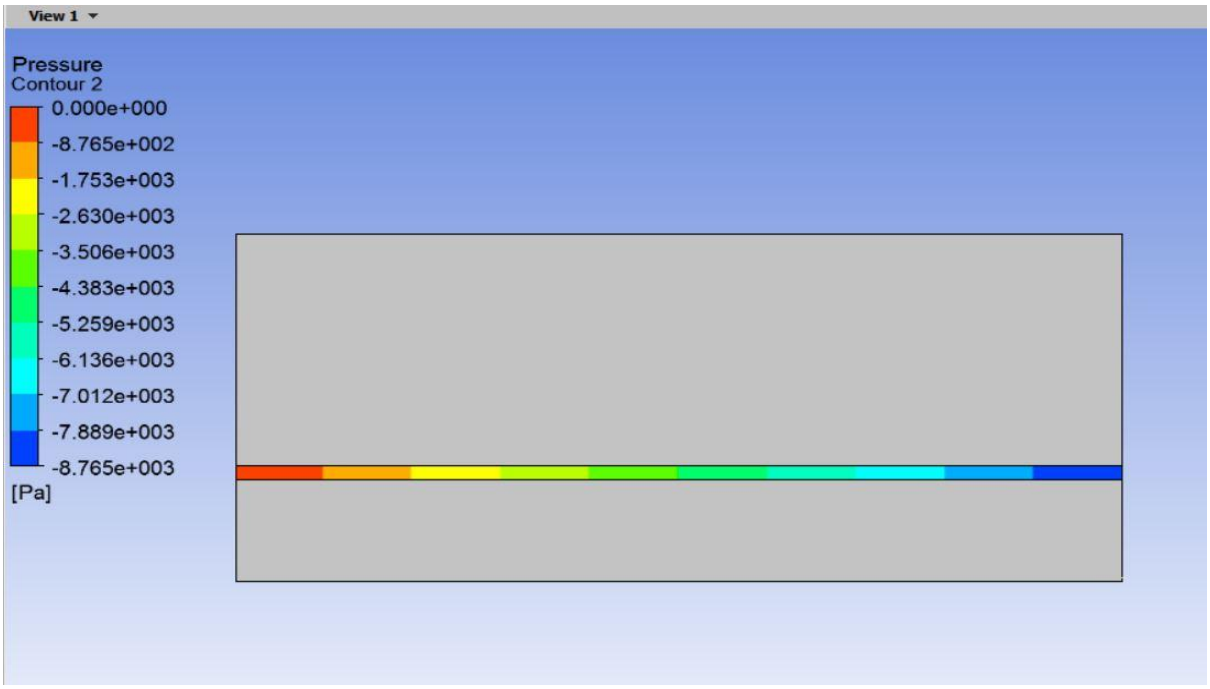

Figure 5.15: Pressure contours for water along channel at Re=400

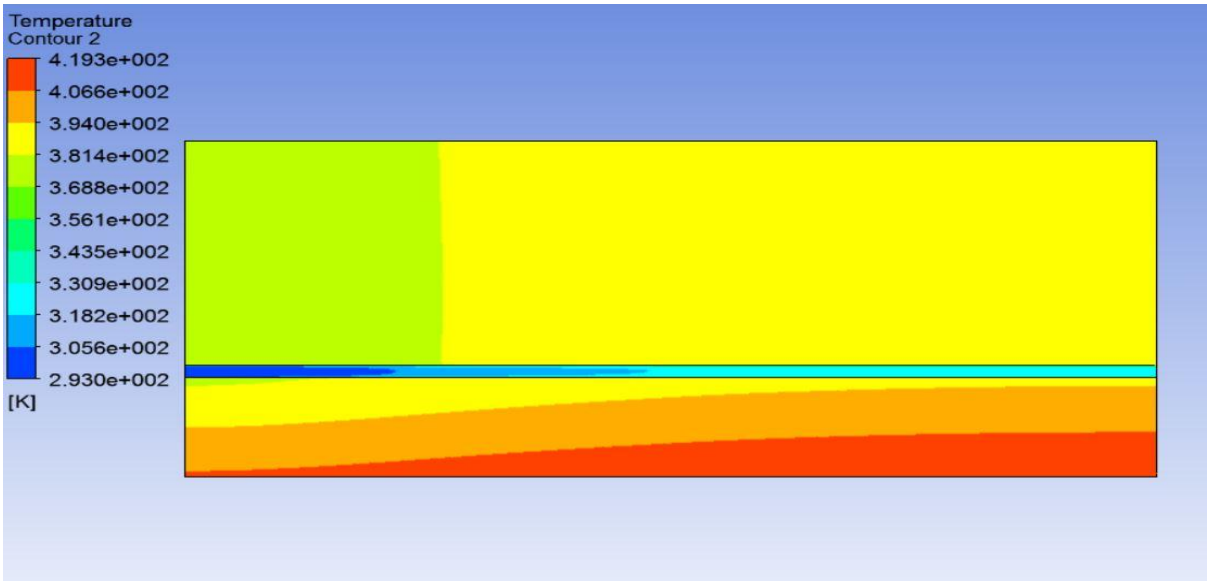

Figure 5.16: Temperature contour for water and heat sink at Re=400

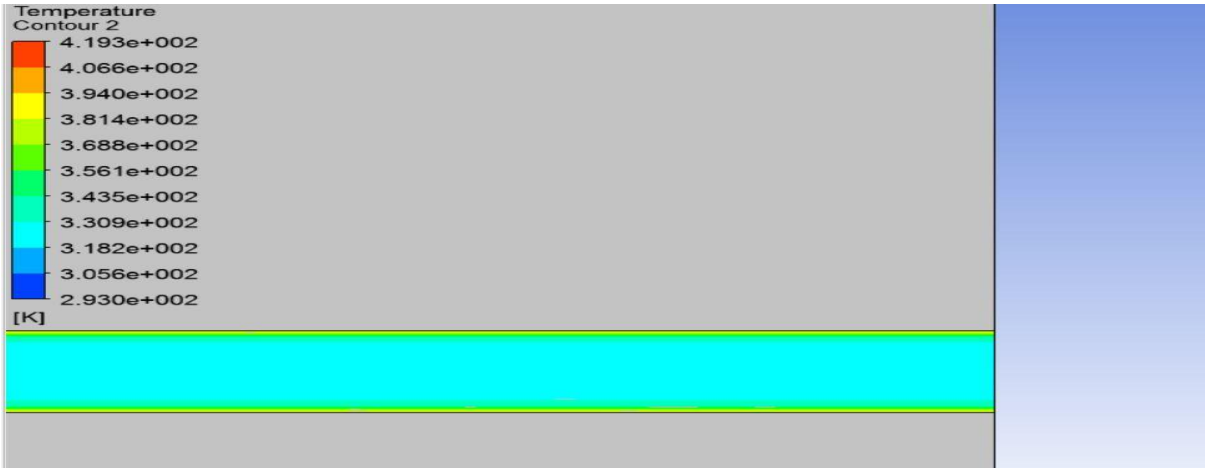

Figure 5.17: Temperature contour at the outlet of channel at Re=400

- In the figures 5.15 to 5.17, the contours for pressure and temperature in a straight rectangular channel for Reynolds number value equal to 400 are shown.
- In figure 5.15 pressure drop along the channel is found to be 0.087 bar.
- In figure 5.17 temperature at the outlet of the channel is found to be 335 K.
- In figure 5.16 maximum wall temperature is at the bottom wall of the heat sink and is found to be 419.3K and further the wall temperature increases in the direction of flow.

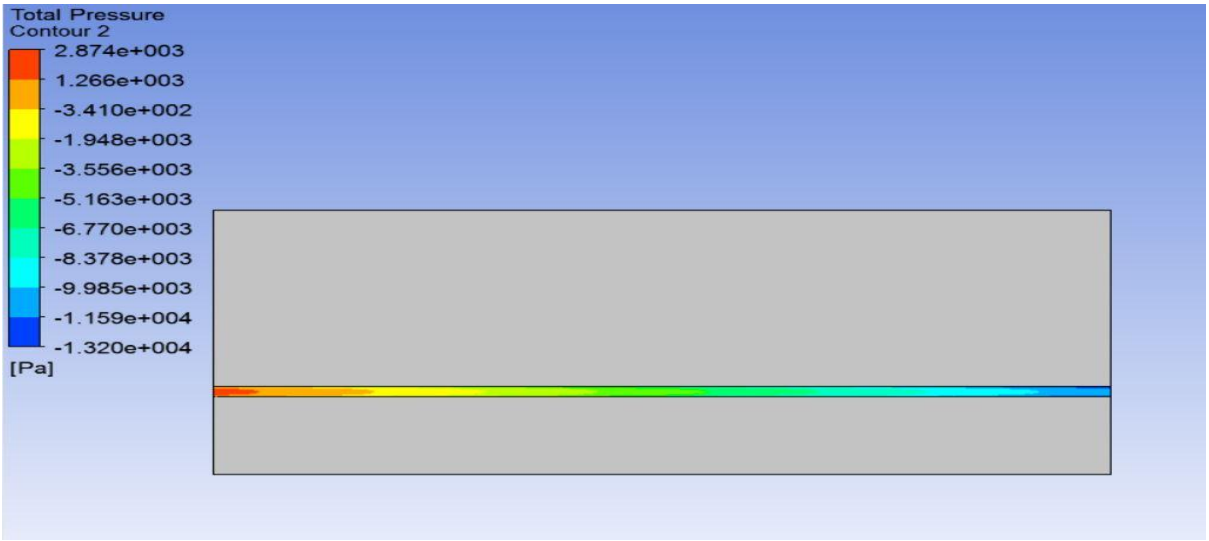

Figure 5.18: Pressure contours for water along the channel at Re=600

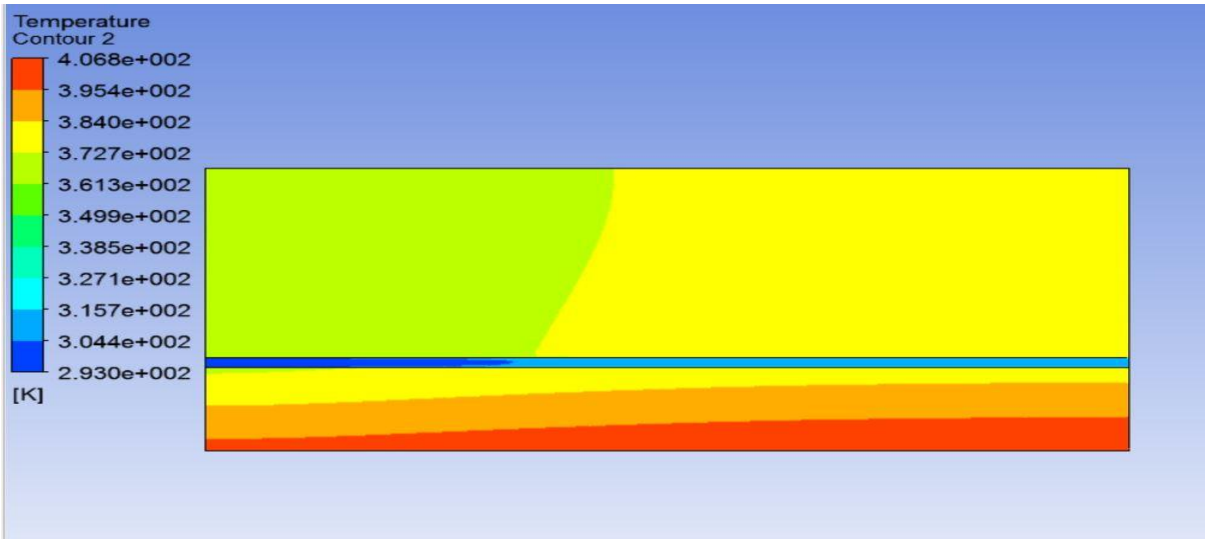

Figure 5.19: Temperature contours for sink wall and water channel at Re=600

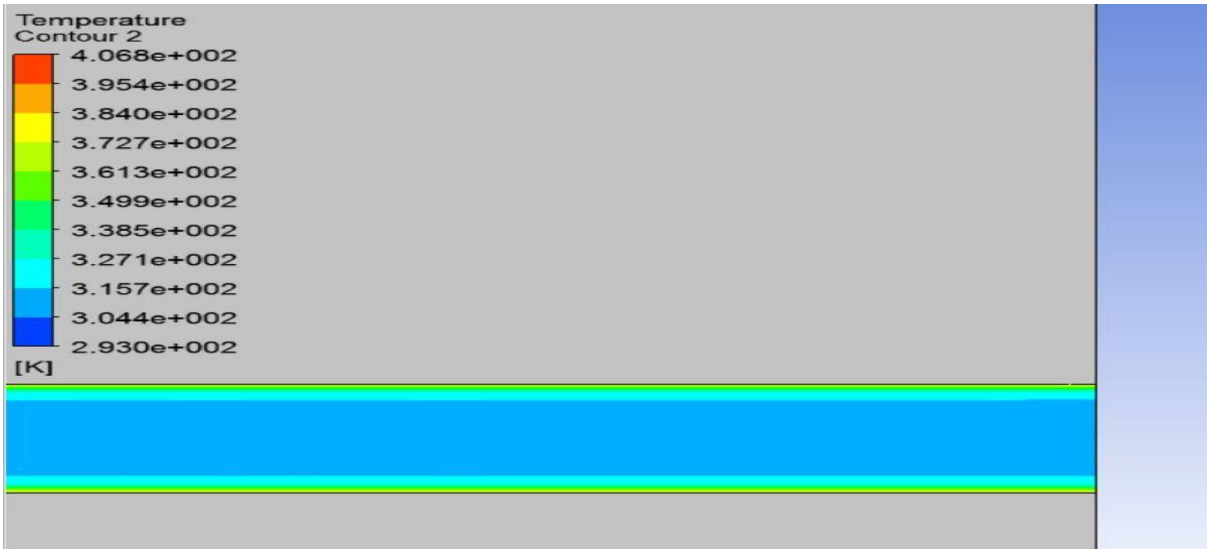

Figure 5.20: Temperature contours of water closer to outlet of channel at Re=600

- In the figures 5.18 to 5.20, the contours for pressure and temperature in a straight rectangular channel for Reynolds number value equal to 600 are shown.
- In figure 5.18 pressure drop along the channel is found to be 0.16 bar.
- In figure 5.20 temperature at the outlet of the channel is found to be 318 K.
- In figure 5.19 maximum wall temperature is at the bottom wall of the heat sink and is found to be 406.8 K and further the wall temperature increases in the direction of flow.

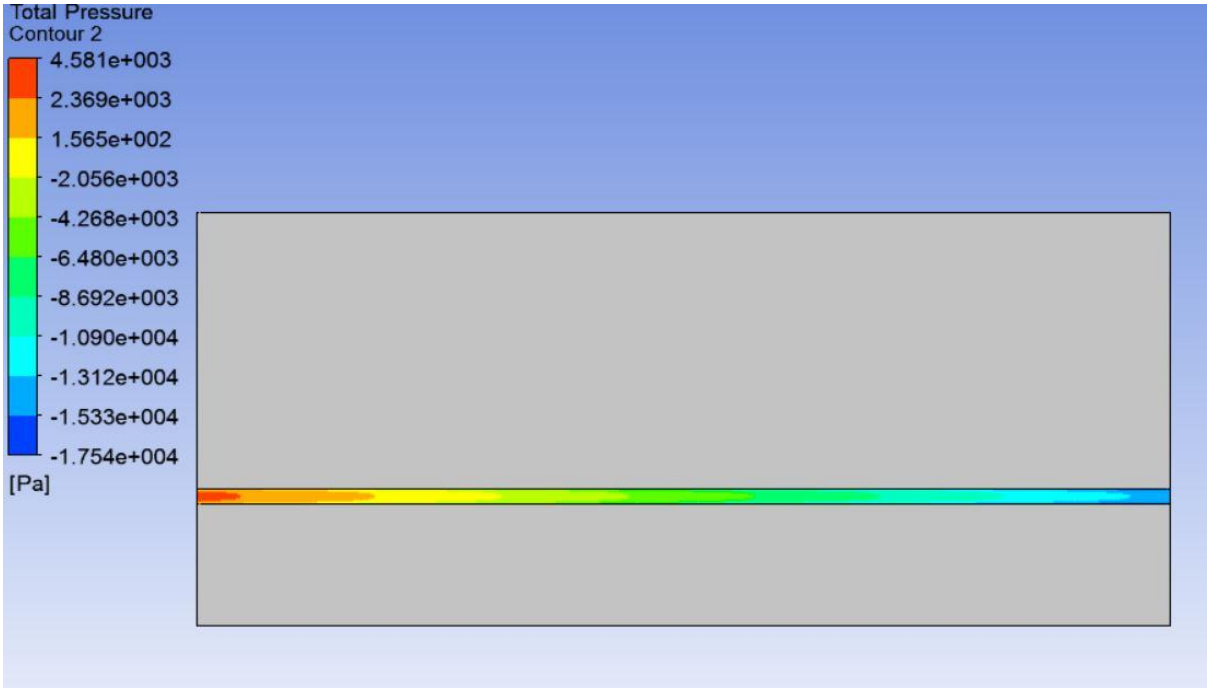

Figure 5.21: Pressure contours for water along channel at Re =800

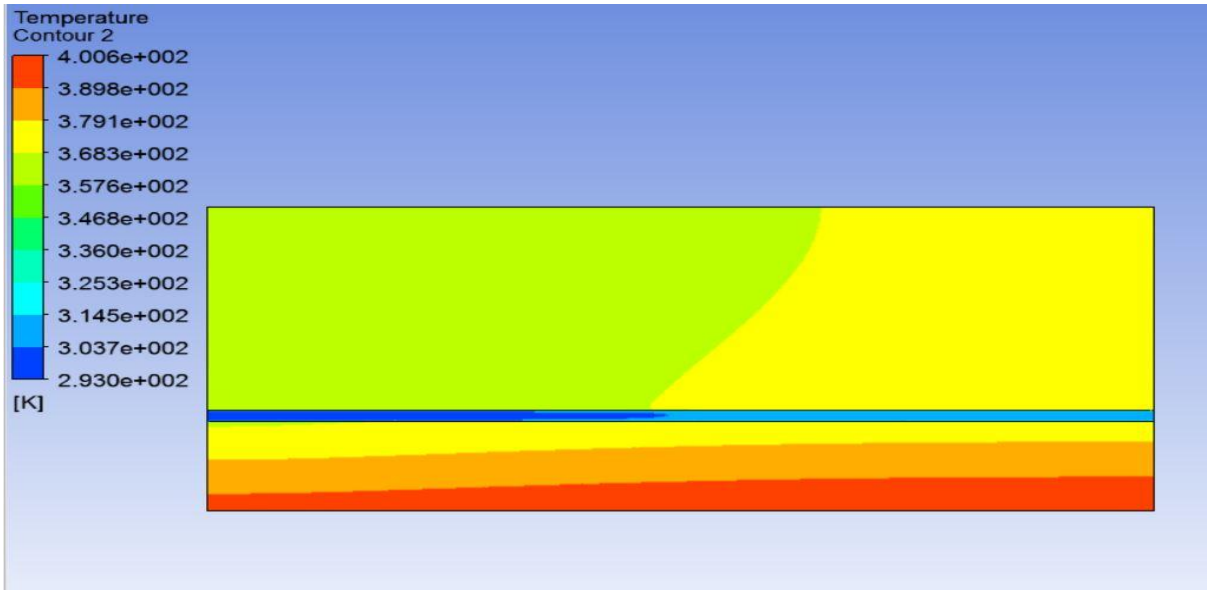

Figure 5.22: Temperature contours for heat sink and water along channel at Re=800

Figure 5.23: Temperature contour of water closer to outlet at Re=800

- In the figures 5.21 to 5.23, the contours for velocity, pressure and temperature in a straight rectangular channel for Reynolds number value equal to 800 are shown.
- In figure 5.21 pressure drop along the channel is found to be 0.22 bar.
- In figure 5.23 temperature at the outlet of the channel is found to be 314.5 K.
- In figure 5.22 maximum wall temperature is at the bottom wall of the heat sink and is found to be 406 K and further the wall temperature increases in the direction of flow.

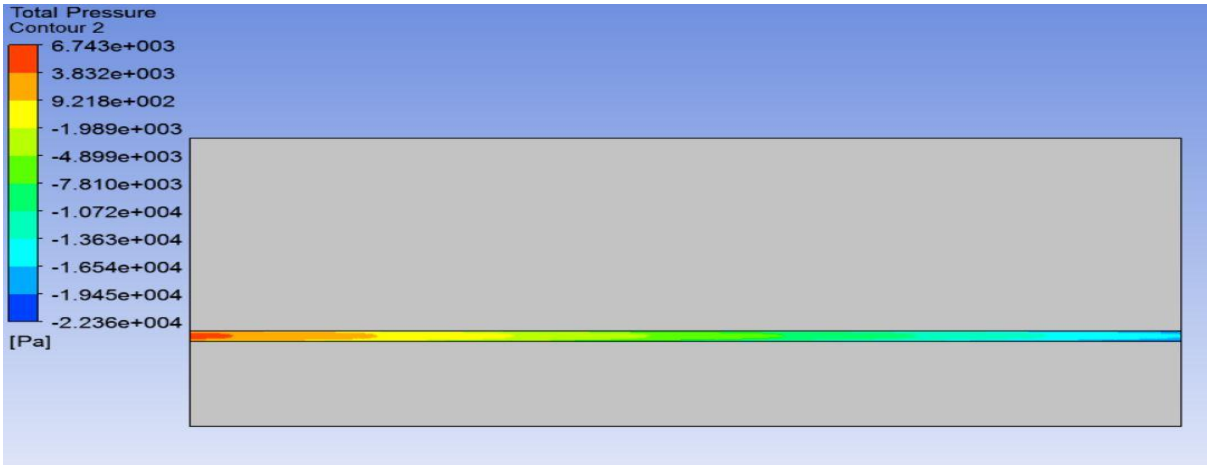

Figure 5.24: Pressure contour for water along the channel at Re=1000

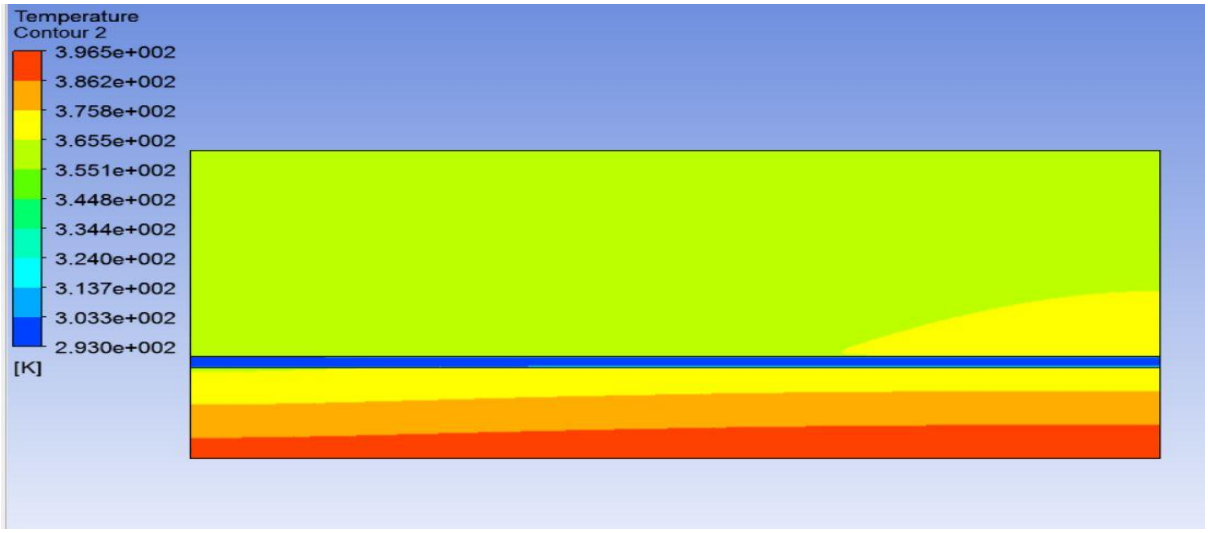

Figure 5.25: Temperature contour for water and heat sink at Re=1000.

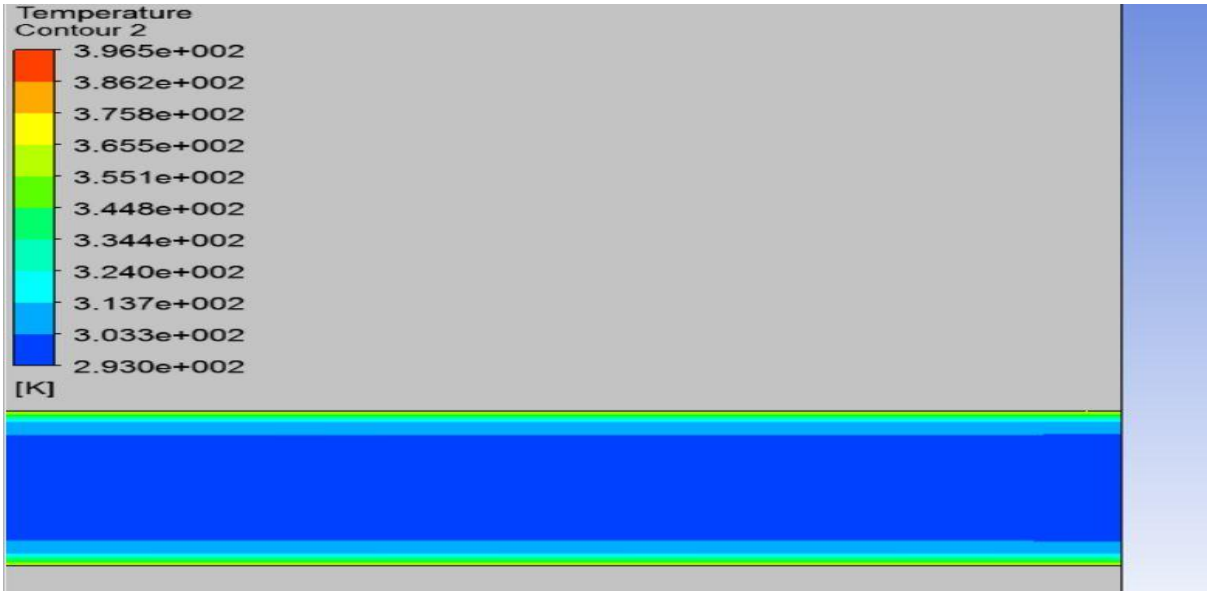

Figure 5.26: Temperature contour of water close to outlet of channel at Re=1000

- In the figures 5.24 to 5.26, the contours for velocity, pressure and temperature in a straight rectangular channel for Reynolds number value equal to 1000 are shown.
- In figure 5.24 pressure drop along the channel is found to be 0.28 bar.
- In figure 5.26 temperature at the outlet of the channel is found to be 307 K.
- In figure 5.25 maximum wall temperature is at the bottom wall of the heat sink and is found to be 396.5 K and further the wall temperature increases in the direction of flow.

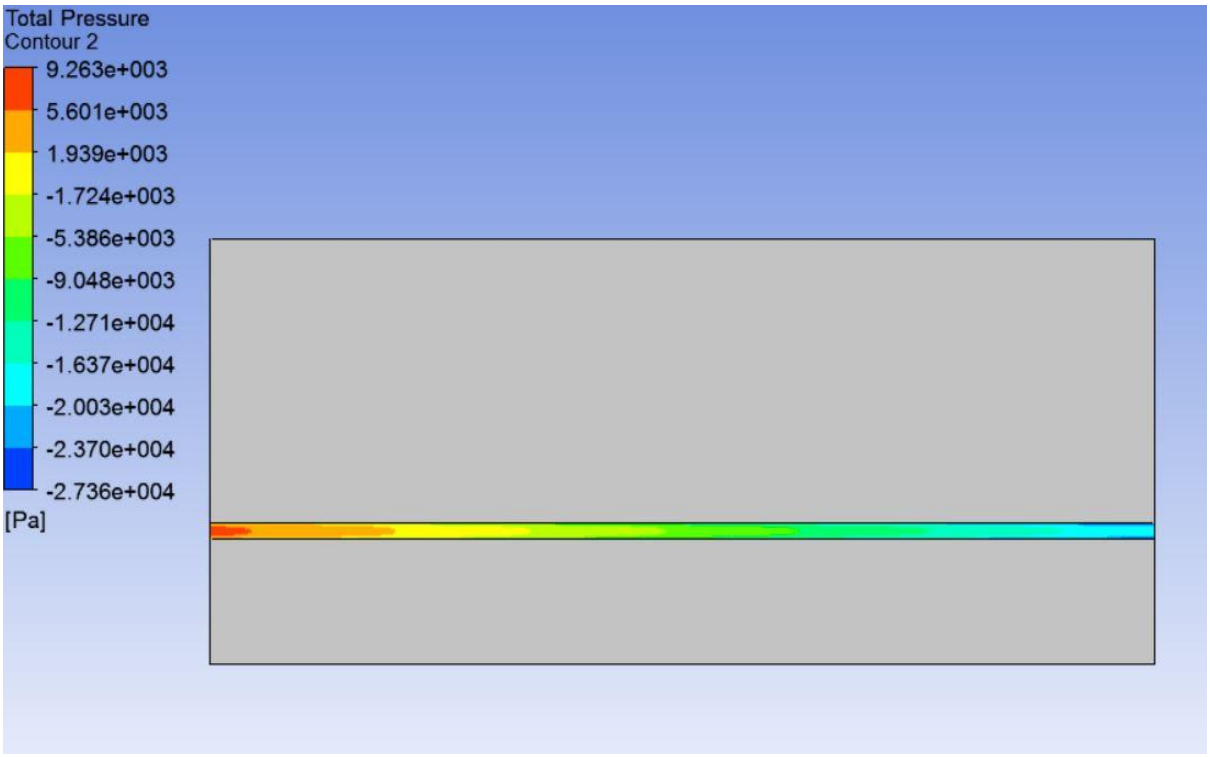

Figure 5.27: Pressure contour along channel at Re=1200.

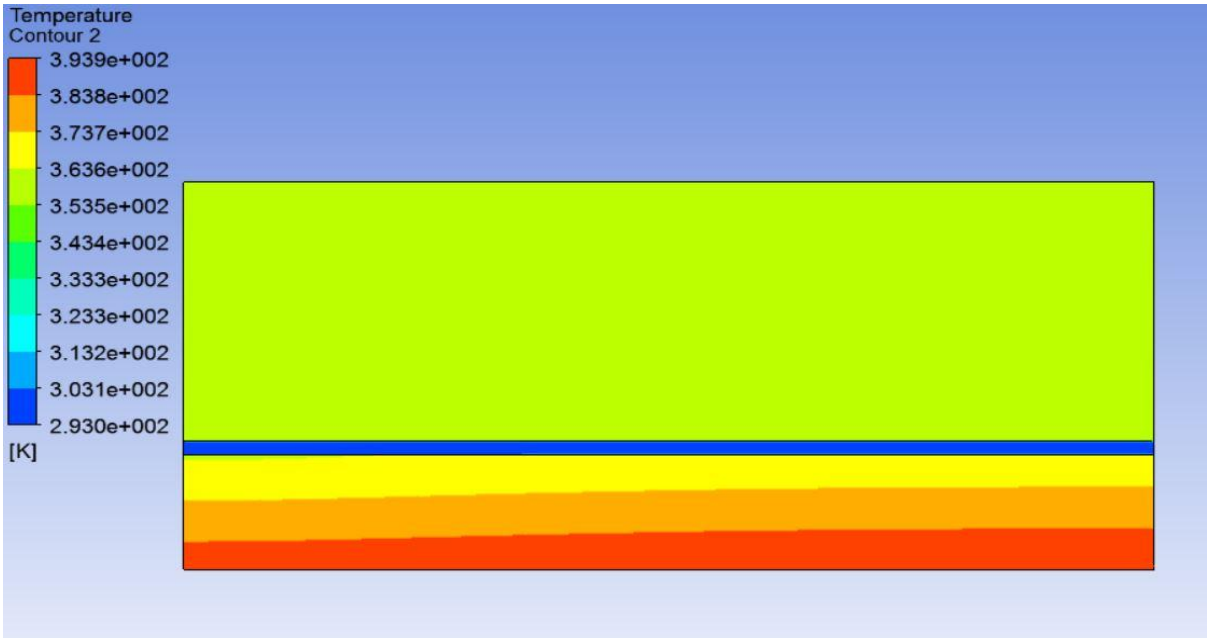

Figure 5.28: Temperature contour along channel and heat sink at Re=1200

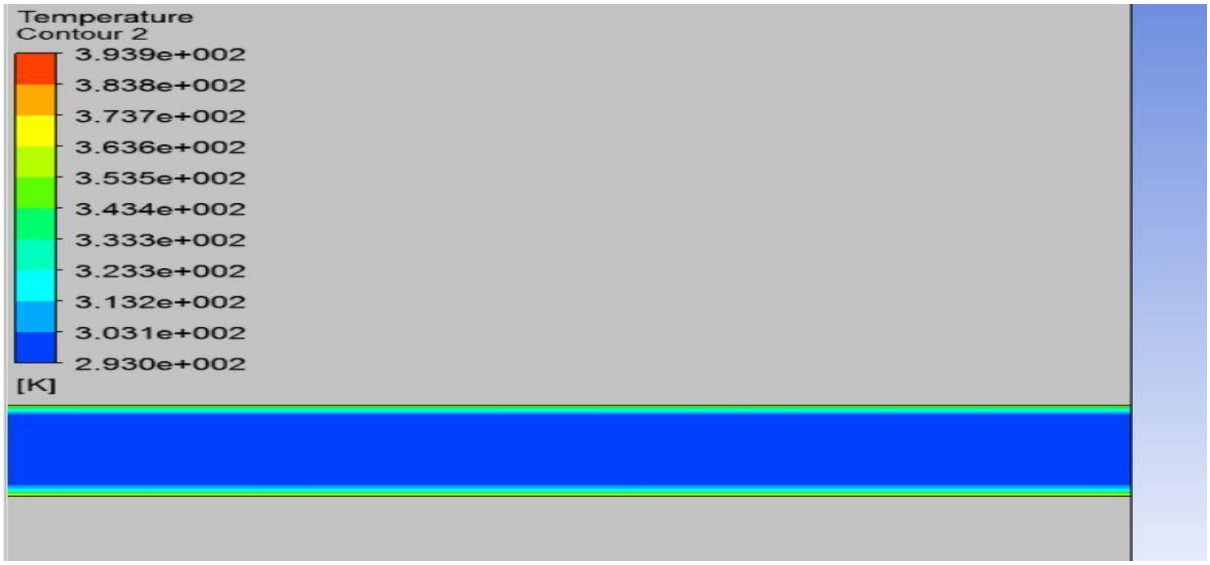

Figure 5.29: Temperature contours for water closer to outlet of channel at Re=1200.

In the figures 5.27 to 5.29, the contours for velocity, pressure and temperature in a straight rectangular channel for Reynolds number value equal to 1200 are shown.

- In figure 5.27 pressure drop along the channel is found to be 0.28 bar.
- In figure 5.29 temperature at the outlet of the channel is found to be 307 K.
- In figure 5.28 maximum wall temperature is at the bottom wall of the heat sink and is found to be 396.5 K and further the wall temperature increases in the direction of flow.

5.2 Problem validation-

Case 1-

For the validation of the problem, the experimental pressure drop along the channel is compared with the computational pressure drop. The computational pressure drop from the pressure contours generated for different values of Reynolds number for 100W/cm^2 bottom wall heat flux are taken from figures 5.1, 5.3, 5.6, 5.9 and 5.12 respectively and for 200W/ cm^2 bottom wall heat flux are taken form figures 5.15, 5.18, 5.21, 5.24, 5.27 respectively.

Table 9: Bottom wall heat flux value=100W/cm^2

Reynolds number	Experimental pressure drop (bar)	Computational pressure drop (bar)
400	0.10	0.11
600	0.17	0.15
800	0.23	0.22
1000	0.32	0.29
1200	0.41	0.366

Table -10: Bottom wall heat flux value=200W/cm^2

Reynolds number	Experimental pressure drop(bar)	Computational pressure drop (bar)
400	0.08	0.10
600	0.15	0.16
800	0.21	0.22
1000	0.30	0.291
1200	0.40	0.37

From table 9 and table 10 the values of computational pressure drop for heat flux values of 100W/cm^2 and 200W/cm^2 are found to be in close agreement with the experimental pressure

drop. Hence ,the computational model is successfully validated on the basis of pressure drop along the channel length.

Case 2- For further validation the experimental temperature rise is compared with the computational temperature rise. The computational temperature rise taken from temperature contours generated for different values of Reynolds number for 100W/cm^2 bottom wall heat flux are taken from figures 5.2, 5.5, 5.8, 5.11 and 5.14 respectively and for 200W/cm^2 are taken from figures 5.17, 5.20, 5.23, 5.26, 5.29 respectively.

Table 11: Bottom wall heat flux value=100W/cm^2

Reynolds number	Experimental temperature rise (°C)	Computational temperature rise (°C)
400	22	20
600	16	14
800	10	10
1000	8	6
1200	6	4

Table 12: Bottom wall heat flux of 200 W/cm^2

Reynolds number	Experimental temperature rise (°C)	Computational temperature rise (°C)
400	44	43
600	31	28
800	22	22
1000	18	16
1200	15	14

From table 11 and table 12 the values of computational temperature rise for heat flux values of 100W/cm^2 and 200W/cm^2 are found to be in close agreement with the experimental temperature rise. Hence, the computational model is successfully validated on the basis of temperature rise along the length of channel.

5.3 Graphical validation –

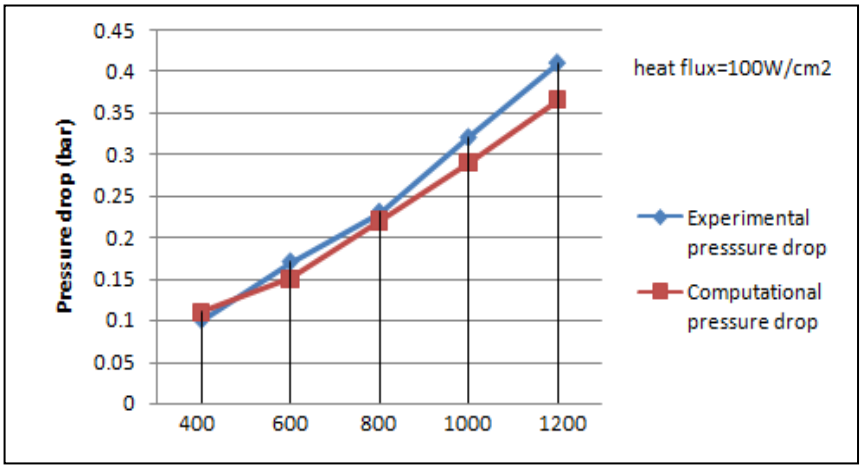

Figure 5.30: Pressure drop vs Reynolds number

Figure 5.30 shows the comparison of experimental and numerical pressure drop results for varying sets of Reynolds number for heat flux =100W/cm^2

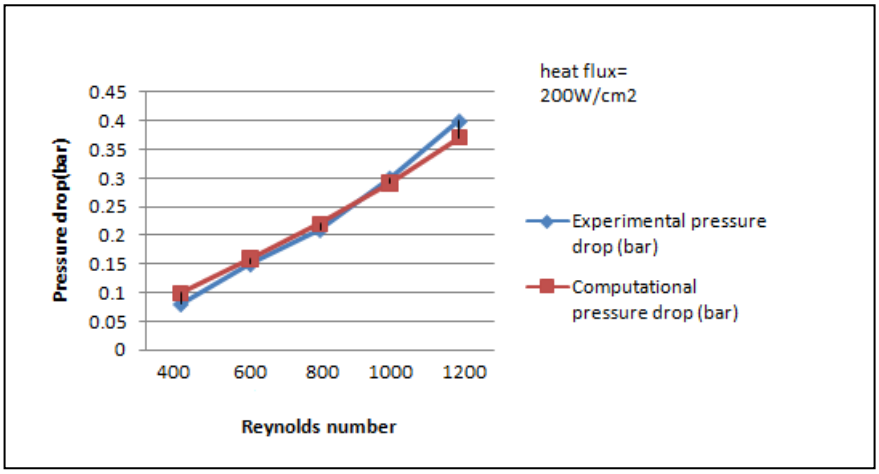

Figure 5.31: pressure drop vs Reynolds number

Figure 5.31 shows comparison of experimental and numerical pressure drop results for varying sets of Reynolds number for heat flux=200W/cm^2.

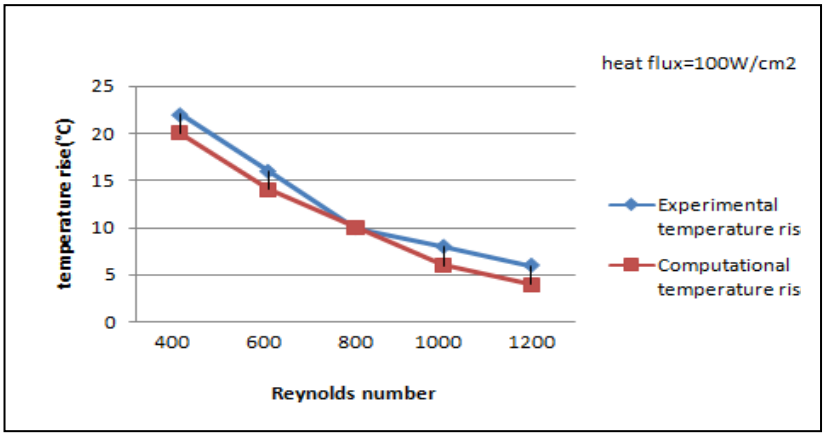

Figure 5.32: Temperature rise vs Reynolds number

Figure 5.32 shows the comparison of experimental and numerical temperature rise results for varying sets of Reynolds number for heat flux =100W/cm^2

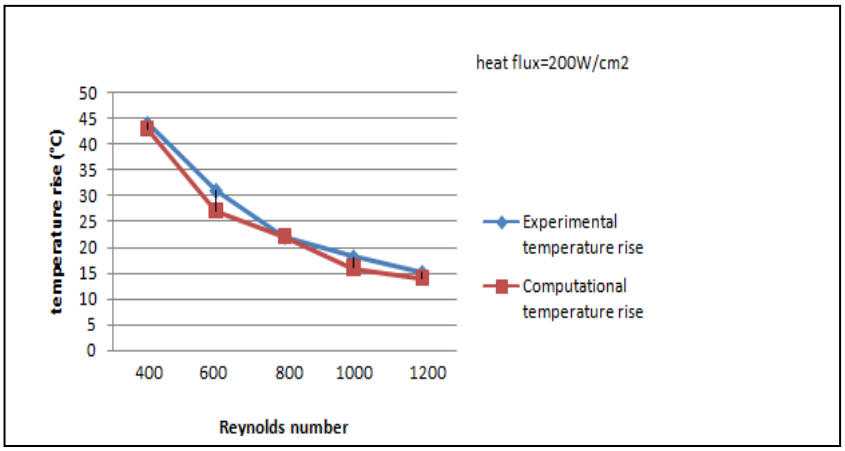

Figure 5.33: Temperature rise vs Reynolds number

Figure 5.33 shows the comparison of experimental and numerical temperature rise results for varying sets of Reynolds number for heat flux =200W/cm^2

CHAPTER 6

SIMULATION RESULTS

6.1 Simulation results for wavy type of channel-

In the following computational fluid dynamics analysis the results are plotted for pressure drop and heat transfer in wavy edge type rectangular micro-channel for two different values of heat fluxes applied at the bottom of the heat sink for varying set of values of Reynolds number. The value of heat flux used in the analysis are 100W/$cm^2$and 200W/cm^2. Five values of Reynolds number are taken for the analysis which are 400, 600, 800, 1000 and 1200 respectively.

Results for heat flux= 100W/$cm^2$for different sets of Reynolds number -

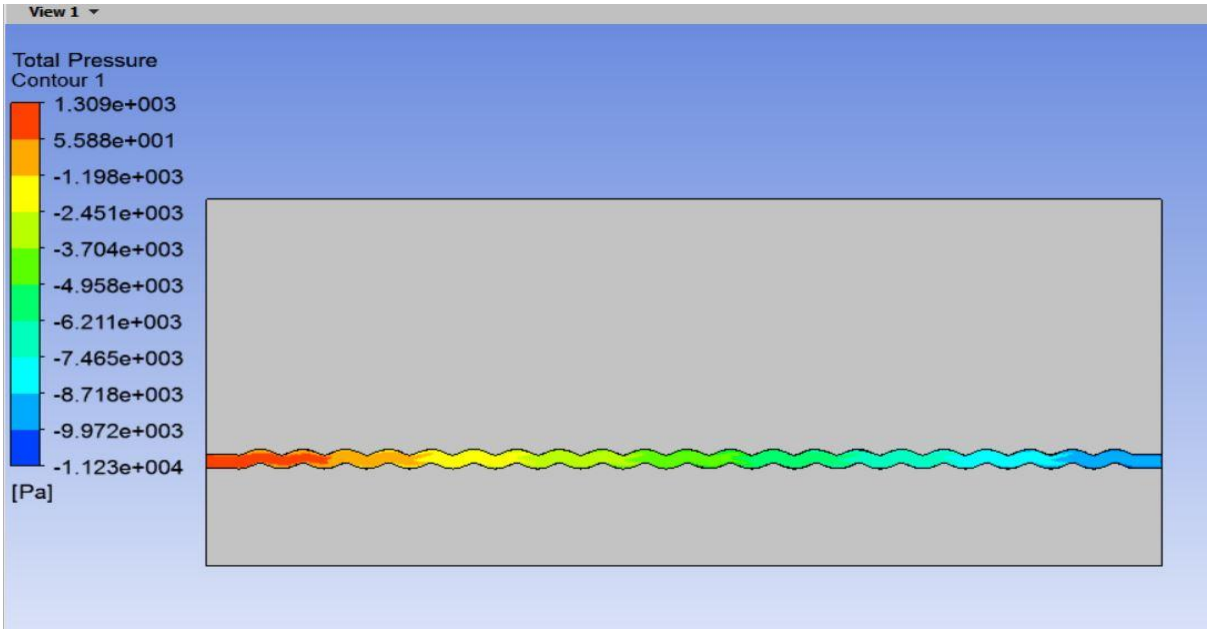

Figure 6.1: Pressure contour of water along wavy channel at Re=400.

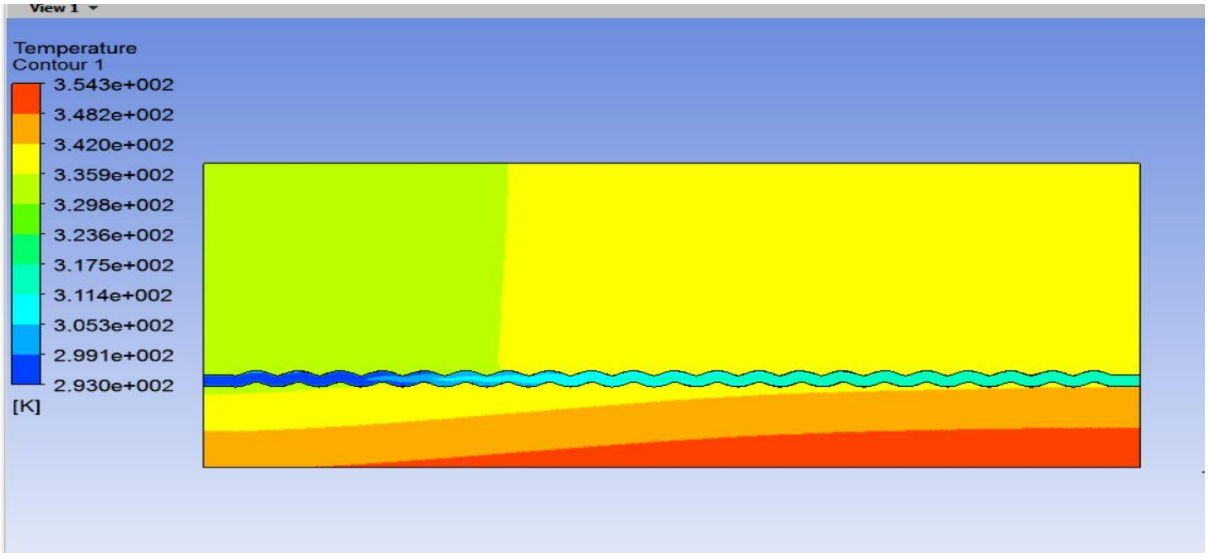

Figure 6.2: Temperature contours of water and heat sink for wavy channel at Re=400.

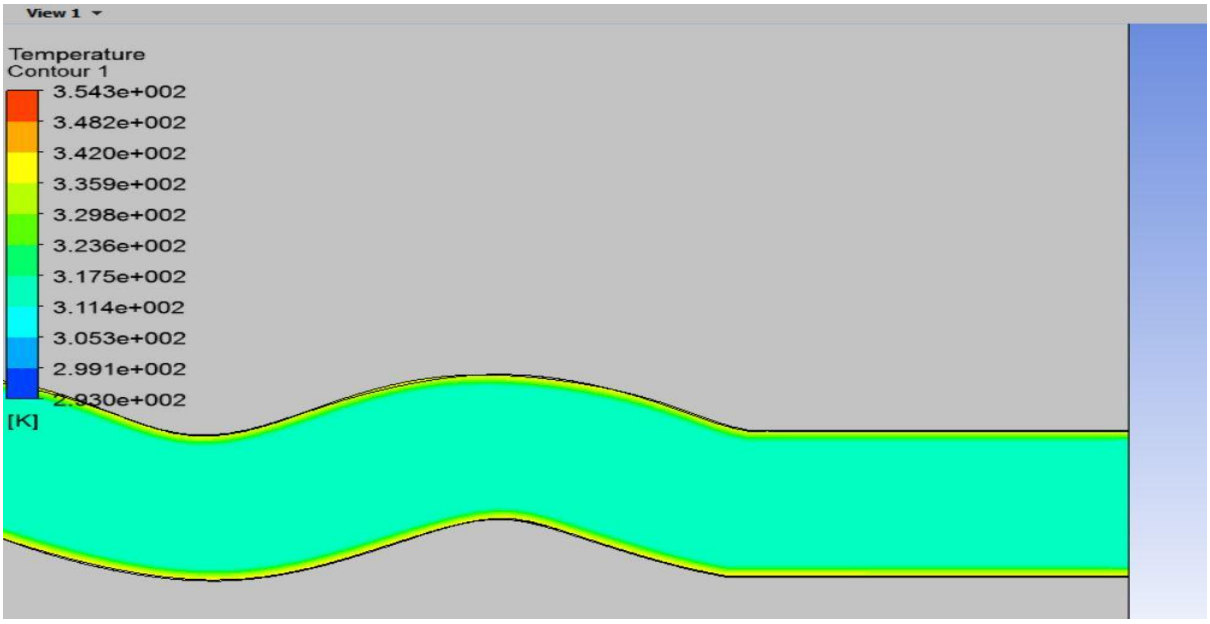

Figure 6.3: Temperature contour at the outlet of wavy channel at Re=400.

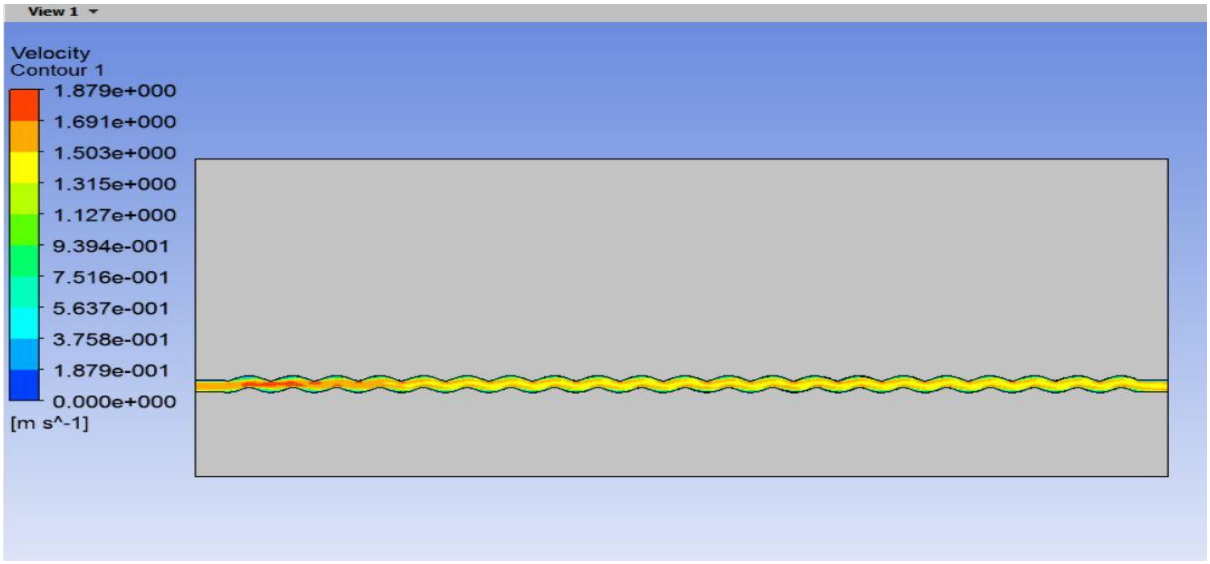

Figure 6.4: velocity contour along wavy channel at Re=400.

In the figures 6.1 to 6.4, the contours for pressure, temperature and velocity in a wavy edge rectangular channel for Reynolds number value equal to 400 are shown.

- In figure 6.1 Pressure drop along the channel is found to be 0.125 bar.
- In figure 6.3 Temperature at the outlet of the channel is found to be 318 K.
- In figure 6.2 Maximum wall temperature is at the bottom wall of the heat sink and is found to be 354.4 K and further the wall temperature increases in the direction of flow.

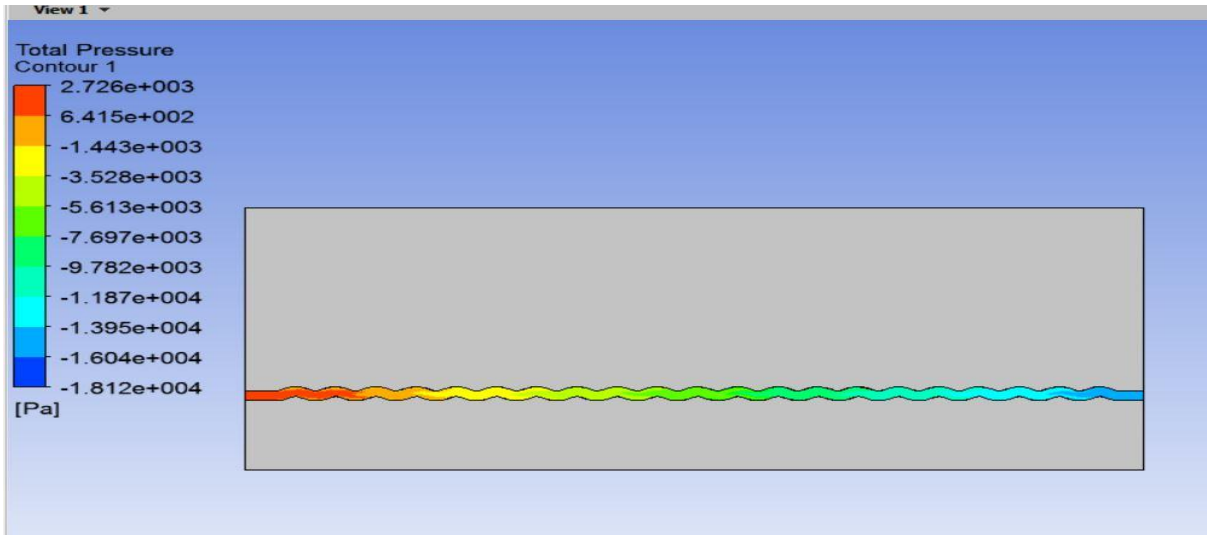

Figure 6.5: Pressure contour of water along wavy channel at Re=600

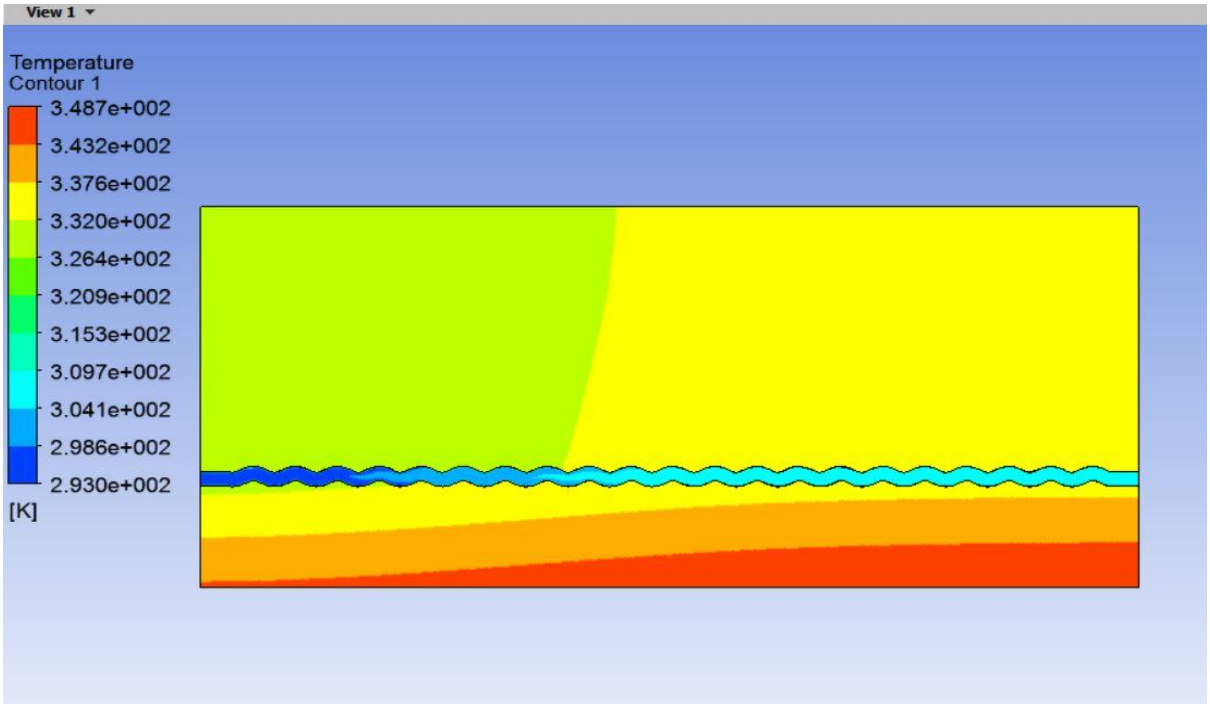

Figure 6.6: Temperature contours for heat sink and water along wavy channel at Re=600

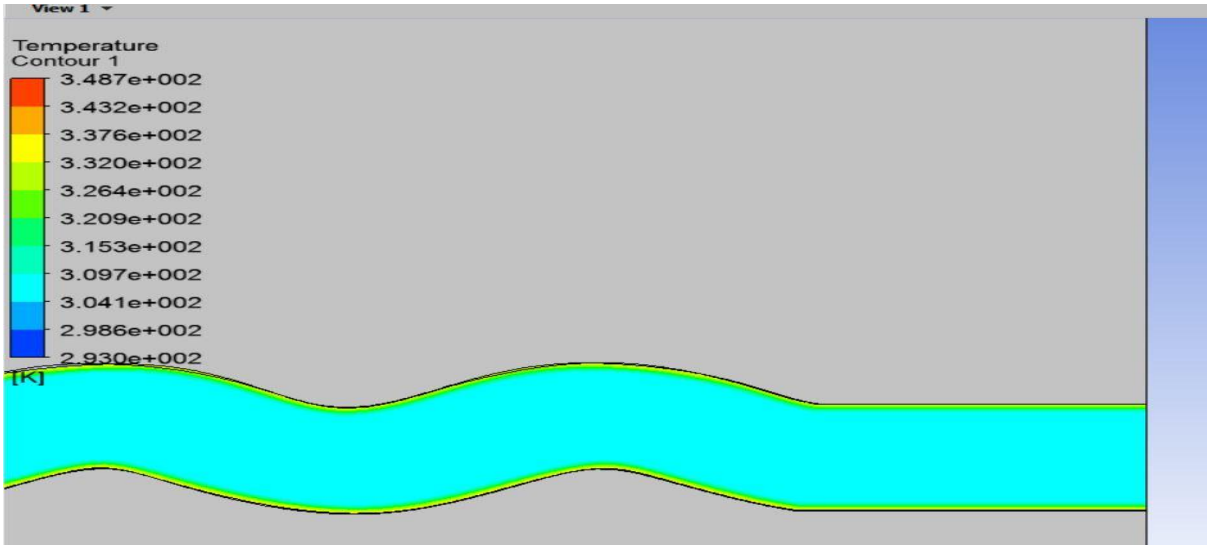

Figure 6.7: Temperature contour closer to outlet of wavy channel at Re=600

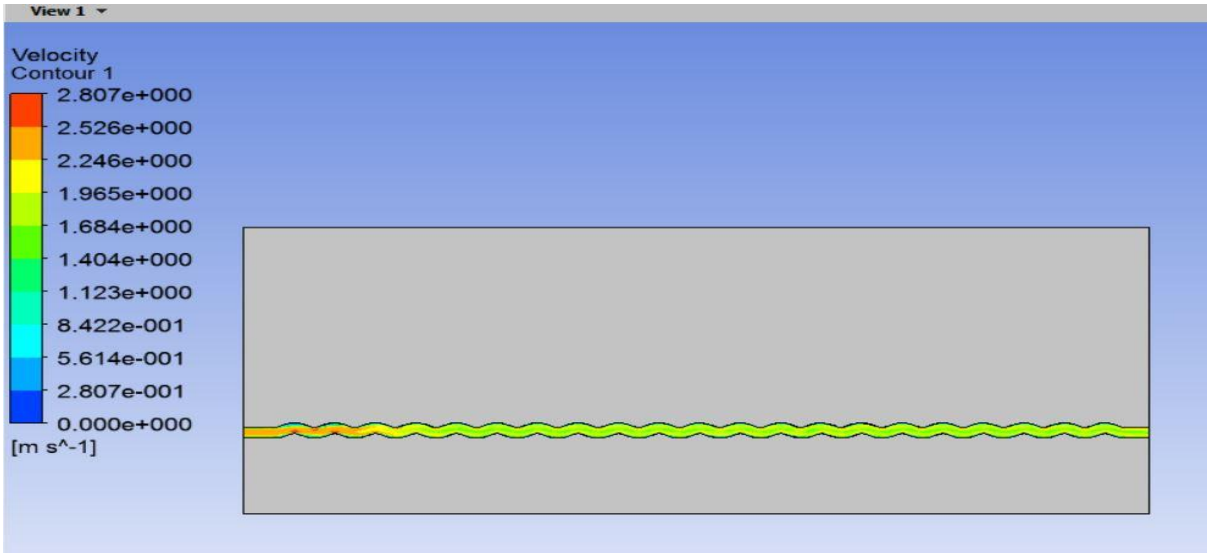

Figure 6.8: Velocity contour along wavy channel at Re=600

In the figures 6.5 to 6.8, the contours for pressure, temperature and velocity in a wavy edge rectangular channel for Reynolds number value equal to 600 are shown.

- In figure 6.5 Pressure drop along the channel is found to be 0.21 bar.
- In figure 6.7 Temperature at the outlet of the channel is found to be 311 K.
- In figure 6.6 Maximum wall temperature is at the bottom wall of the heat sink and is found to be 348.7 K and further the wall temperature increases in the direction of flow.

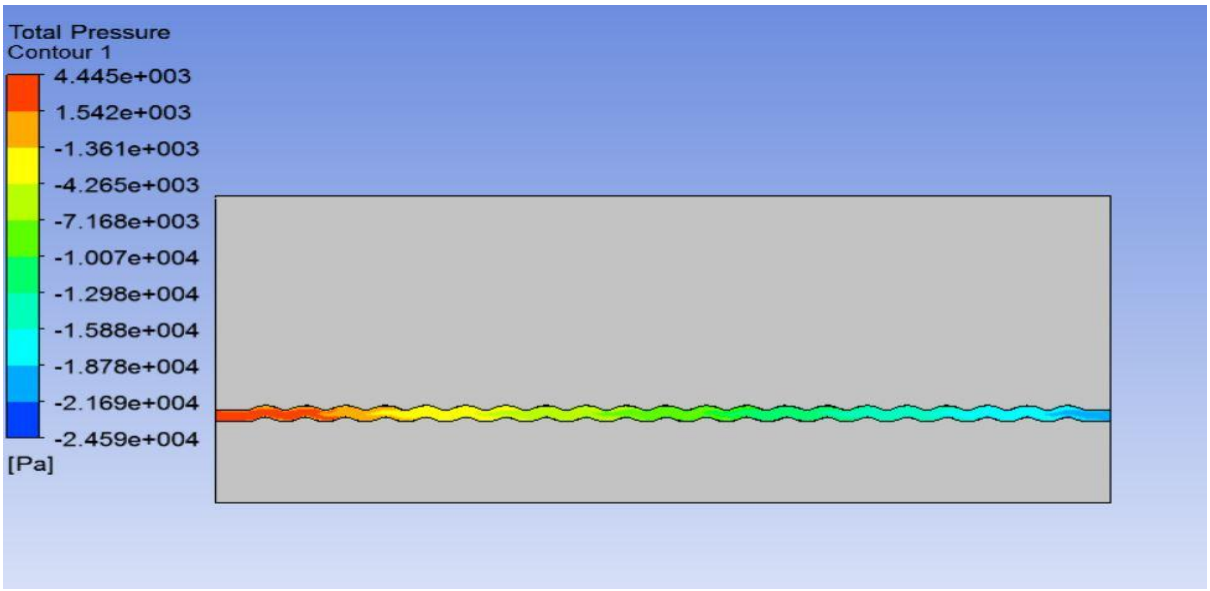

Figure 6.9: pressure contour of water along wavy channel at Re=800

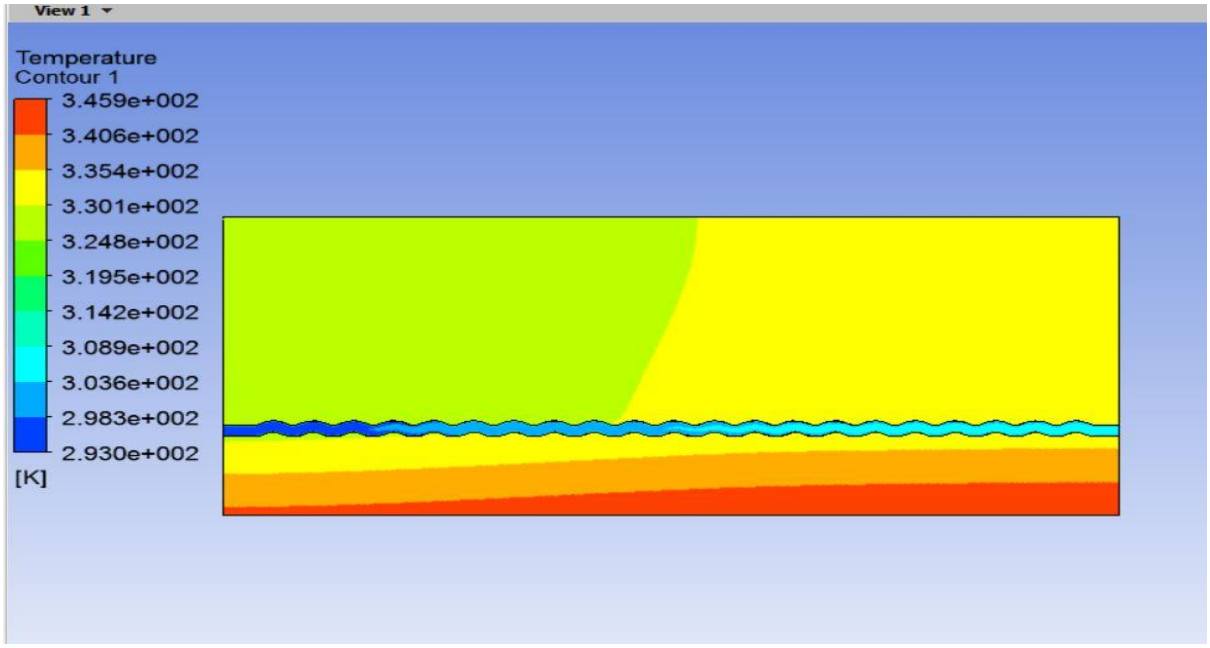

Figure 6.10: temperature contour of heat sink and water along wavy channels at Re=800.

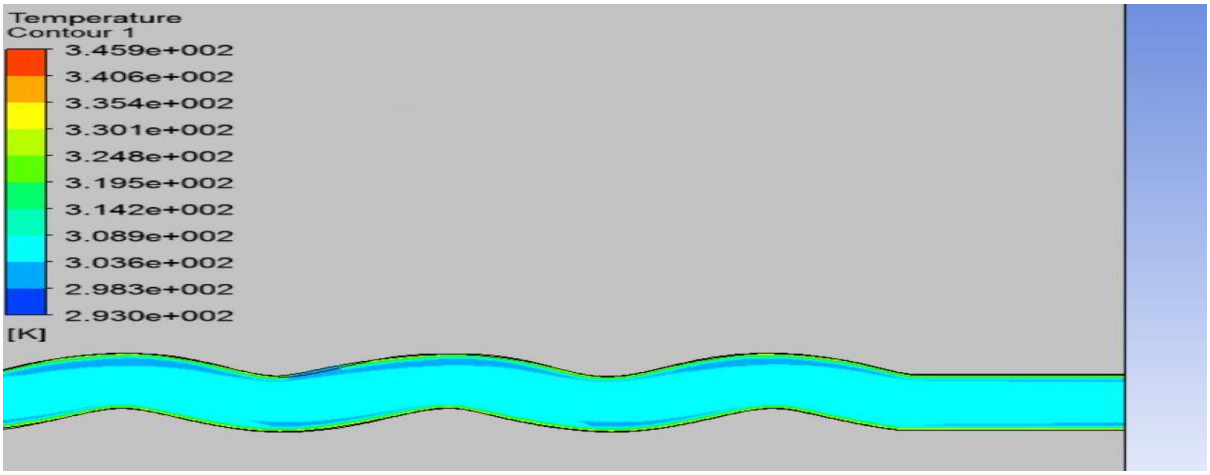

Figure 6.11: Temperature contour closer to outlet of channel at Re=800.

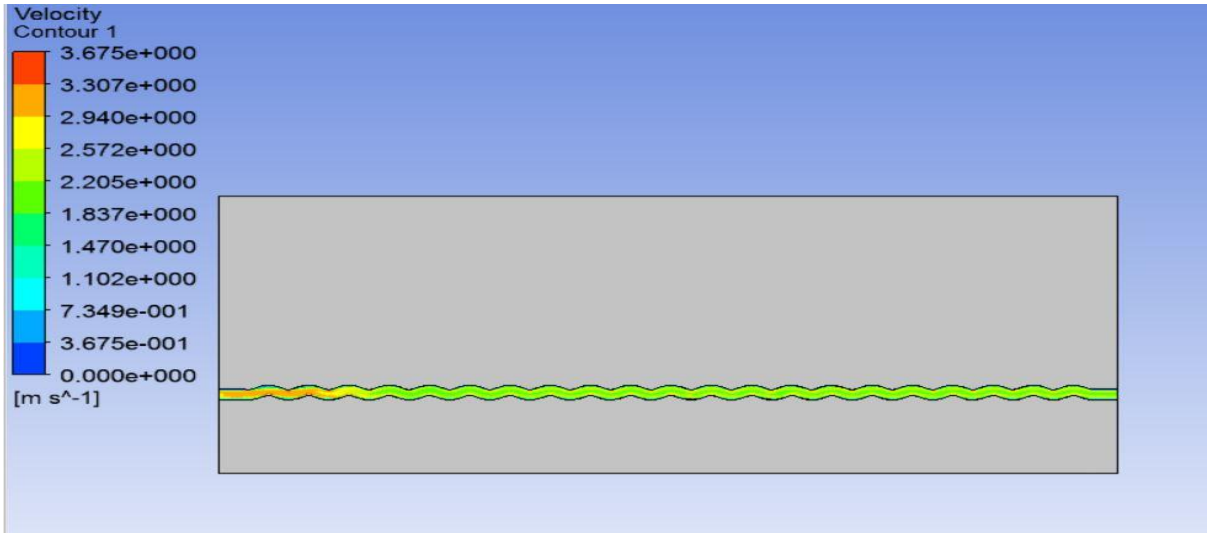

Figure 6.12: velocity contour along wavy channel at Re=800.

In the figures 6.9 to 6.12, the contours for pressure, temperature and velocity in a wavy edge rectangular channel for Reynolds number value equal to 800 are shown.

- In figure 6.9 Pressure drop along the channel is found to be 0.292 bar.
- In figure 6.11 Temperature at the outlet of the channel is found to be 309 K.
- In figure 6.10 Maximum wall temperature is at the bottom wall of the heat sink and is found to be 345.9 K and further the wall temperature increases in the direction of flow.

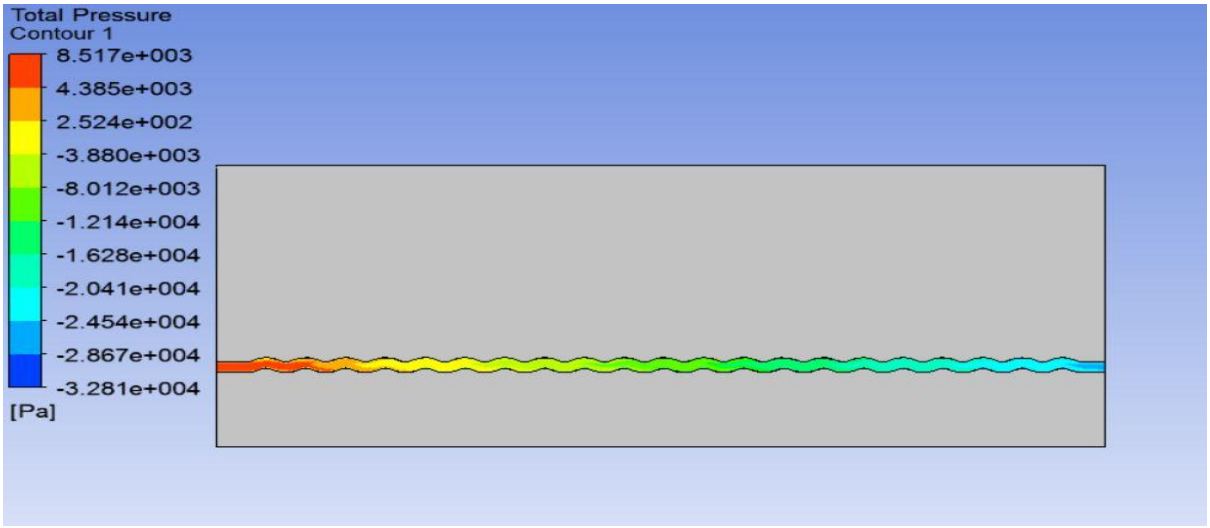

Figure 6.13: pressure contour of water along wavy channel at Re=1000.

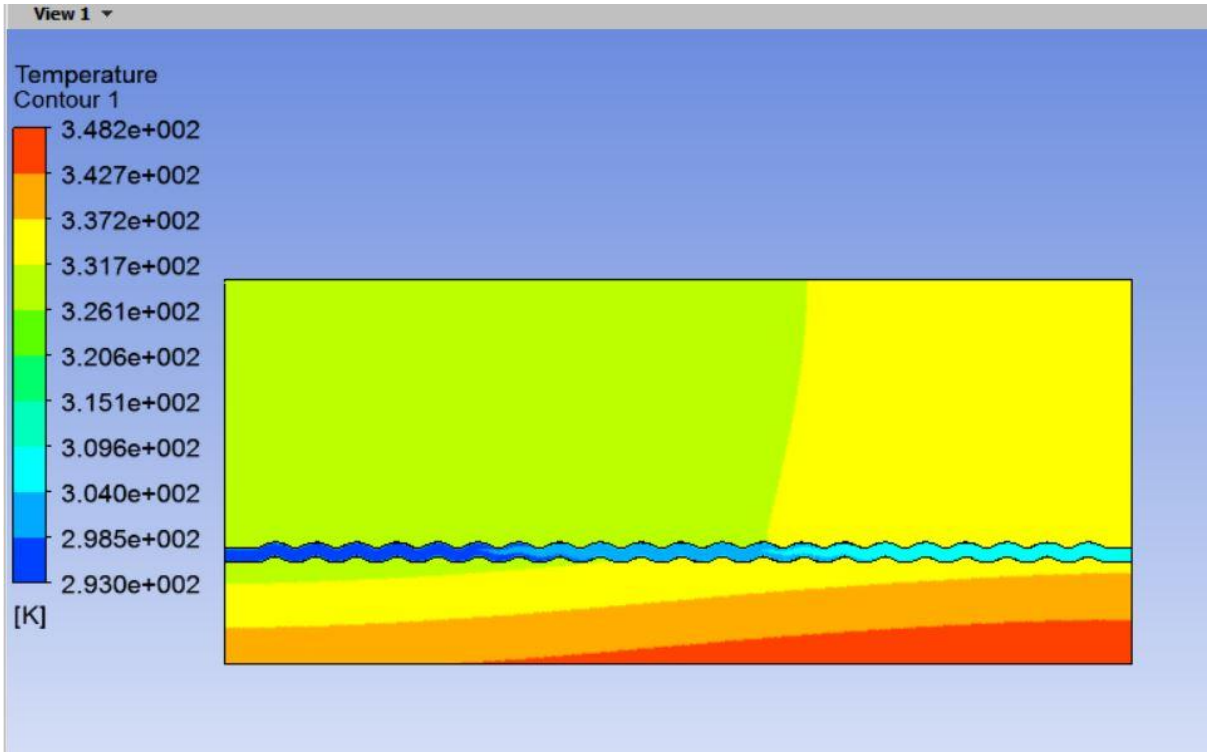

Figure 6.14: temperature contour of heat sink and water along wavy channel at Re=1000.

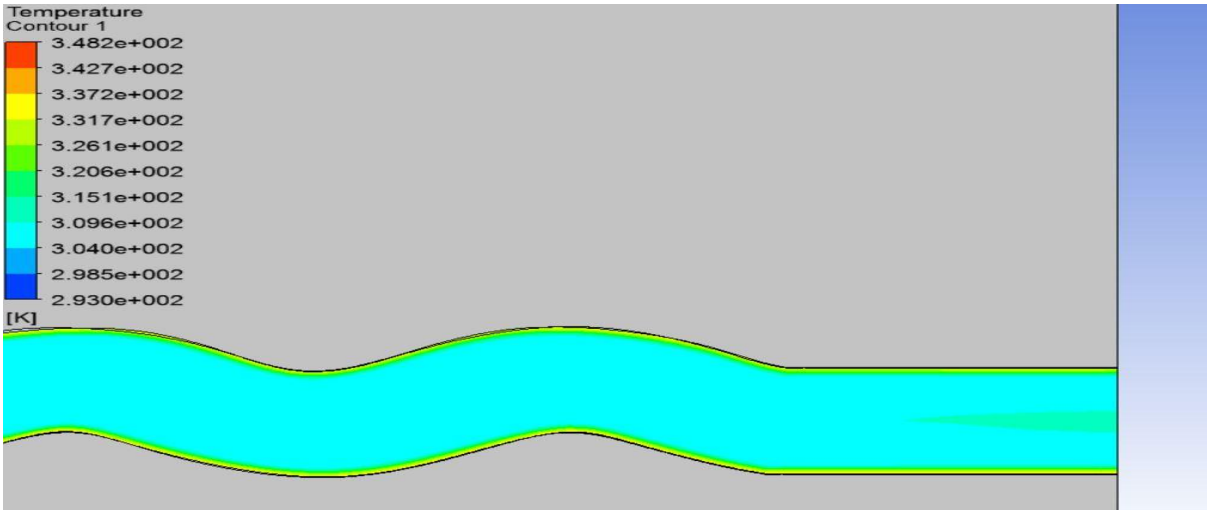

Figure 6.15: temperature contour closer to outlet of wavy channel at Re=1000

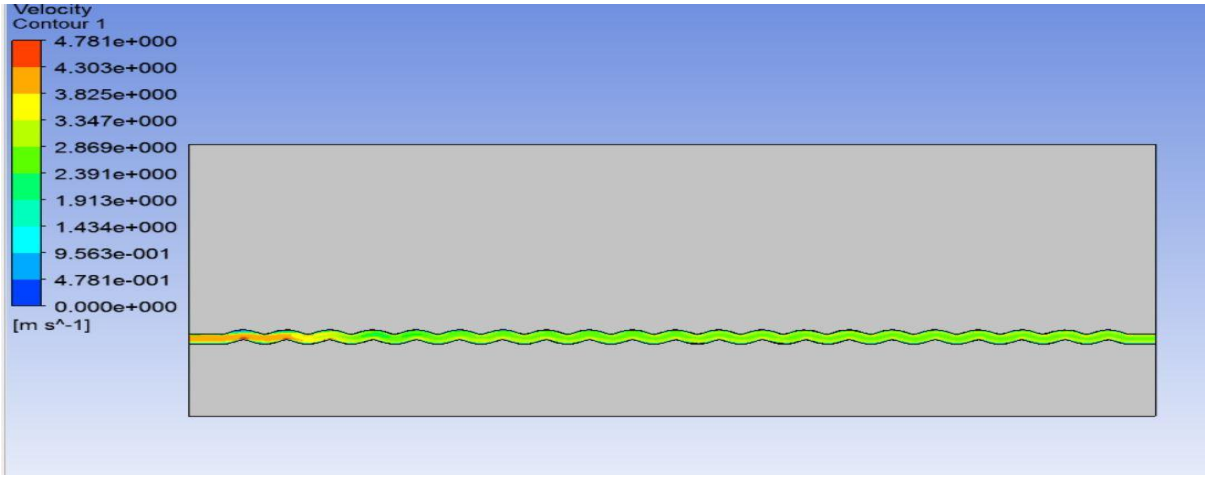

Figure 6.16: velocity contour along wavy edge channel at Re=1000.

In the figures 6.13 to 6.16, the contours for pressure, temperature and velocity in a wavy edge rectangular channel for Reynolds number value equal to 1000 are shown.

- In figure 6.13 Pressure drop along the channel is found to be 0.412 bar.
- In figure 6.15 Temperature at the outlet of the channel is found to be 307 K.
- In figure 6.14 Maximum wall temperature is at the bottom wall of the heat sink and is found to be 342 K and further the wall temperature increases in the direction of flow.

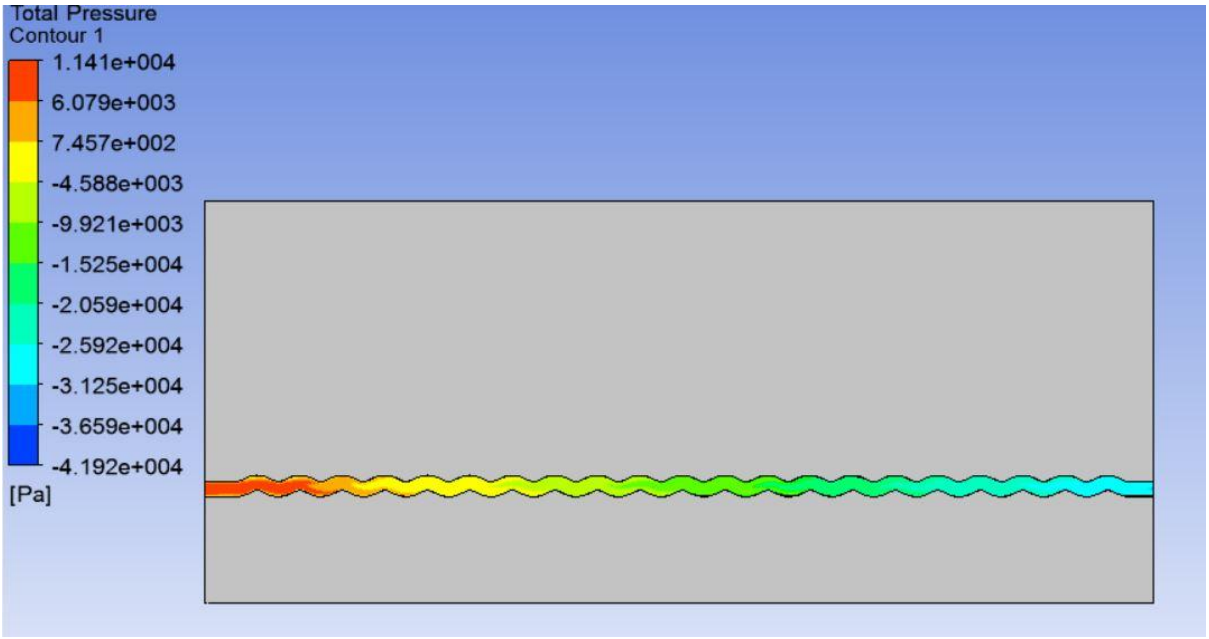

Figure 6.17: pressure contour along wavy edge channel at Re=1200.

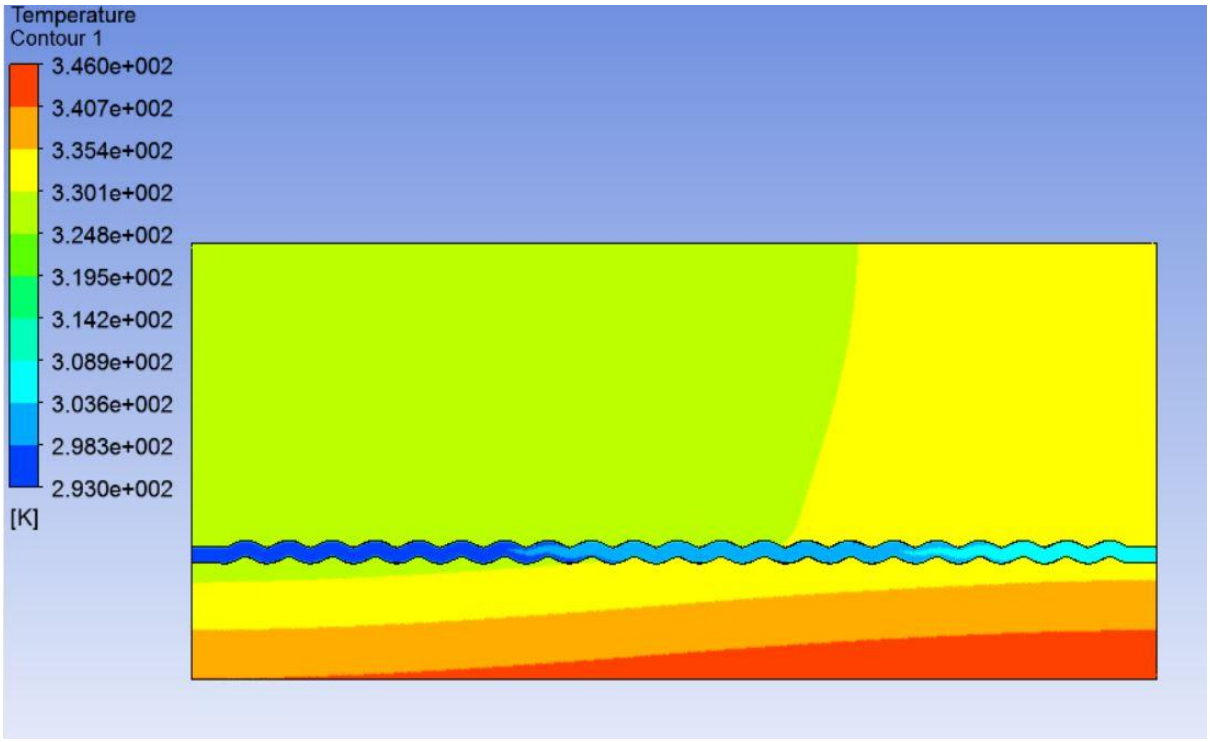

Figure 6.18: temperature contour of water and heat sink along wavy channel at Re=1200.

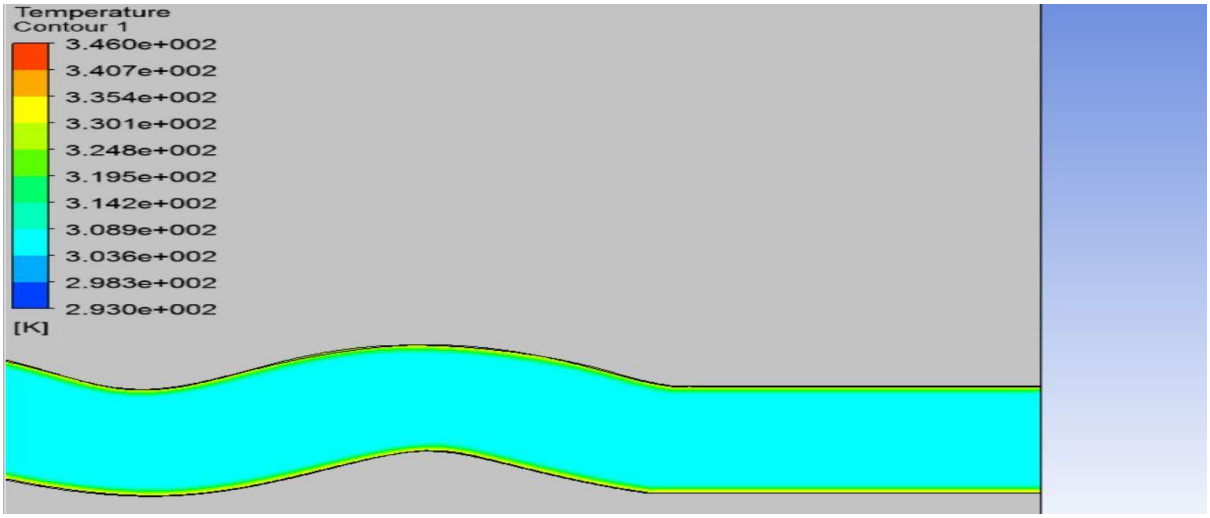

Figure 6.19: temperature contour closer to outlet of wavy channel at Re=1200.

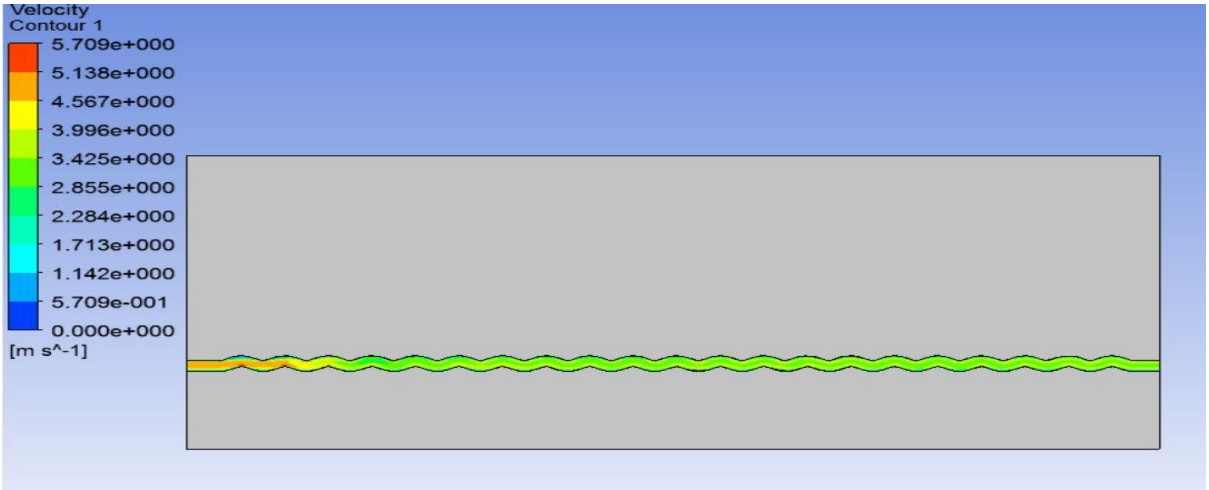

Figure 6.20: velocity contour along wavy edge channel at Re=1200.

In the figures 6.17 to 6.20 the contours for pressure, temperature and velocity in a wavy edge rectangular channel for Reynolds number value equal to 1200 are shown.

- In figure 6.17 Pressure drop along the channel is found to be 0.53 bar.
- In figure 6.19 Temperature at the outlet of the channel is found to be 304 K.
- In figure 6.18 Maximum wall temperature is at the bottom wall of the heat sink and is found to be 347 K and further the wall temperature increases in the direction of flow.

Results for heat flux of 200 W/cm^2 and different sets of Reynolds number-

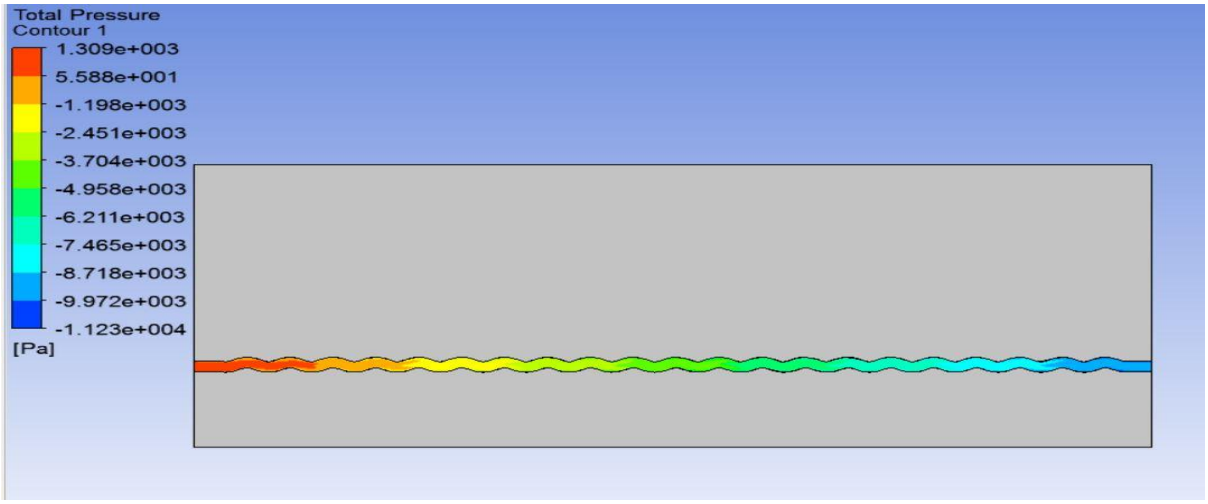

Figure 6.21: pressure contour along wavy channel at Re=400.

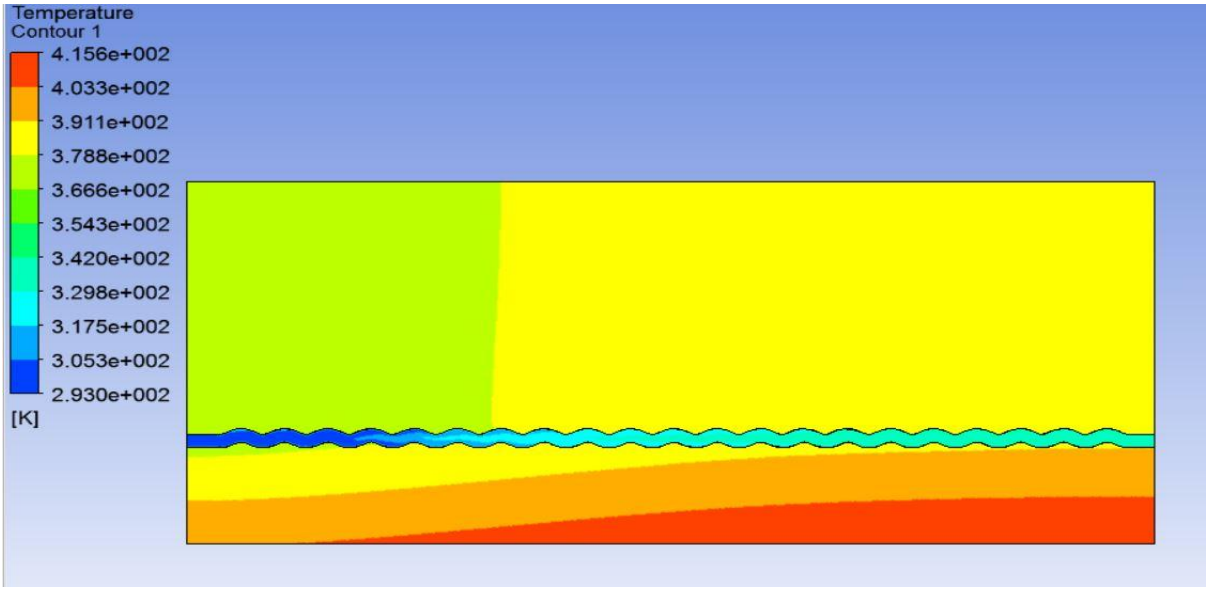

Figure 6.22: Temperature contour of water and heat sink for wavy channel at Re=400.

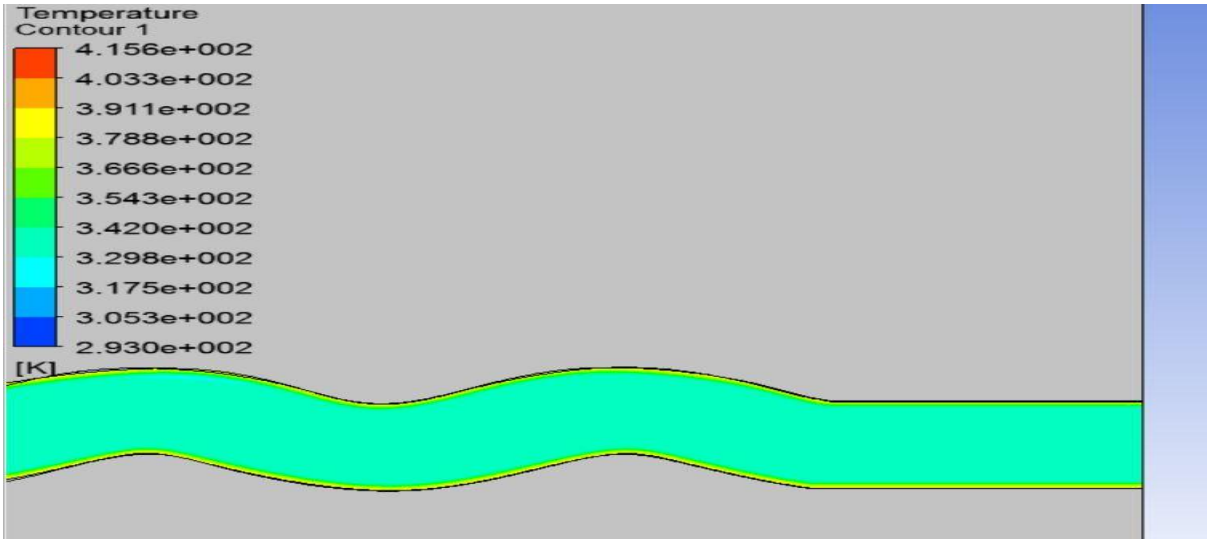

Figure 6.23: Temperature contour closer to outlet of wavy channel at Re=400

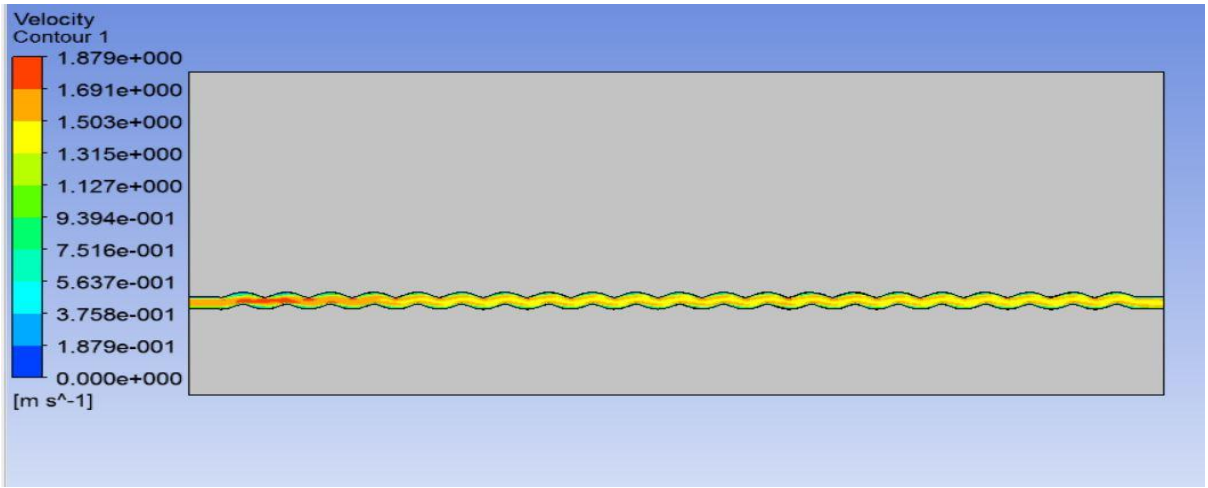

Figure 6.24: velocity contour along wavy channel at Re=400.

In the figures 6.21 to 6.24, the contours for pressure, temperature and velocity in a wavy edge rectangular channel for Reynolds number value equal to 400 are shown.

- In figure 6.21 pressure drop along the channel is found to be 0.126 bar.
- In figure 6.23 temperature at the outlet of the channel is found to be 342 K.
- In figure 6.22 maximum wall temperature is at the bottom wall of the heat sink and is found to be 415.6 K and further the wall temperature increases in the direction of flow.

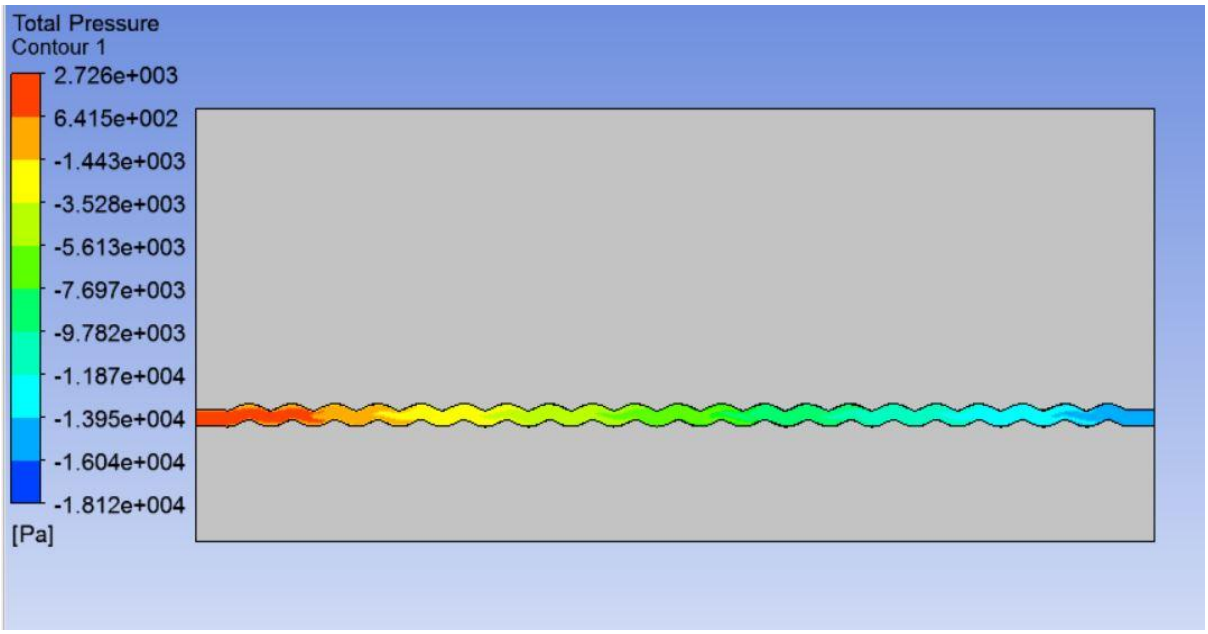

Figure 6.25: pressure contour of water along wavy channel at Re=600.

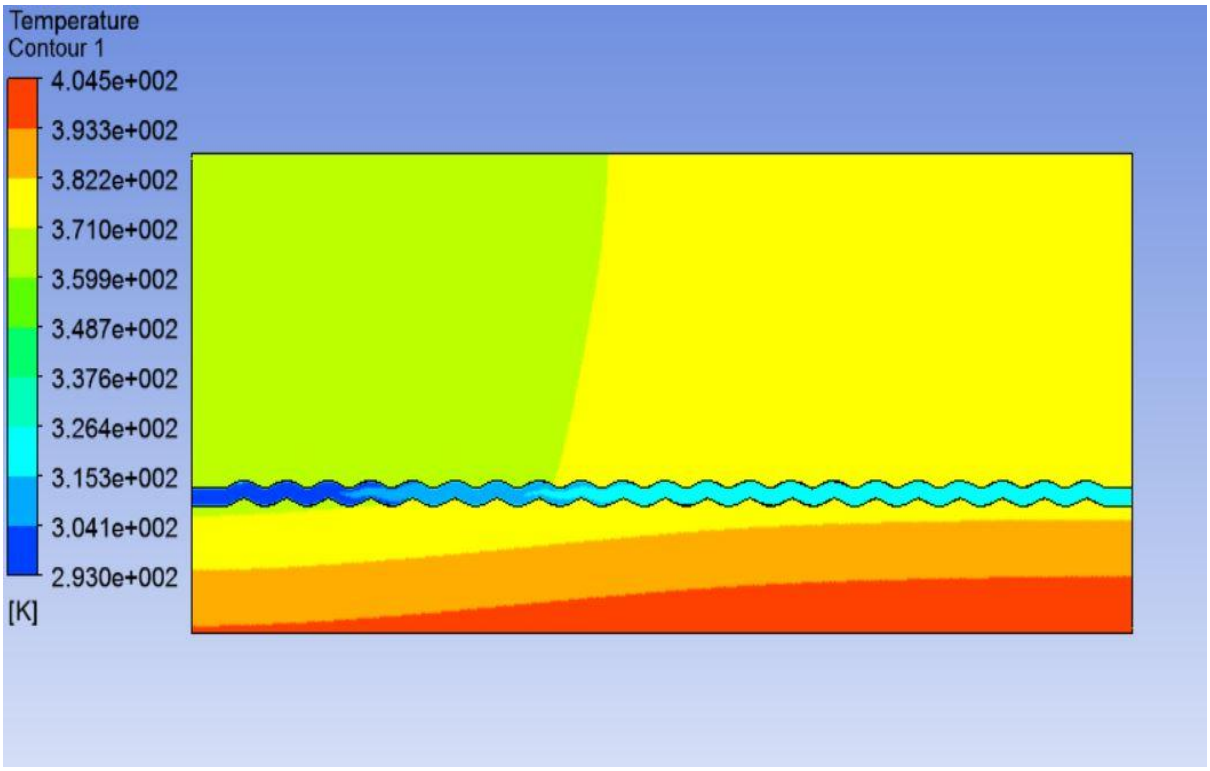

Figure 6.26: temperature contour of water and heat sink at Re=600

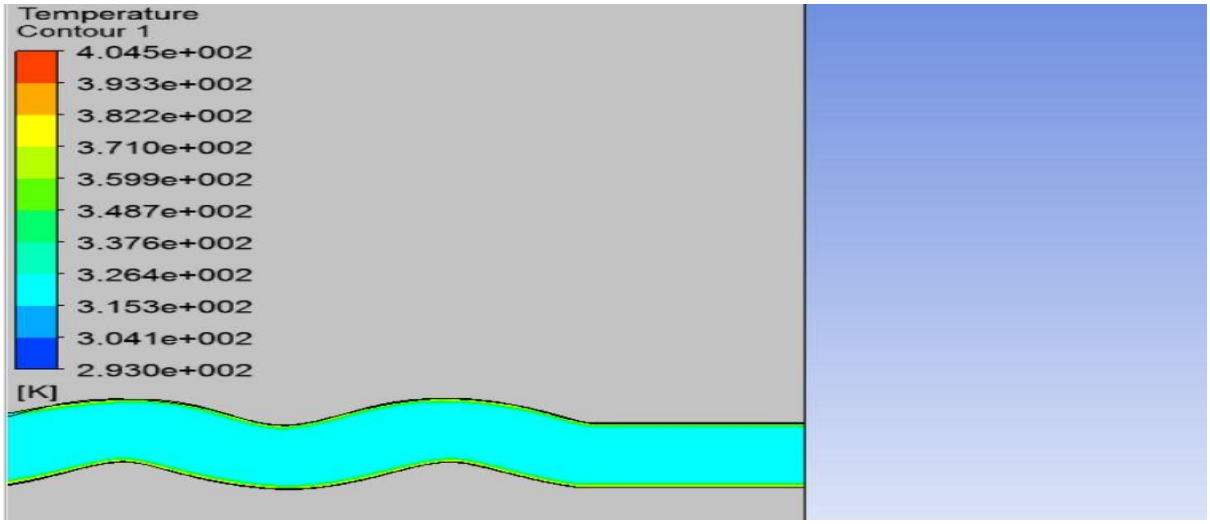

Figure 6.27: Temperature contour closer to outlet of wavy channel at Re=600.

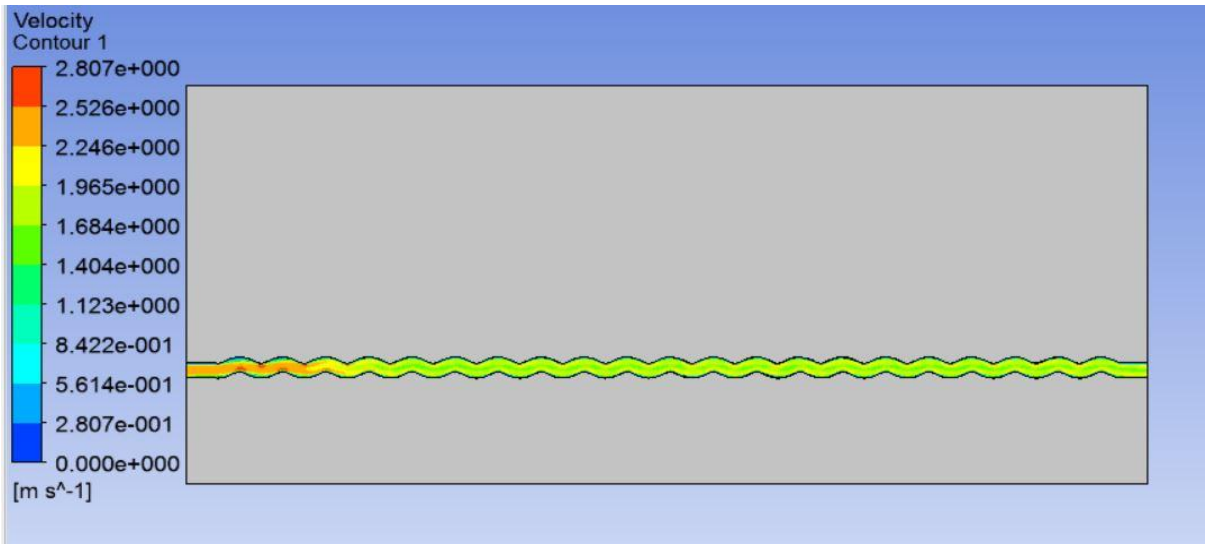

Figure 6.28: velocity contour along wavy edge channel at Re=600

In the figures 6.25 to 6.28, the contours for pressure, temperature and velocity in a wavy edge rectangular channel for Reynolds number value equal to 600 are shown.

- In figure 6.25 pressure drop along the channel is found to be 0.20 bar.
- In figure 6.27 temperature at the outlet of the channel is found to be 332 K.
- In figure 6.26 Maximum wall temperature is at the bottom wall of the heat sink and is found to be 404.6 K and further the wall temperature increases in the direction of flow.

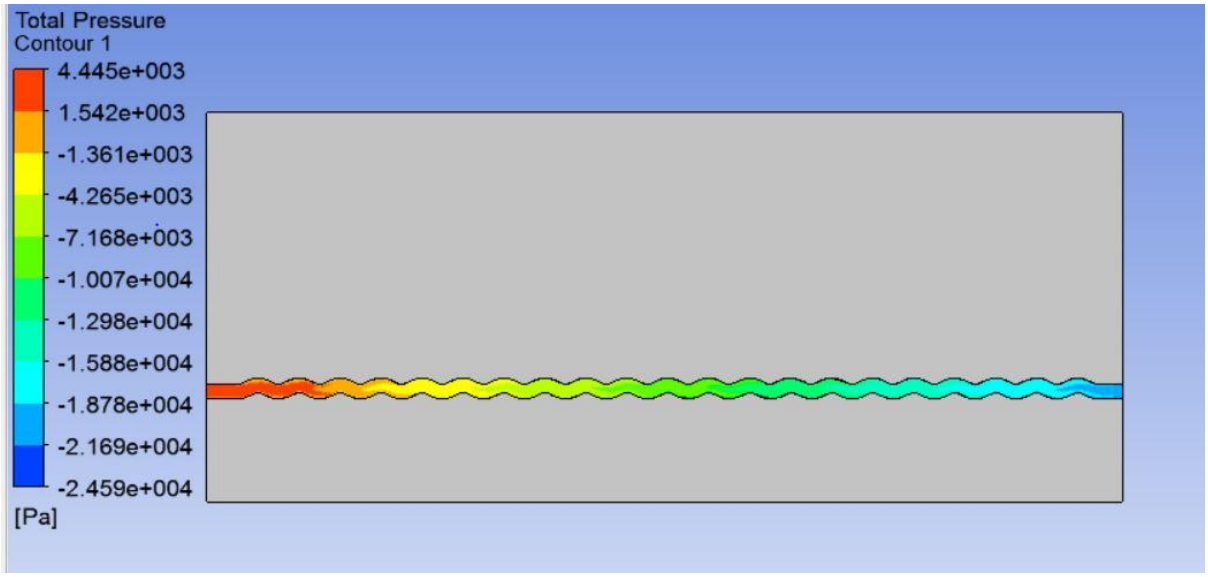

Figure 6.29: pressure contour along wavy channel at Re=800.

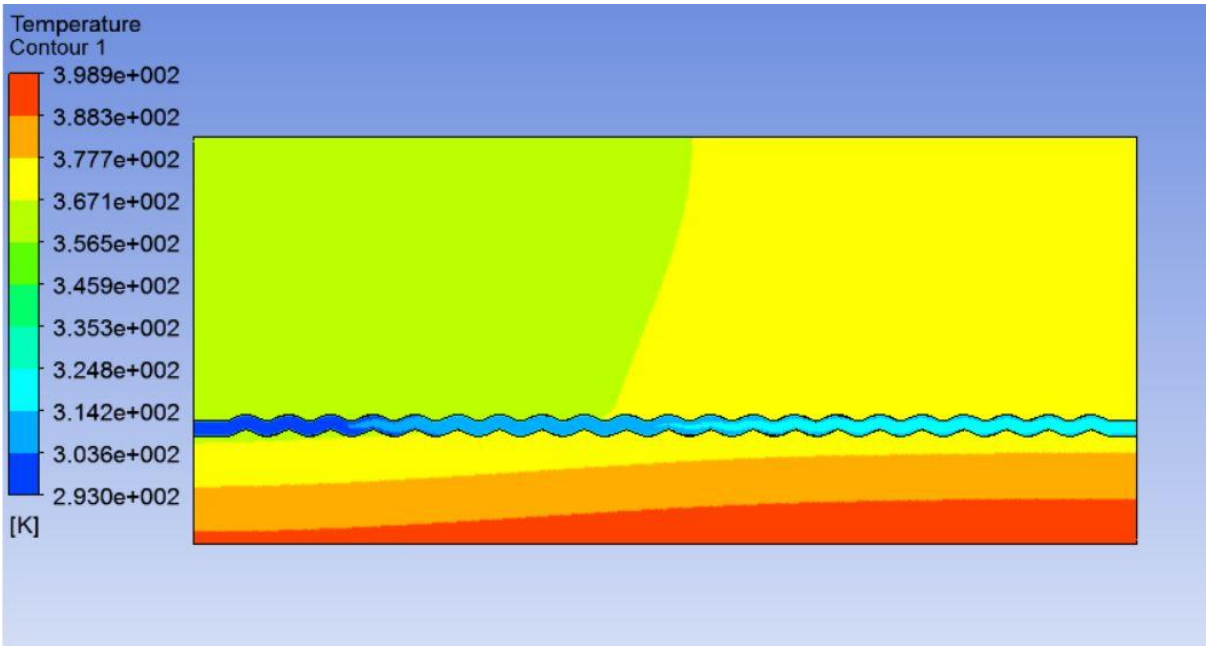

Figure 6.30: Temperature contour for heat sink and water at Re=800

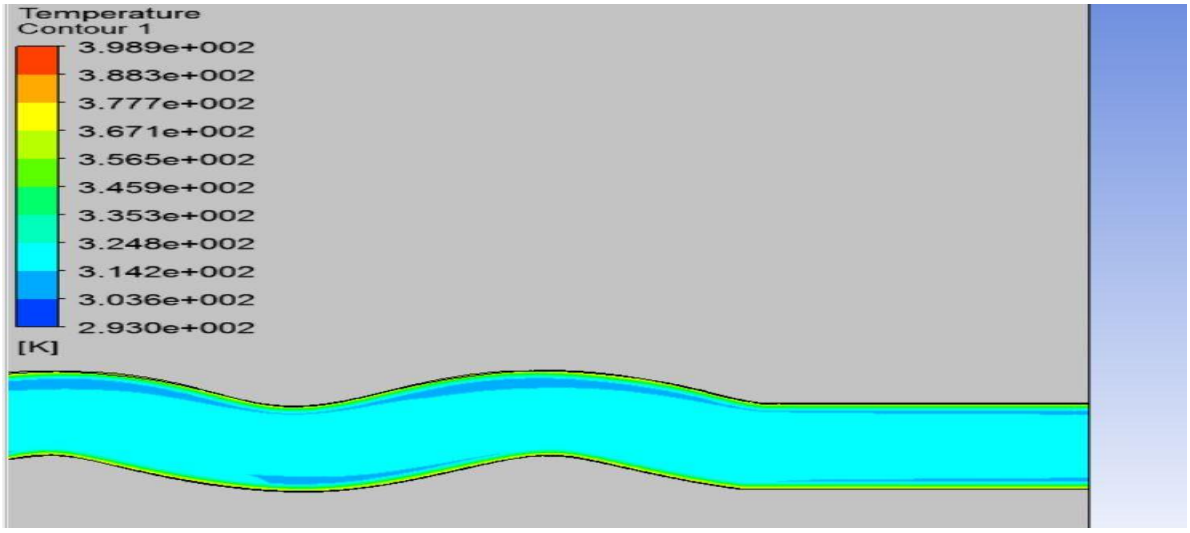

Figure 6.31: Temperature contour closer to outlet of wavy channel at Re=800.

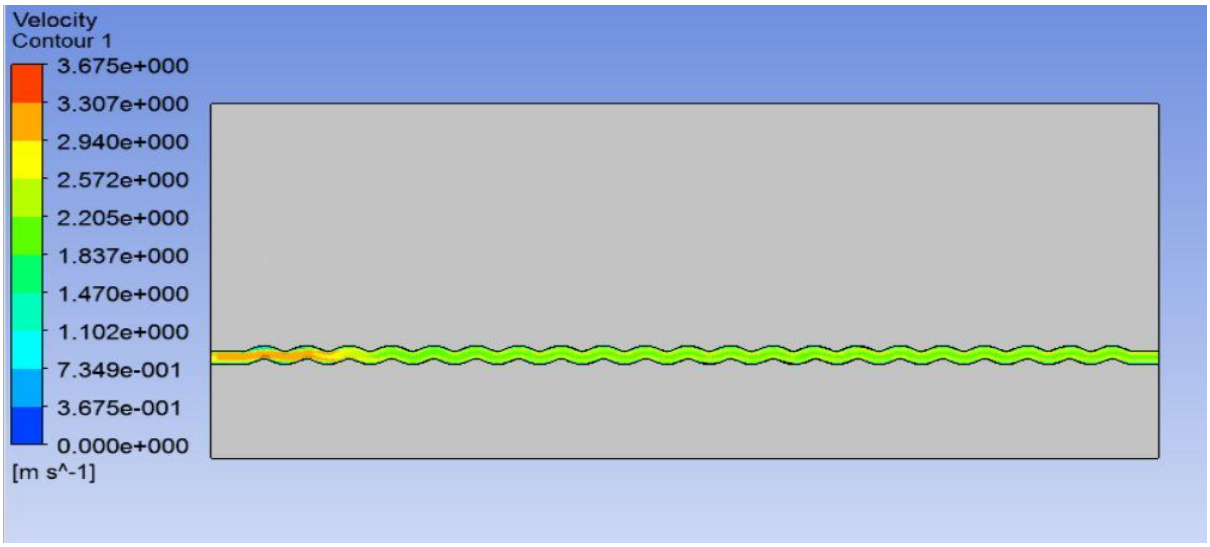

Figure 6.32: velocity contour for wavy edge channel at Re=800.

In the figures 6.29 to 6.32, the contours for pressure, temperature and velocity in a wavy edge rectangular channel for Reynolds number value equal to 800 are shown.

- In figure 6.29 Pressure drop along the channel is found to be 0.28 bar.
- In figure 6.31 Temperature at the outlet of the channel is found to be 324 K.
- In figure 6.30 Maximum wall temperature is at the bottom wall of the heat sink and is found to be 398.9 K and further the wall temperature increases in the direction of flow.

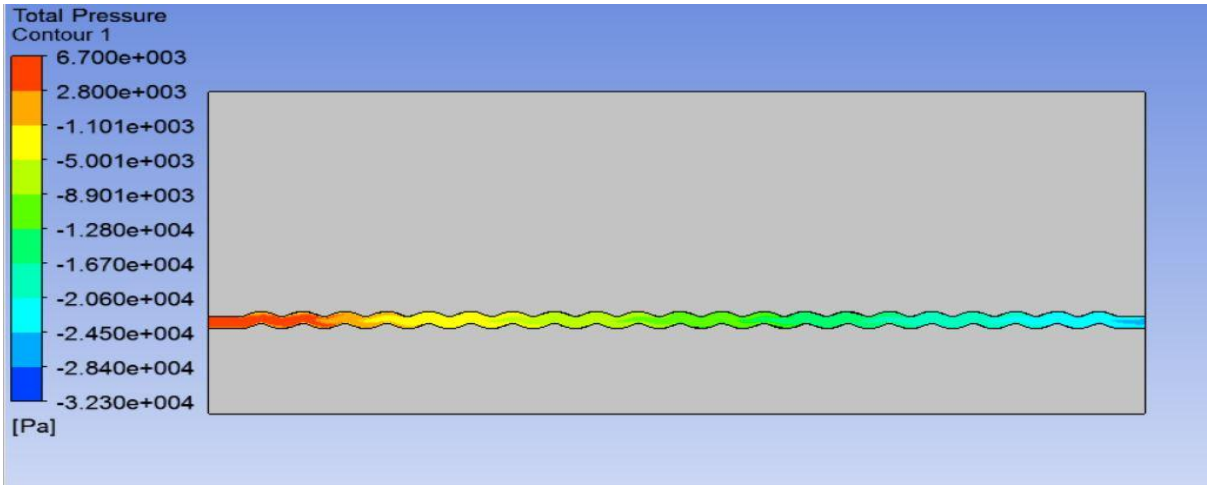

Figure 6.33: pressure contour of water along wavy channel at Re=1000.

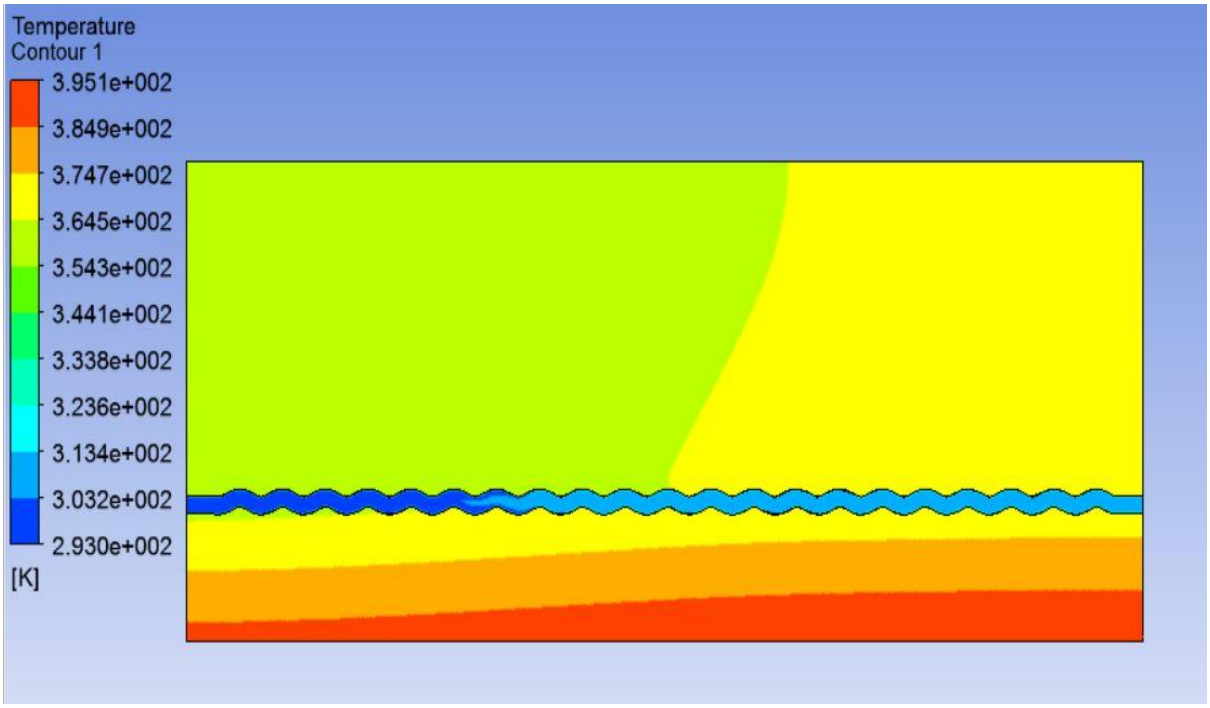

Figure 6.34: Temperature contour of water and heat sink at Re=1000.

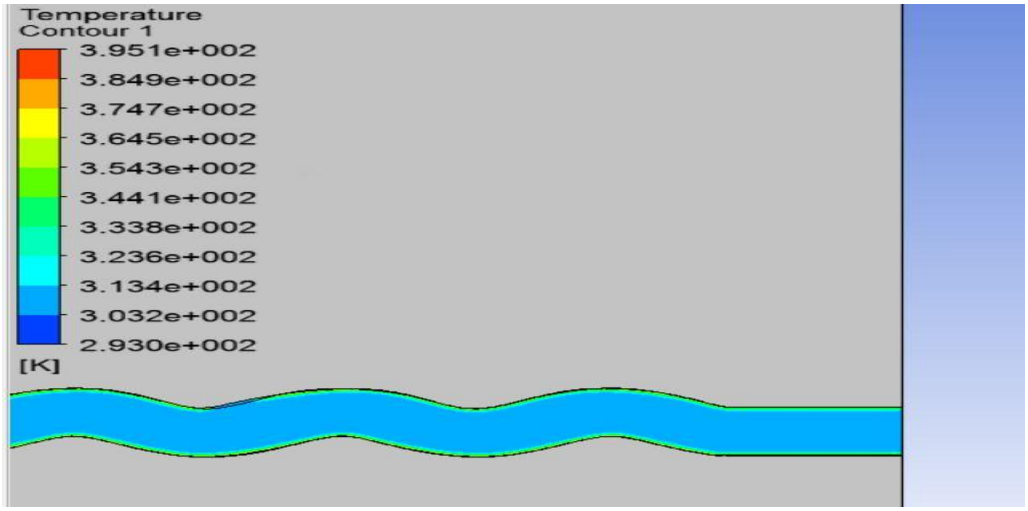

Figure 6.35: Temperature contour closer to outlet of wavy channel at Re=1000.

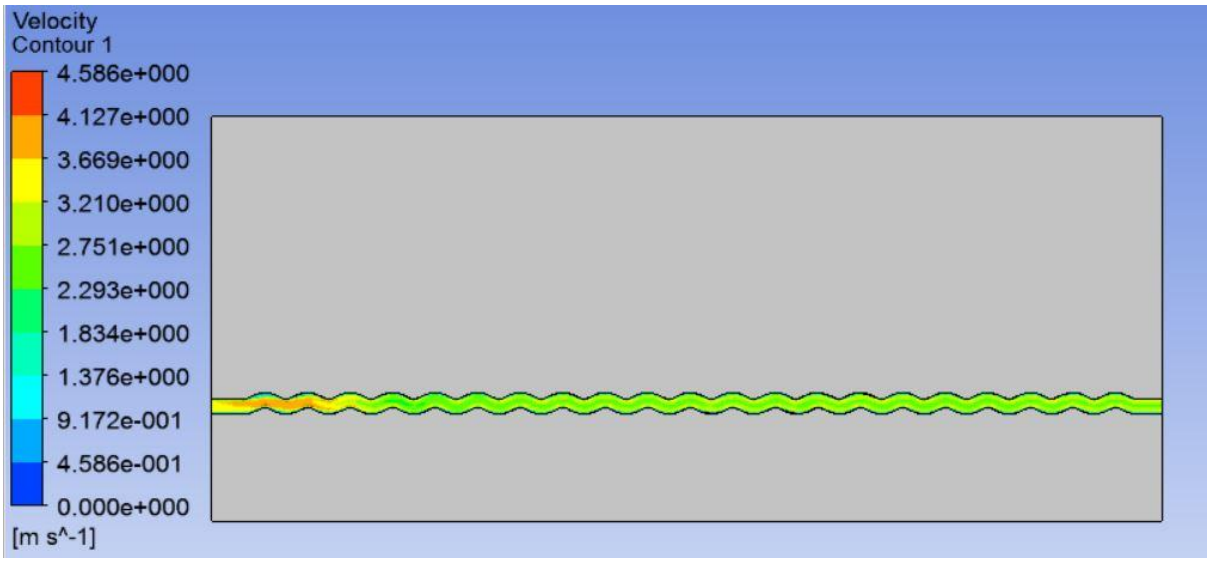

Figure 6.36: velocity contour along wavy channel at Re=1000.

In the figures 6.33 to 6.36, the contours for pressure, temperature and velocity in a wavy edge rectangular channel for Reynolds number value equal to 1000 are shown.

- In figure 6.33 pressure drop along the channel is found to be 0.39 bar.
- In figure 6.35 temperature at the outlet of the channel is found to be 319 K.
- In figure 6.34 Maximum wall temperature is at the bottom wall of the heat sink and is found to be 395.1 K and the wall temperature increases in the direction of flow.

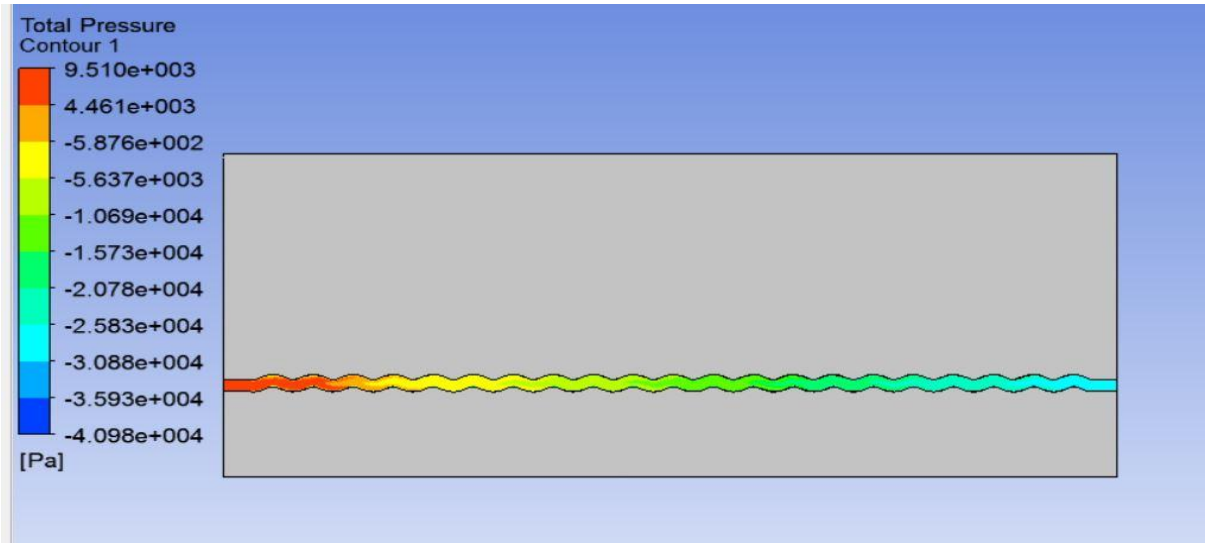

Figure 6.37: pressure contour along wavy edge channel at Re=1200.

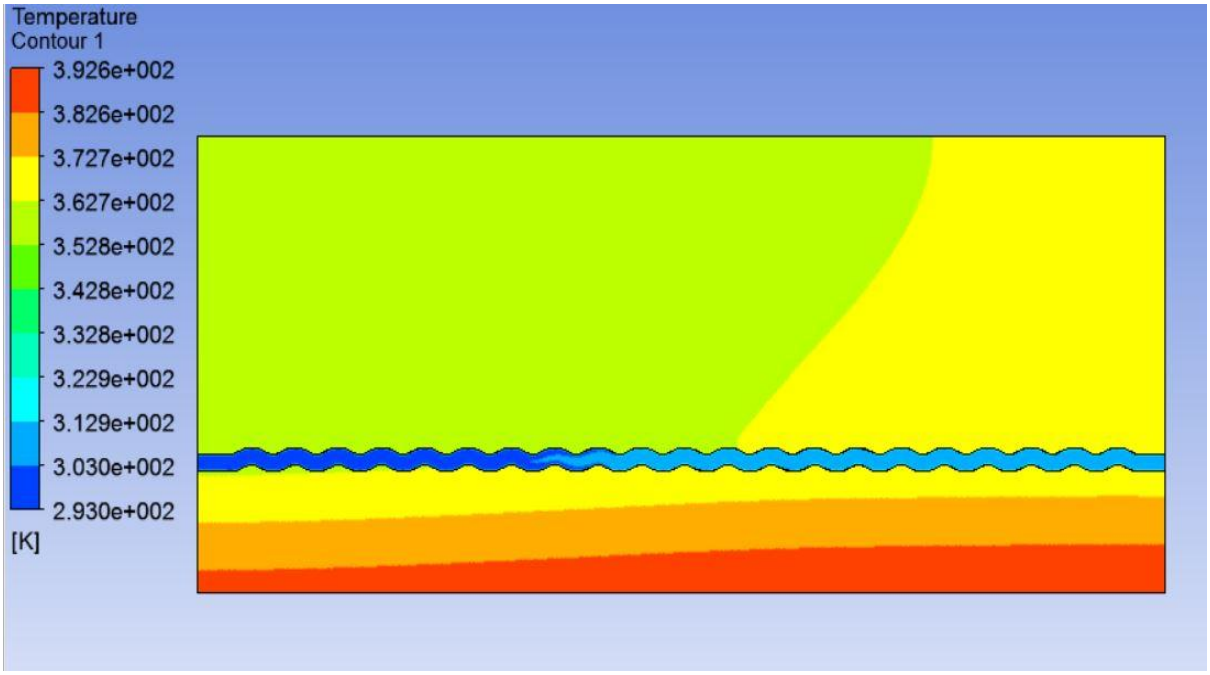

Figure 6.37: temperature contour of heat sink and water at Re=1200.

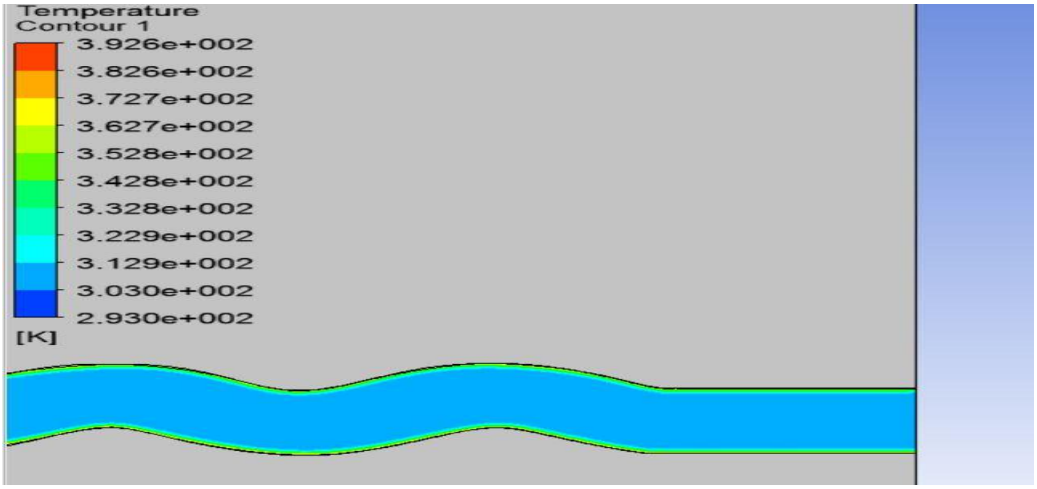

Figure 6.38: temperature contour closer to outlet of wavy channel at Re=1200.

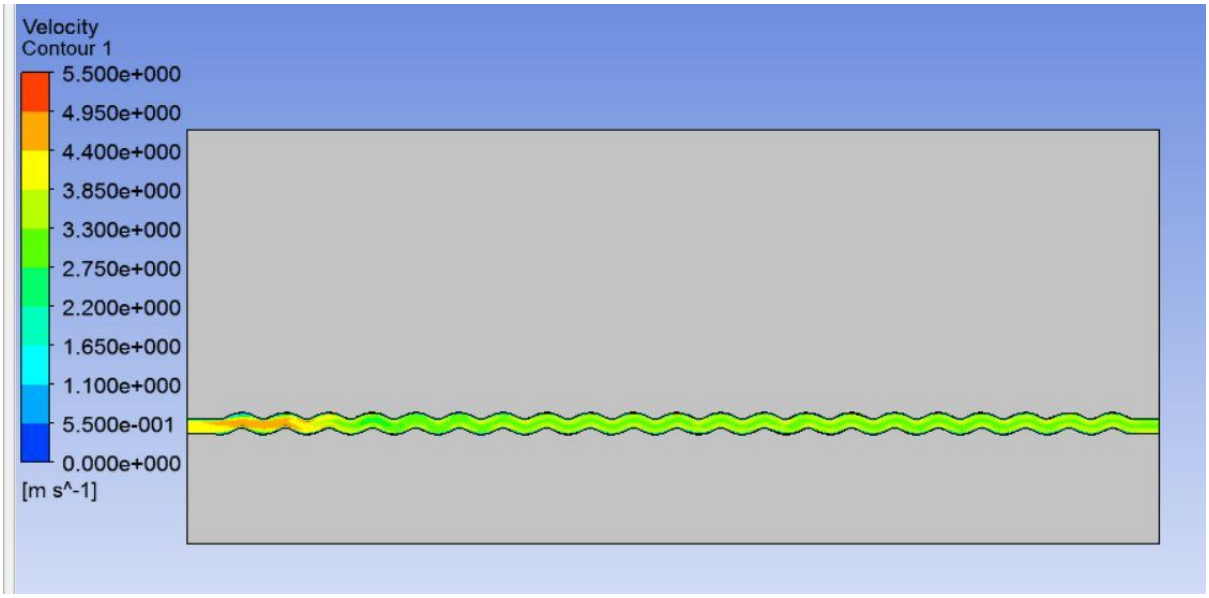

Figure 6.40: velocity contour along wavy edge channel at Re=1200.

In the figures 6.37 to 6.40, the contours for pressure, temperature and velocity in a wavy edge rectangular channel for Reynolds number value equal to 1200 are shown.

- In figure 6.37 Pressure drop along the channel is found to be 0.504 bar.
- In figure 6.39 Temperature at the outlet of the channel is found to be 309 K.
- In figure 6.38 Maximum wall temperature is at the bottom wall of the heat sink and is found to be 392.6 K and further the wall temperature increases in the direction of flow.

The computational pressure drop taken from the pressure contours generated for different sets of Reynolds number for 100W/cm^2 bottom wall heat flux are taken from figures 6.1, 6.5, 6.9, 6.13 and 6.17 respectively.

Table 13: Pressure drop for different Reynolds number for heat flux=100W/cm^2

Reynolds number	Computational pressure drop(bar)
400	0.125
600	0.208
800	0.291
1000	0.413
1200	0.533

The computational temperature rise taken from the temperature contours generated for different sets of Reynolds number for 100W/cm^2 bottom wall heat flux are taken from figures 6.3, 6.7, 6.11, 6.15 and 6.19 respectively.

Table 14: Temperature rise for different Reynolds number for heat flux=100W/cm^2

Reynolds number	Computational temperature rise(°C)
400	25
600	18
800	16
1000	14
1200	11

The maximum computational velocity taken from velocity contours generated for different sets of Reynolds number for 100W/cm^2 bottom wall heat flux are taken from figures 6.4, 6.8, 6.12, 6.16 and 6.20 respectively.

Table 15: Maximum velocity for different Reynolds number for heat flux =100W/cm^2

Reynolds number	Maximum computational velocity(m/s)
400	1.879
600	2.807
800	3.674
1000	4.781
1200	5.709

The computational pressure drop taken from the pressure contours generated for different sets of Reynolds number for 200W/cm^2 bottom wall heat flux are taken from figures 6.21, 6.25, 6.29, 6.33 and 6.37 respectively.

Table 16: pressure drop for different Reynolds number for heat flux =200W/cm^2

Reynolds number	Computational pressure drop(bar)
400	0.124
600	0.204
800	0.286
1000	0.39
1200	0.504

The computational temperature rise taken from the temperature contours generated for different sets of Reynolds number for 200W/cm^2 bottom wall heat flux are taken from figures 6.23, 6.27, 6.31, 6.35 and 6.39 respectively.

Table 17: Temperature rise for different Reynolds number for heat flux =200W/cm^2

Reynolds number	Computational temperature rise (°C)
400	49
600	39
800	31
1000	26
1200	21

The maximum computational velocity taken from velocity contours generated for different sets of Reynolds number for 200W/cm^2 bottom wall heat flux are taken from figures 6.24, 6.28, 6.32, 6.36 and 6.40 respectively

Table 18: maximum velocity for different Reynolds number for heat flux =200W/cm^2

Reynolds number	Maximum computational velocity(m/s)
400	1.870
600	2.77
800	3.672
1000	4.586
1200	5.50

CHAPTER 7

CONCLUSION

7.1 Conclusion-

Based on the numerical study on both straight and wavy edge type micro-channel following conclusions can be made-

- Water temperature rise is more at the outlet of wavy edge type of micro-channels in comparison to straight micro-channels for same values of Reynolds number and heat flux.
- From the above results both for straight rectangular micro-channel and wavy edge type micro-channel the thermal performance of wavy edge micro-channel is found to be better in comparison to that of straight micro-channel of same hydraulic diameter.
- Pressure drop is found to be more in wavy edge micro-channels in comparison to that of straight micro-channels, however the loss in pressure is compensated by the better heat transfer characteristics of the wavy micro-channel.
- Velocity of water is more in wavy type of micro-channels closer to inlet for different values of Reynolds number .
- Velocity of water decreases along the flow direction in wavy micro-channels due to loss in energy of fluid while travelling along wavy channel.
- As the value of heat flux in wavy type of channel is increased from 100W/cm^2 to 200W/cm^2 there is an increase in the outlet temperature of water,however the pressure drop along the channel decreases. But the difference in pressure drop is very less .

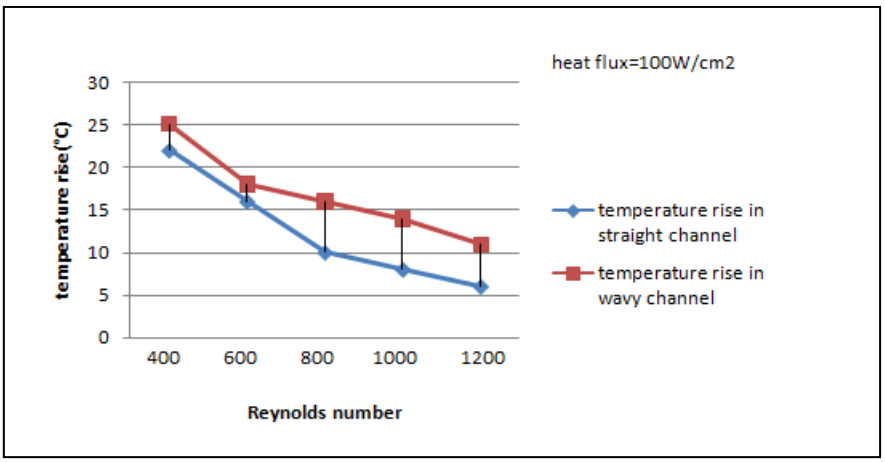

Figure 7.1: Comparison of temperature rise for both straight and wavy type of micro-channel for q=100W/cm^2

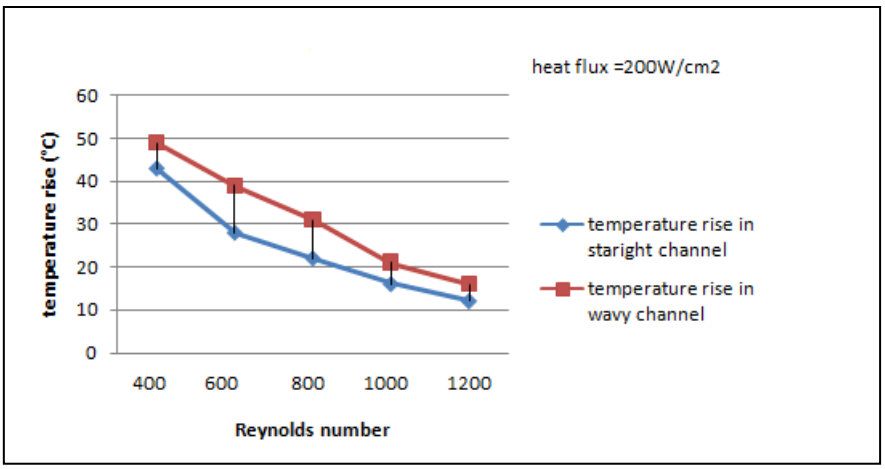

Figure 7.2: Comparison of temperature rise for both straight and wavy type of micro-channel for q=200W/cm^2

From figure 7.1 and figure 7.2 it is clear that there is an increase in the temperature at the outlet of wavy type channel in comparison to that of straight channels for same values of heat flux. Thus in this way heat transfer characteristics of wavy type of micro-channels are better than straight micro-channel for the same dimensions.

7.2 Future scope –

- Analysis of Rectangular micro-channel with refrigerants.
- Analysis of wavy type of micro-channels with refrigerants.
- Analysis of zig zag type of mico-channels with water.

References -

[1] I. Mudawar, W. Qu, Analysis of three dimensional heat transfer in micro-channels, Int. J. Heat and Mass Transfer 45 (2002) 3973-3985.

[2] G.M. Mala, D. Li, J.D. Dale, Heat transfer and fluid flow in micro-channels, International Journal of Heat and Mass Transfer 40 (1997) 3079-3088.

[3] L.T. Yeh, Review of heat transfer technologies in electronic equipment, ASME J. Electron. Packag. 117 (1995) 333–339.

[4] D.B. Tuckerman, R.F.W. Pease, High-performance heat sinking for VLSI, IEEE Electron. Dev. Lett. EDL-2 (1981) 126–129.

[5] I. Mudawar, M.B. Bowers, Ultra-high critical heat flux (CHF) for subcooled water flow boiling —I: CHF data and parametric effects for small diameter tubes, Int. J. Heat Mass Transfer 42 (1999) 1405–1428.

[6] I. Mudawar, W. Qu, Experimental and numerical study of pressure drop and heat transfer in a single-phase micro-channel heat sink, Int. J. Heat and Mass Transfer 45(2002) 2549-2565.

[7] K. Kawano, K. Minakami, H. Iwasaki, M. Ishizuka, Micro channel heat exchanger for cooling electrical equipment, Application of Heat Transfer in Equipment, Systems and Education, ASME HTD-361-3/PID-3, 1998, pp. 173–180.

[8] A. Bejan, A.M. Morega, Optimal arrays of pin fins and plate fins in laminar forced convection, ASME J. Heat Transfer 115 (1993) 75–81.

[9] A.G. Fedorov, R. Viskanta, Three-dimensional conjugate heat transfer in the microchannel heat sink for electronic packaging, Int. J. Heat Mass Transfer 43 (2000) 399–415.

[10] X.F. Peng, G.P. Peterson, Convective heat transfer and flow friction for water flow in microchannel structures, Int. J. Heat Mass Transfer 39 (1996) 2599–2608.

[11] K.K. Ambatipudi, M.M. Rahman, Analysis of conjugate heat transfer in microchannel heat sinks Numer. Heat Transfer A, 37 (2000), pp. 711–731.

[12] Y. Sui, C.J. Teo, P.S. Lee, Y.T. Chew, C. Shu, Fluid flow and heat transfer in wavy micro-channels Int. J. Heat Mass Transfer, 53 (2010), pp. 2760–2772.

[13] P. Gunnasegaran, H.A. Mohammed, N.H. Shuaib, R. Saidur, The effect of geometrical parameters on heat transfer characteristics of micro-channels heat sink with different shapes Int. Commun. Heat Mass Transfer, 37 (8) (2010), pp. 1078–1086

[14] E. Utriainen, B. Sunden ,Numerical analysis of primary surface trapezoidal cross wavy duct Int. J. Numer. Method Heat Fluid Flow, 10 (6) (2000), pp. 634–648.

[15] S. Kandlikar, S. Garimella, D. Li, S. Colin, M.R. King, Heat Transfer and Fluid Flow in Minichannels and Microchannels, Elsevier, USA, 2005.

[16] E. Utriainen, B. Sunden, Numerical analysis of primary surface trapezoidal cross wavy duct, Int. J. Numer. Method Heat Fluid Flow 10 (6) (2000) 634–648.

[17] W. Yang, J. Zhang, H. Cheng, The study of flow characteristics of curved microchannel, Appl. Therm. Eng. 25 (2010) 1894–1907.

[18] R.K. Shah, A.L. London, Laminar Flow Forced Convection in Ducts, Academic Press, New York, 1978.

[19] S.G. Kandlikar, W.J. Grande, Evaluation of single phase flow in microchannels for high heat flux chip cooling – thermohydraulic performance enhancement and fabrication technology, Heat Transfer Eng. 25 (8) (2004) 5–16.

[20] S.V. Garimella, C.B. Sobhan, Transport in microchannels – a critical review, Annu. Rev. Heat Transfer 13 (2003) 1–50.

[21] S.V. Patankar, Numerical Heat Transfer and Fluid Flow, Hemisphere, New York, 1980.

[22] J.D. Anderson, Computational Fluid Dynamic: The Basics with Applications, McGraw-Hill, New York, 1995.